TNO Building and Construction Research

TNO report

97-BT-R0574

Concrete resistivity and reinforcement corrosion rate as a function of temperature and humidity of the environment

Date   5 March 1997

Authors   Dr. Luca Bertolini (Politecnico di Milano, Italy)
                Dr. R.B. Polder

Copy no
No. of copies
Number of pages   85
Number of appendices 2
Sponsor
Project name   Corrosion
Project number   7.20.8.4435.600

SUMMARY

This report describes the analysis of experimental measurements carried out at TNO within the research project NL-1: "Corrosion rate and resistivity of reinforced concrete" which was part of the European research programme COST 509: "Corrosion of metals in contact with concrete".

The results obtained during five years on specimens with concrete mixed with blast furnace slag cement and ordinary portland cement exposed to environments with different humidity and temperature were studied. Aim of the work was the investigation of the relationship between corrosion rate of steel and resistivity of concrete, in chloride contaminated and/or in carbonated concrete. The influence of concrete composition and environmental variables on resistivity of concrete and corrosion rate and potential of steel was also discussed.

Although a relationship between corrosion rate of steel and concrete resistivity applicable to all types of concrete and environment was not found, good linear trends were observed for given specimens when the environmental variables were changed. The same linear relationship between corrosion rate steel in carbonated or chloride contaminated concretes and conductivity of concrete was found when both temperature or the humidity of the environment changed.

However, other factors (namely, cement type, w/c ratio, carbonation, chloride content) had different influences on corrosion rate of steel and resistivity of concrete, so that they changed also the relationship between them.

The mechanisms that control corrosion of steel in different types of concrete or conditions of exposure were also investigated. In particular it was shown that in carbonated and/or chloride contaminated concrete exposed to 75-95% R.H. and 20-40°C both corrosion rate and corrosion potential are related to resistivity of concrete, in accordance to the anodic resistance control theory.

The analysis of the influential factors on corrosion rate and resistivity showed a strong influence of moisture content in concrete, temperature, cement type, carbonation and chloride contamination. A linear dependence on R.H. and an exponential dependence on temperature was found both for conductivity of concrete and corrosion rate of steel.

INDEX

1. INTRODUCTION

Resistivity of concrete plays an important role in corrosion of steel. Several research works show a inverse relationship between corrosion rate of reinforcement and electrical resistivity of concrete [1-4]. To explain this correlation, it has been suggested that corrosion rate is under resistive control [3]. Furthermore, Glass et al. [1] discussing experimental results on carbonated mortars, proposed a theory based on anodic resistance control, i.e. the corrosion rate of steel is under anodic control with the anodic reaction rate being limited by the mortar resistivity.

A long term research project was carried out at TNO aimed at studying concrete resistivity and corrosion rate of embedded steel in concretes of different composition, exposed to different climates. Five year tests were performed on reinforced concrete specimens exposed to wet (fog room) and semi-dry (80% R.H.) environments. The influences of temperature (0-40°C) and relative humidity (>75%) were also investigated.

The research was part of the European research programme COST 509 "Corrosion of metals in contact with concrete", project NL-1 "Corrosion rate and resistivity of reinforced concrete". The tests were carried out by several students from Universitá La Sapienza of Rome (M.Valente, A.Tondi, A.Mazzoni, S.Fiore, M.Scotto di Carlo) and the results are presented in TNO reports [5-9].

A significant number of experimental results is available, suggesting a relationship between corrosion rate of steel and resistivity of concrete. In some cases a linear relation between corrosion rate and conductivity (the inverse of resistivity) was found. However different fitting straight lines were found in different specimen. Some relationships were also found between resistivity of concrete and temperature, relative humidity, chloride content, etc. However, this matter needs to be investigated in more details.

In this report, the parameters that influenced both resistivity of concrete and corrosion rate are analysed in order to better evaluate the mechanisms which control the corrosion rate of steel in carbonated or chloride contaminated concrete and to discuss the relationship between corrosion rate of steel and resistivity of concrete.

Firstly, all the experimental results are presented as a function of time and exposure condition. Then, the influence of several parameters (such as concrete composition, environment humidity, temperature) on resistivity of concrete, corrosion rate and corrosion potential is studied. Finally, an attempt to correlate concrete resistivity and corrosion rate of steel, also in relation to the mechanisms of corrosion control proposed in the literature, will be made.

2. EXPERIMENTAL RESULTS

2.1 *Specimens*

Figure 1 shows the specimens (prisms) used for the tests, which were cast in September 1991 [5]. Eight types of concrete were used, by changing:

- cement type: an ordinary portland cement (OPC) and a blast furnace slag cement (BFSC) with a slag content of about 70%;

- water to cement ratio (w/c): 0.45 and 0.65;

- chloride content: no addition and 2% chloride ions by cement weight (added as $CaCl_2 \cdot 2H_2O$).

Cement content was 330 kg/m^3 for specimens with w/c 0.45 and 300 kg/m^3 for those with w/c 0.65. River sand and gravel with a size up to 8 mm were used as aggregate.

For each type of concrete composition, four prism specimens were cast (two cubes were also cast for carbonation depth and weight change measurements); Table 1 reports the designation of the specimens.

Six steel rebars were embedded in the concrete: three on one side of the specimens at a depth of 30 mm and three on the opposite side at a depth of 10 mm, as shown in Fig. 1 (the surface exposed to concrete was 11.4 cm^2). Also four brass bars were embedded in the middle of the specimens at different depths (2 bars at 10 mm and 2 bars at 50 mm) in order to measure the resistivity of concrete.
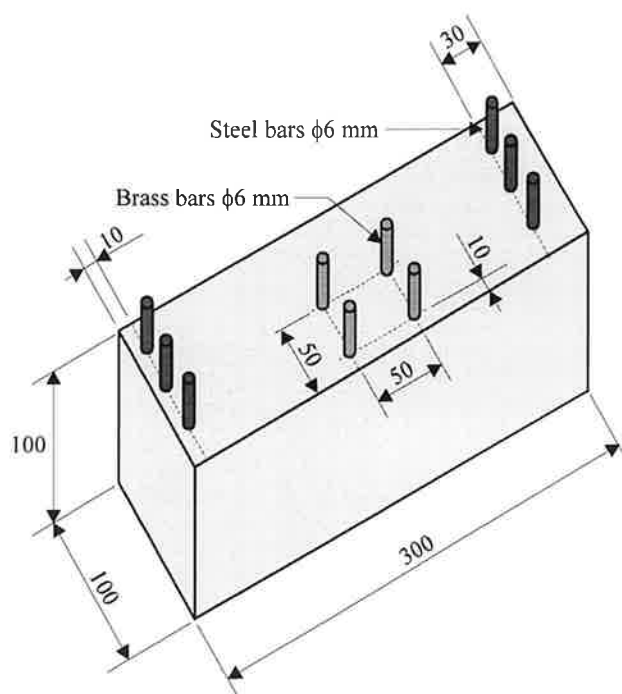
Figure 1 - Schematic representation of the prism specimens (dimensions in mm).

Table 1 - Designation of reinforced concrete specimens.

w/c	Chloride addition	BFSC	OPC
0.45	no	A1, A2, A3, A4	E1, E2, E3, E4
	2%	B1, B2, B3, B4	F1, F2, F3, F4
0.65	no	C1, C2, C3, C4	G1, G2, G3, G4
	2%	D1, D2, D3, D4	H1, H2, H3, H4

2.2 Exposure conditions

During the first years [5-8] the specimens were divided in two groups and exposed to:

- a climate room with 80% R.H. and a temperature of 20°C (specimens designated with numbers 1 and 2);

- a fog room with a temperature of 20°C (specimens designated with numbers 3 and 4).

The exposure started on 1 October 1991, 5 or 8 days after casting [5].

In November 1992, 8 specimens (those designated with number 2) were removed from the 80% R.H. room and were subjected to accelerated carbonation in a cabinet with high CO_2 content (5% by volume) and 50% R.H. at 20°C [6]. The specimens remained in this cabinet from day 406 to day 510, when they were again exposed to the 80% R.H. room. At the end of the carbonation treatment, carbonation depth (measured in cubic specimens) varied between about 10 and 30 mm in the different types of concrete [7]. Table 2 reports the carbonation depths measured after five years [9].

After about 5 years [9] the exposure conditions were changed:

- specimens at 80% R.H. and 20°C were still exposed to 80% R.H. but the temperature was increased to 40°C (on day 1788, autumn 1996); however, measurements were carried out in a laboratory with 20°C and 50% R.H. so that specimens were cooling; indicatively resistivity with two point method was measured when temperature of the specimen was about 38°C, corrosion rate at 30-32°C, potential at 24°C;

- specimens in the fog room were exposed outside, under the action of natural precipitation (wetting and drying), on day 1774 (late 1996); however, for measurements the specimens were moved to a laboratory at 20°C and 80% R.H. for 12 hours.

Also short term tests were carried out in order to evaluate the influence of R.H. and temperature on corrosion rate and resistivity. At a concrete age of about 3 years, relative humidity influence was studied by changing R.H. in four steps from 75% to 95% and waiting until a stable condition was reached (as an average, about 25 days were necessary for each step in order to reach a steady state) [8]. At a concrete age of about 5 years, influence of temperature was studied with dynamic tests during which the specimens at 80% R.H. slowly cooled from 40°C to 20°C [9]. In a limited set of experiments, resistivity and corrosion rate were measured regularly during cooling, giving data from 23 to 37°C.

2.3 Tests

Corrosion rate and corrosion potential of steel, as well as resistivity of concrete, were regularly measured in the different conditions of exposure.

Table 2 - Carbonation depth (mm) measured on concrete cubes after about 5 years [9].

Cement	w/c	Chloride	80% R.H. - 20°C	80% R.H. - 20°C + accelerated carbonation
BFSC	0.45	0%	3	12
BFSC	0.45	2%	1	12
BFSC	0.65	0%	11	27
BFSC	0.65	2%	9	28
OPC	0.45	0%	3	6
OPC	0.45	2%	5	8
OPC	0.65	0%	8	25
OPC	0.65	2%	5	20

Corrosion rate was measured with the linear polarization technique on steel bars both with 10 mm and 30 mm concrete cover. The central of the three bars was used as working electrode (and thus its corrosion rate was measured), while the two external bars were used as counter and reference electrodes respectively. No ohmic drop correction was made. Some measurements were also carried out by using in turn the different bars as working, counter and reference electrode [9], but in this report only measurements of corrosion rate of the central bar (designated 'C') have been considered. Corrosion rate is expressed in μm/year.

Potential of rebars at 10 and 30 mm depth was measured with a Ag/AgCl reference electrode placed in ionic contact to the concrete surface by means of a wet sponge. Three measurements were taken along the length of each bar. In this report only the average value of all the measurements on the rebars at the same depth has been considered. Potential of steel is expressed in mV versus Ag/AgCl reference electrode.

Resistivity of concrete was measured by means of two methods: a two-point method (using the embedded pairs of brass bars) and a 4-point method (Wenner method) applied from the concrete surface. In this report only the 'two-point-resistivity' is considered, since with this method it was possible to measure the resistivity of concrete at two depths, named '10 mm' and '50 mm' respectively, in correspondence of the two pairs of brass bars. In order to evaluate the resistivity from the resistance measured between the brass bars, calibration tests were carried out with solutions of known resistivity [5]. Resistivity of concrete is expressed in $\Omega \cdot m$.

The details of the experimental procedures for each type of measurement can be found in the reports [5-9].

2.4 Results

In appendix A, all the measurements are plotted against time. Every figure refers to a single specimen and shows the time evolution of corrosion rate of rebars with 10 mm cover (CR-10 mm) and with 30 mm cover (CR-30 mm), the average corrosion potential of the rebars at 10 mm (E-10 mm) and at 30 mm (E-30 mm) and the resistivity of concrete measured with the two-point method applied to the brass bars embedded at 10 mm (R-10 mm) and at 50 mm (R-50 mm). A logarithmic scale has been used for corrosion rate and resistivity.

Figs. A.1-A.8 report the results on specimens of series 1, exposed to 80% R.H. During the first 100 days, in all types of concrete a decrease in corrosion rate and an increase in concrete resistivity can be observed. Afterwards, however, corrosion rate tends to reach a constant value. Also resistivity of concrete tends to approach a constant value; however a slight increase with time is evident up to 1800 days.

On day 1788 temperature was increased to 40°C and since then a decrease in resistivity and an increase in corrosion rate in most of the specimens was observed.

Corrosion rate of rebars at 10 mm has a general trend similar to that of bars at 30 mm, although the latter tends to show lower values (in several specimens, however, after 1700 days values at 30 mm are higher than those at 10 mm). Also concrete resistivity is similar at 10 mm and 50 mm depth, although it is slightly lower at 50 mm.

Figs. A.9-A.16 show the results on specimens of series 2, exposed to 80% R.H. and subjected to accelerated carbonation (from day 406 to day 510). In the first days, similarly to specimens of series 1, a progressive decrease in corrosion rate and increase in resistivity of concrete can be observed. Nevertheless, at 400 days, more or less stable values are reached. After the accelerated carbonation treatment an increase in corrosion rate takes place, especially on rebars with 10 mm cover. Some specimens show this increase immediately after the treatment (measurement on day 510), others specimens only in the following measurement (on day 701). Also resistivity of concrete slightly increases owing to carbonation of concrete (although this is not very evident in the figures, owing to the logarithmic scale). A remarkable resistivity increase can be observed in specimen G2 (Fig. A.15) on the measurement with the brass bars at 10 mm. Corrosion potentials (which were measured only after the carbonation treatment) show stable values.

The increase of temperature to 40°C has, in general, a slight influence on corrosion rate, resistivity and corrosion potential.

The measurements carried out on specimens of series 3 and 4, exposed to fog room and then outside, are plotted in Figs. A.17-A.32. Specimens of both series were exposed to the same conditions (act as duplicates) and the results are in good agreement. After an initial transitory of about 100 days, both corrosion rate and resistivity reached a steady value (with a few exceptions). Only slight differences in corrosion rate between rebars with 10 mm cover and rebars with 30 mm cover were observed. No practical differences in resistivity of concrete were observed between measurements with the brass bars at 10 mm depth and those at 50 mm depth.

When the specimens were moved from the fog room to outside, both temperature and relative humidity decreased (values between 1 and 13°C were measured for temperature and R.H. ranged from 65 to 85%), but the specimens were exposed to rain. The weight of cubic specimens decreased with time showing a loss of water; however the weight loss after sixty days ranged between 0.07% and 0.7% [9], and thus during the period studied, only a small fraction of the pore water had evaporated.

Some increase in resistivity and decrease in corrosion rate was observed (it should be noted that measurements were carried out at 20°C in the lab). The more evident effect, however, was on corrosion potential; specimens that had a very negative corrosion potential in the fog room (i.e. below -400 mV Ag/AgCl) showed a remarkable increase towards much more

noble values (see for instance Figs. A.19-A.21). The trend of potential evolution during the exposure outside suggests that a stable condition was not reached even when the last measurement was carried out (60 days after moving the specimens from the fog room).

In the next paragraphs, the results presented in Appendix A will be analysed by considering separately corrosion rate, corrosion potential and resistivity of concrete, in order to asses the influence of concrete composition and exposure conditions. Then, the correlation between these three parameters will be discussed.

3. CORROSION RATE

The average values of corrosion rate in the various conditions of exposure are reported in Figs. 2-5. Fig. 2 refers to specimens exposed to 80% R.H. and 20°C; the average is calculated over the period subsequent to the accelerated carbonation treatment of specimens of series 2. Rebars in concrete without chloride showed very low corrosion rates, lower than 1 µm/year (and often lower than 0.1 µm/year). These are the typical values of passive steel in non carbonated and chloride free concrete [4]. Corrosion rate was also low in the specimens subjected to accelerated carbonation, although slightly higher values were observed in the rebars at 10 mm depth. No significant influence of cement type and w/c ratio was observed.

Corrosion rate in concrete with 2% chloride was higher, often above 1 µm/year. The water cement ratio influenced the corrosion rate; in fact, higher corrosion rates were measured in concrete with w/c 0.65 compared to concrete with 0.45 w/c, particularly for OPC concrete. No substantial differences were observed in specimens subjected to accelerated carbonation with respect to the others.

By increasing the temperature from 20°C to 40°C (Fig. 3), corrosion rate values increased several times both in the presence and in the absence of chlorides. However, values lower than 1 µm/year were still measured in chloride free concrete (the actual temperature during measurement of corrosion rate was about 30-32°C).

Corrosion rate in specimens exposed in the fog room was much higher due to the high moisture content in concrete (Fig. 4).
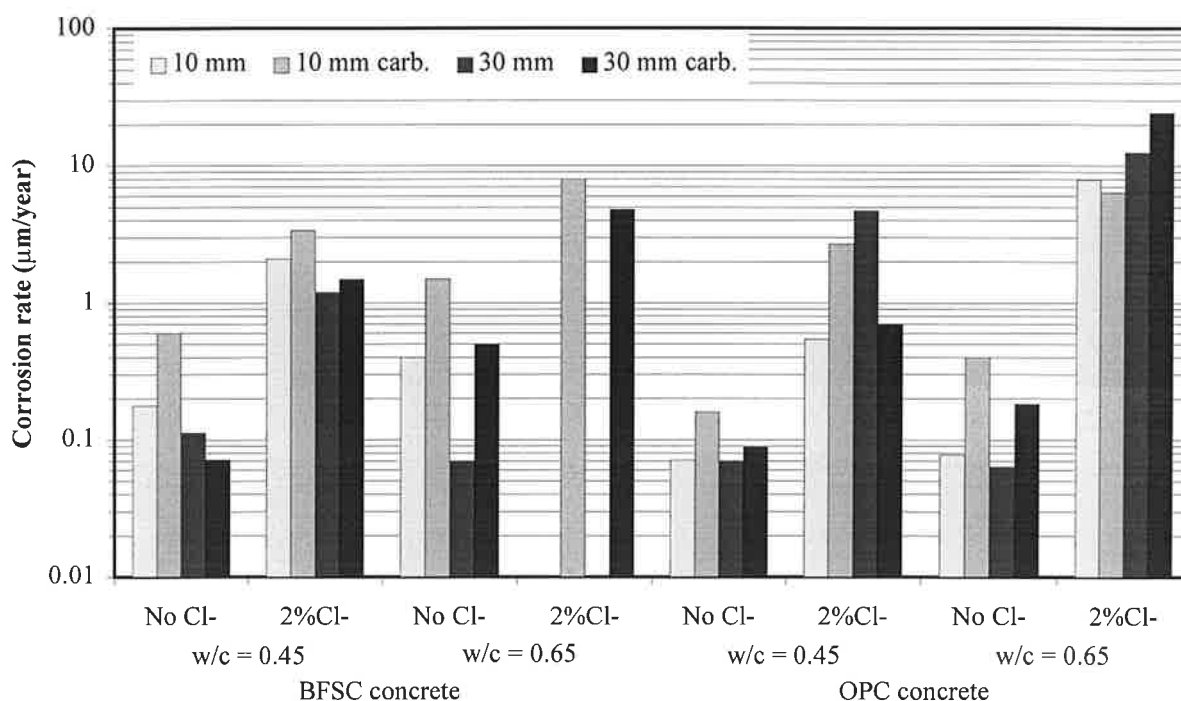
Figure 2 - Corrosion rate in specimens exposed at 80% R.H. and 20°C (average value days 514-1075).

Even in specimens without chloride addition, values up to 20 μm/year were measured (only in concrete with BFSC cement and w/c 0.45, corrosion rate was always lower than 1 μm/year). This was explained with the onset of crevice corrosion under the coating that partially covered the steel bars [8].
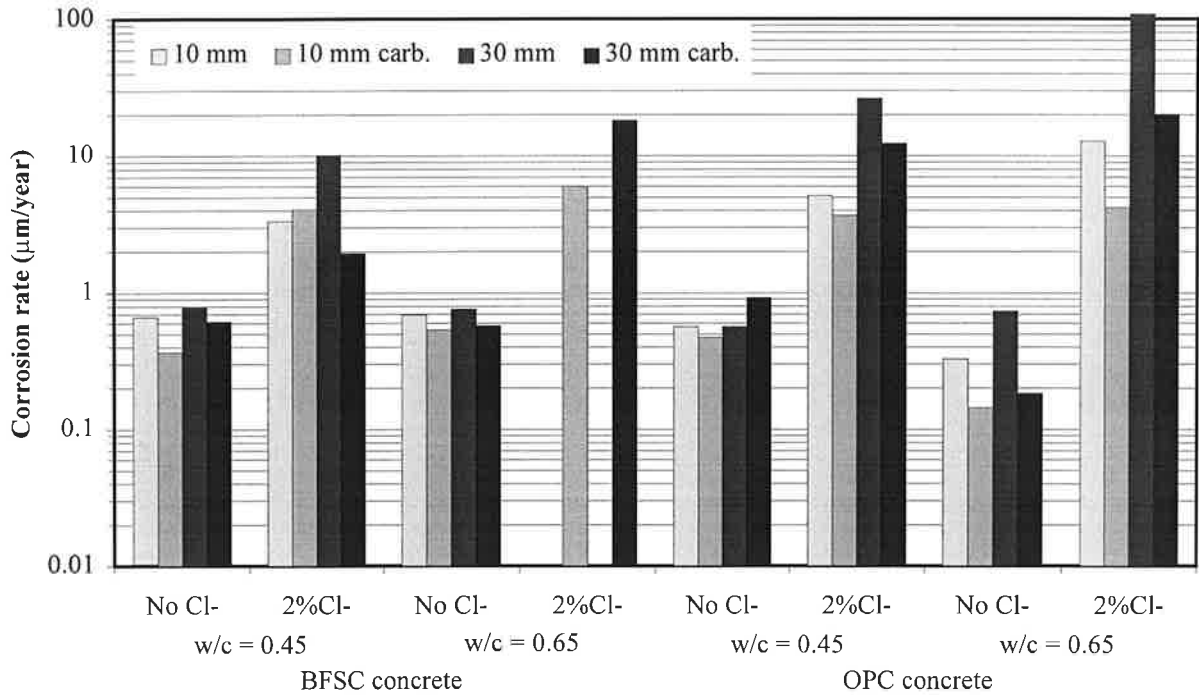
Figure 3 - Corrosion rate in specimens exposed at 80% R.H. and 40°C (average value days 1808-1837). Measurements were carried out when temperature of specimens was about 30-32°C.
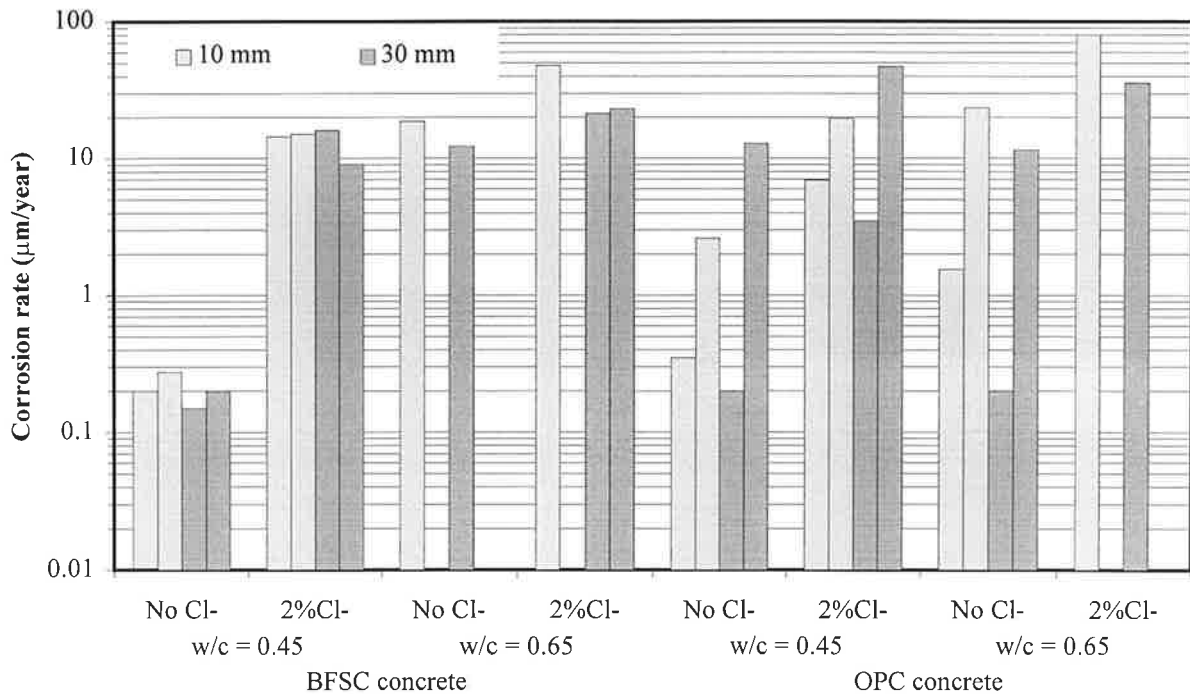
Figure 4 - Corrosion rate in specimens exposed in the fog room at 20°C (average value days 382-1165).
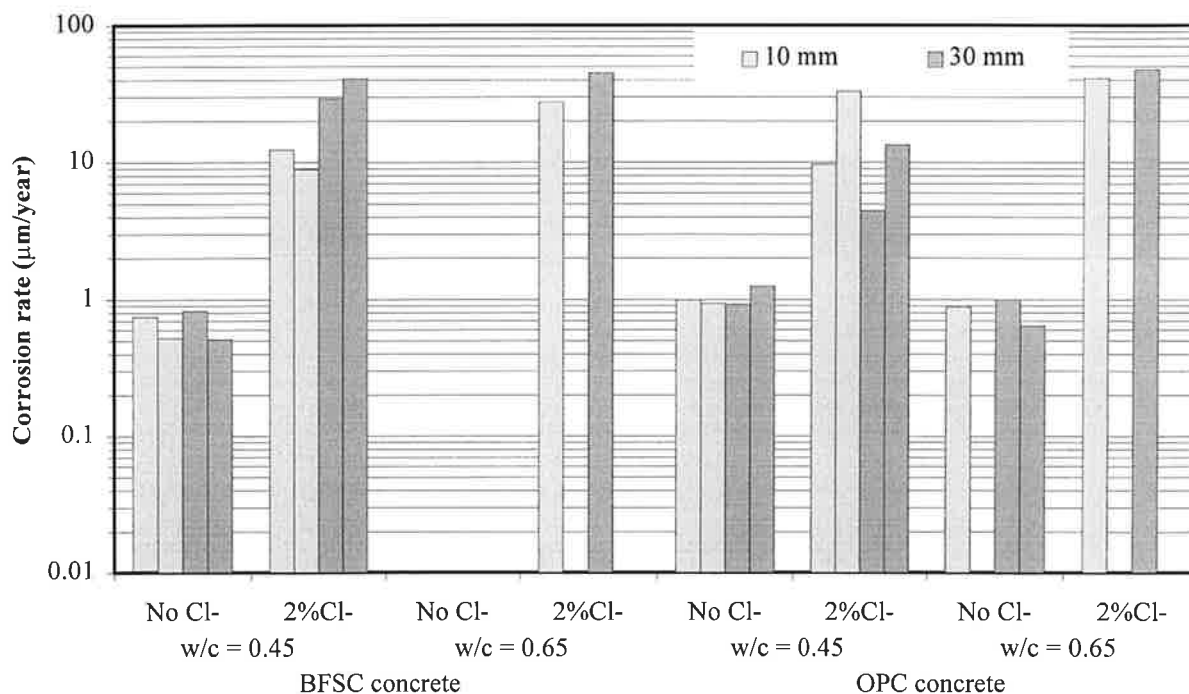
Figure 5 - Corrosion rate in specimens exposed outside after the fog room (average value days 1808-1837). Measurements were carried out after the specimens were left for 12 hours at 20°C and 50% R.H.

Bars in concrete contaminated with 2% chloride had almost always corrosion rates higher than 10 μm/year, regardless of the cement type and the w/c ratio. No significant differences were observed between the rebars at 10 mm and at 30 mm.

When these specimens were exposed outside, the corrosion rate of steel in concrete without chloride always became lower than 1 μm/year (Fig. 5) in accordance with passivity of steel which is expected in that condition. Vice versa, no decrease in corrosion rate was observed in steel in contact with chloride contaminated concrete. This suggests that the slight decrease in moisture content of concrete with 2% chloride, during the sixty days after the removal from the fog room, was not influential on the corrosion conditions.

The previous figures show that the major parameters that influenced corrosion rate of steel during the tests here discussed were: presence of chloride or carbonation, moisture content, and temperature. Only a small influence of carbonation was observed, but this point will be discussed in paragraph 6.

3.1 *Chloride contamination or carbonation*

In chloride free and non carbonated concrete, steel is passive and its corrosion rate should be negligible (usually lower than 1 μm/year [4,10]) regardless of the conditions of exposure. Indeed, results obtained at 80% R.H. and in the outside exposure show these very low corrosion rates[1].

---

[1] The high values of corrosion rate measured in the specimens without chloride exposed in the fog room are not in agreement with the expected passive condition. However the same specimens have also very negative corrosion potentials (see paragraph 4) and this was explained with the onset of crevice corrosion in the very wet (and thus low resistive) concrete. This was confirmed by destructive analysis of a few specimens [8].

Higher corrosion rates were always measured in concretes that contained chloride ions, in all exposure conditions. It is well known that chloride ions can destroy the passive film and then induce pitting corrosion on the steel [10-12]. For instance, at 80% R.H. and 20°C corrosion rate increased from values of the order of 0.1 μm/year in concretes without chloride to values between 1 and 10 μm/year in concrete with 2% chloride. In concrete exposed to the fog room, the corrosion rate reached values up to 70 μm/year (OPC, w/c 0.65, 2%Cl⁻).

Depassivation of steel can occur also owing to carbonation of concrete. The effect of carbonation can be observed only on specimens maintained at 80% R.H. (since carbonation is not expected in the wet concrete exposed in the fog room). The higher corrosion rates measured in some specimens on rebars at 10 mm depth with respect to those at 30 mm depth are probably a consequence of carbonation (according to carbonation depth measurements in the cubic specimens, Table 2). However in the environment at 80% R.H. corrosion rate was low even in this case (below the threshold of 1 μm/year, usually assumed to distinguish corroding from non corroding steel).

3.2 Moisture content

The amount of water in the concrete pores has a remarkable influence on corrosion rate. This is clearly evident by comparing Figs. 2 and 4 concerning respectively 80% R.H. and fog room conditions (both at 20°C).

The only reason for the much higher corrosion rates measured in specimens in the fog room (when the same type of concrete is considered) can be the moisture content. For concretes always maintained in the fog room it is reasonable to assume that most of the pores are filled by water, whereas in concretes at 80% R.H. only a fraction of them is filled.

The content of condensed water in concrete can be related to the relative humidity of the environment. In fact, by increasing the R.H. also the moisture content of concrete will increase as well as the fraction of pores filled by water [11]. Nevertheless, this equilibrium can be reached only slowly and a long time may be necessary before a steady state is achieved, especially during drying [11]. This can be observed by comparing corrosion rate in the fog room (Fig. 4) and in the subsequent exposure outside (Fig. 5).

Even 60 days after the removal from the fog room and the exposure outside, corrosion rates were still similar to those previously measured in the fog room, especially for specimens with chloride. This is probably a consequence both of the hygroscopic properties of these ions, that slow down the drying of concrete, and of the mechanism of pitting corrosion induced by chlorides that produces very aggressive conditions inside pits [12].

The influence of relative humidity on corrosion rate was studied by S.Fiore [8] for R.H. values ranging from 75% to 95%. Figs. 6 and 7 show the corrosion rates measured in steady conditions on specimens of series 1 and 2 (only rebars with 10 mm cover are considered).

Corrosion rate increased with increasing R.H. both in corroding specimens (i.e. with chloride or carbonated) and in passive specimens. Figs. 6 and 7 show a linear relationship when the relative humidity of the environment varies from 75% to 95%. Corrosion rate of rebars with 10 mm cover was higher in specimens subjected to carbonation, but the same ranking with regard to concrete composition was observed.
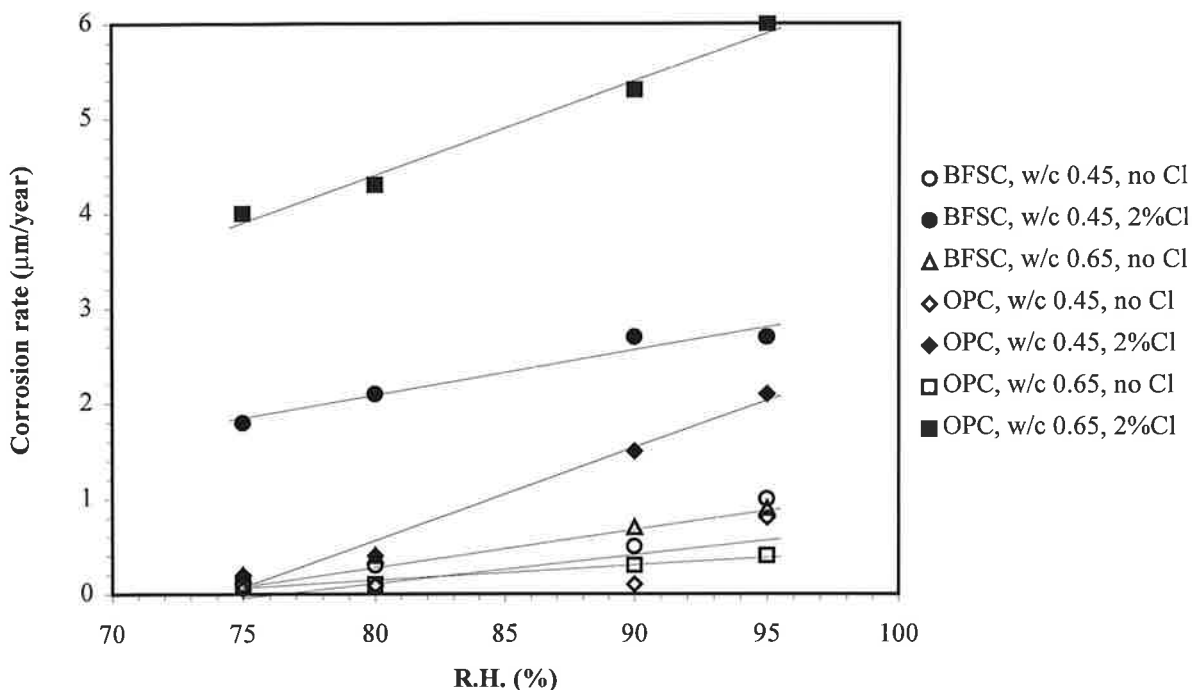
Figure 6 - Corrosion rate of rebars at a depth of 10 mm, during tests at different relative humidity (measurements carried out after a stable condition was reached).
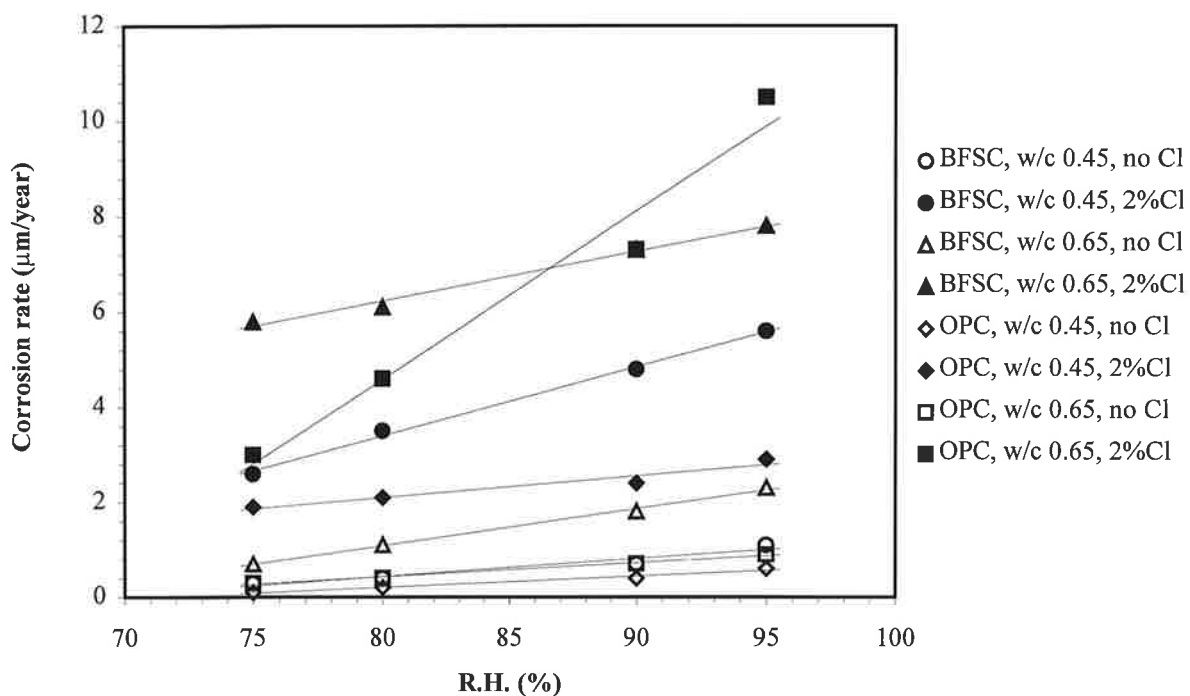
Figure 7 - Corrosion rate of rebars at a depth of 10 mm in specimens previously subjected to accelerated carbonation, during tests at different relative humidity (measurements carried out after a stable condition was reached).

3.3 *Temperature*

The corrosion process is influenced by temperature [13,14]. Tests in 80% R.H. environments showed that the raise in temperature from 20°C to 40°C increased the corrosion rate, both in chloride free and in chloride contaminated concrete.

The ratio of corrosion rate of specimens in the cabinet at 80% R.H. and 40°C to that of the same specimens in the room at 80% R.H. and 20°C is shown in Fig. 8 (calculated from data in Figs. 2 and 3). It should be reminded that corrosion rate of specimens exposed at 40°C was measured when the actual temperature of the specimen was about 30-32°C [9].

The higher increases in corrosion rate were observed on rebars in specimens not subjected to accelerated carbonation, with only a few exceptions (such as OPC concrete with w/c 0.45). For bars at 30 mm depth, corrosion rate increased up to one order of magnitude. Significant, although lower, increase was observed also in rebars with a concrete cover of 10 mm.

In most of the specimens subjected to accelerated carbonation, bars with 10 mm concrete cover did not show any appreciable increase in corrosion rate (the ratio was about 1) even in the presence of chlorides. The increase in corrosion rate was higher in bars at 30 mm and was more than an order of magnitude for bars in OPC concrete with w/c 0.45. In general it seems that the lower corrosion rates are 'activated' by the temperature increase; already active corrosion is less influenced.

The influence of temperature was also studied with dynamic tests, by measuring the corrosion rate when cooling the specimens from 40°C to 20°C. Fig. 9 shows the results on concretes with BFSC cement.
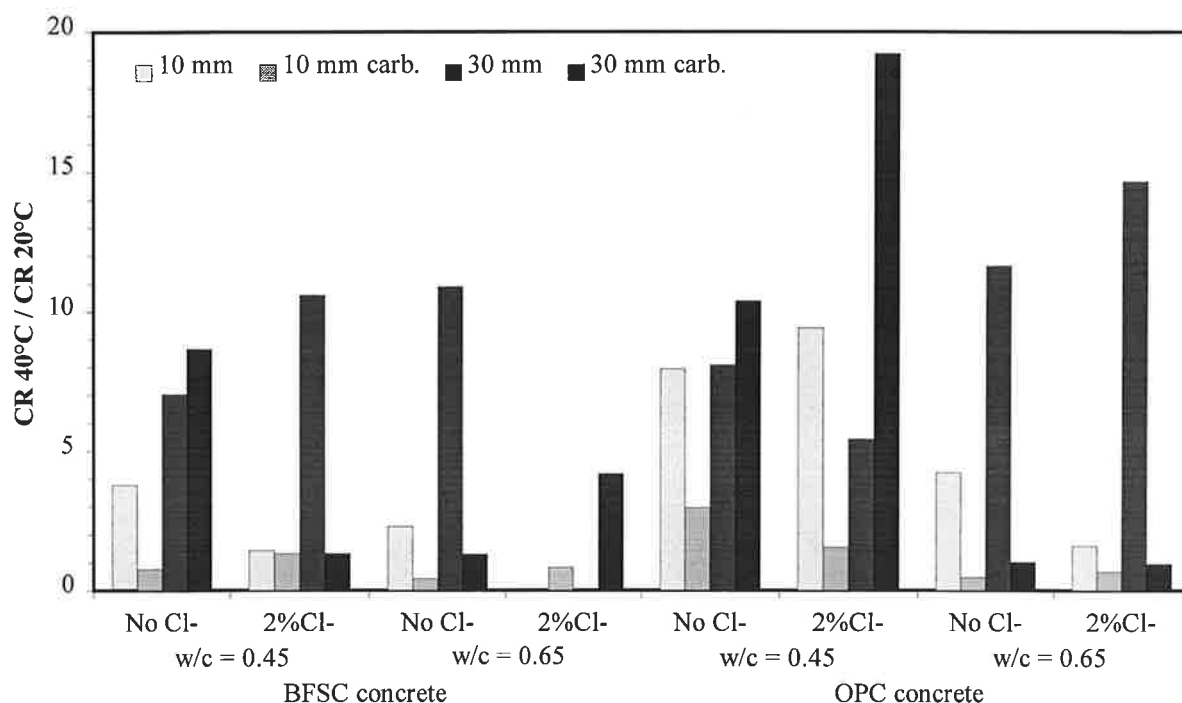
Figure 8 - Ratio of corrosion rate of specimens exposed at 80% R.H. and 40°C to corrosion rate of the same specimens at 80% R.H. and 20°C. Measurements of specimens exposed to 40°C were carried out at temperature of about 30-32°C, while they were cooling.
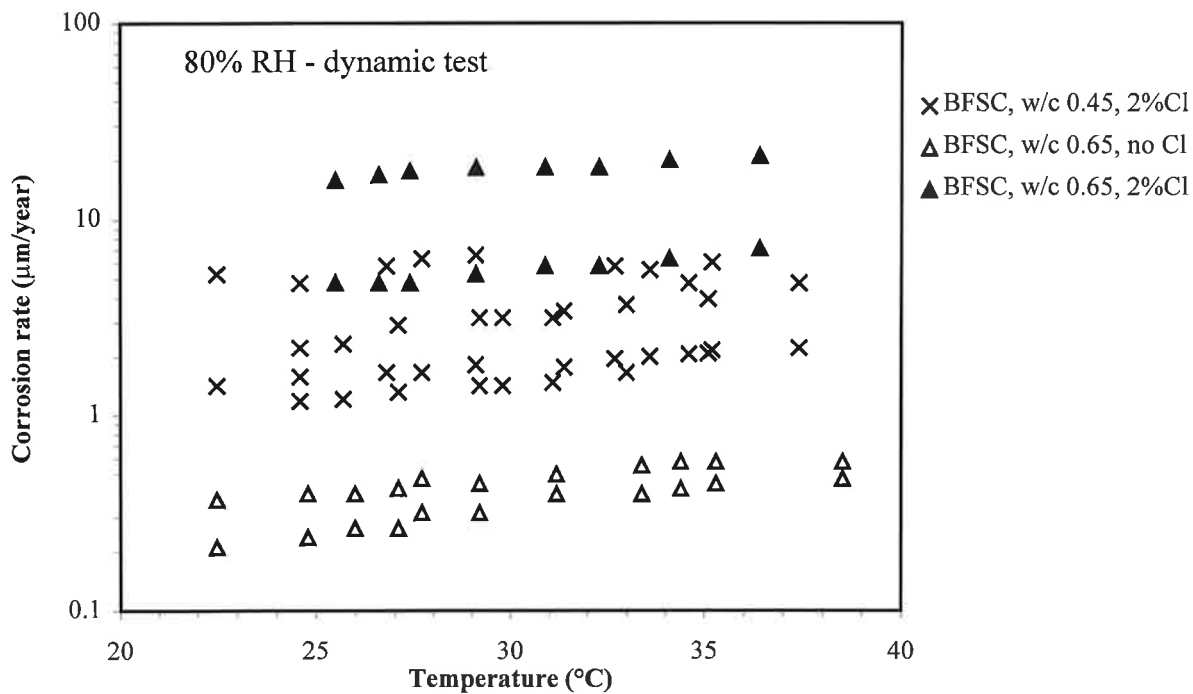
Figure 9 - Corrosion rate of bars at a depth of 10 mm in specimens with BFSC concrete, during dynamic cooling tests from 40°C to 20°C.
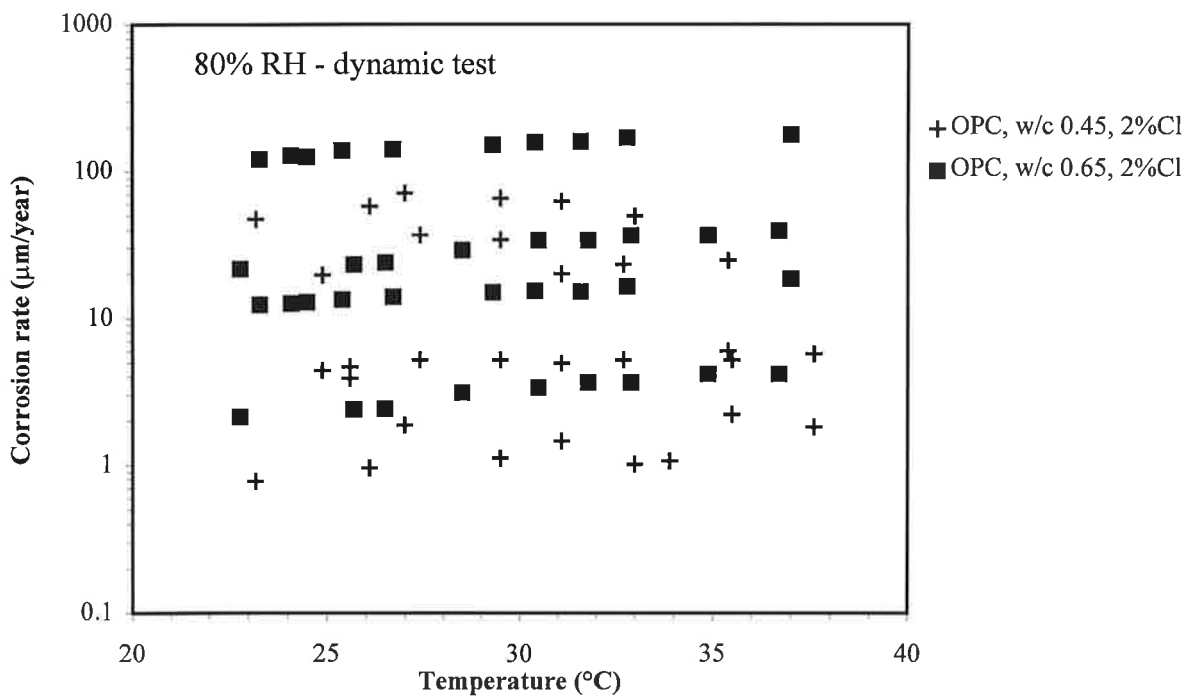
Figure 10 - Corrosion rate of bars at a depth of 10 mm in specimens with OPC concrete, during dynamic cooling tests from 40°C to 20°C.

A significant scatter of results is evident since all the specimens with the same type of concrete (both with and without accelerated carbonation treatment) have been plotted with the same marker. However, the behaviour of the single specimens can be clearly observed: corrosion rate decreased from 40°C to 20°C with a linear trend in semilogarithmic scale, i.e. an exponential relationship between corrosion rate and temperature is suggested. Furthermore, the slope of the curves seems to be roughly the same in all the specimens, being only slightly influenced by the initial value of the corrosion rate. Values calculated on the fitting lines of each specimens range from 0.023 to 0.055 (the lowest values were obtained in the specimens with the highest corrosion rate). These results suggest that the corrosion rate can double for an increase of temperature between 13°C (slope 0.055) and 30°C (slope 0.023).

A similar figure was obtained with steel in OPC concrete with 2% Cl⁻ (Fig. 10): the slope of the curves varied between 0.029 and 0.054.

4. CORROSION POTENTIAL

Corrosion potential is correlated to the corrosion conditions of rebars in concrete (potential mapping is often used for inspection of corroding structures). In general, strongly negative values of potential are associated with corrosion of steel and more positive potential values are typical of passive steel [4]. However this is not always the case. Low potential values can be found even when steel is passive, when concrete is wet and there is lack of oxygen in the pore solution [15]. Conversely, active steel in carbonated concrete can have high potential values (similar to those of passive steel) if the environment is dry (in this case corrosion rate is usually low) [4,16].

Corrosion potential of specimens at 80% R.H. and 20°C (Fig. 11) seems not to depend on cement type, but strongly depends on chloride content. All rebars in chloride free concrete have positive potential values (between -50 and +150 mV vs Ag/AgCl), even with 10 mm cover in the specimens subjected to accelerated carbonation (this does not necessarily mean that steel is still passive, since in this dry environment also active steel in carbonated concrete could have high potential values).

Rebars in concretes with 2% Cl⁻ have much lower potential values (usually between -200 and -400 mV vs Ag/AgCl, with the exception of some measurements in OPC concrete with w/c 0.45). These low potential values are a consequence of corrosion occurring at the steel surface (in fact, corrosion rate was higher than 1 μm/year, Fig. 3); furthermore chloride might also have increased the moisture content of concrete in equilibrium with the environment at 80% R.H. (resistivity is significantly lower in those cases, see further).
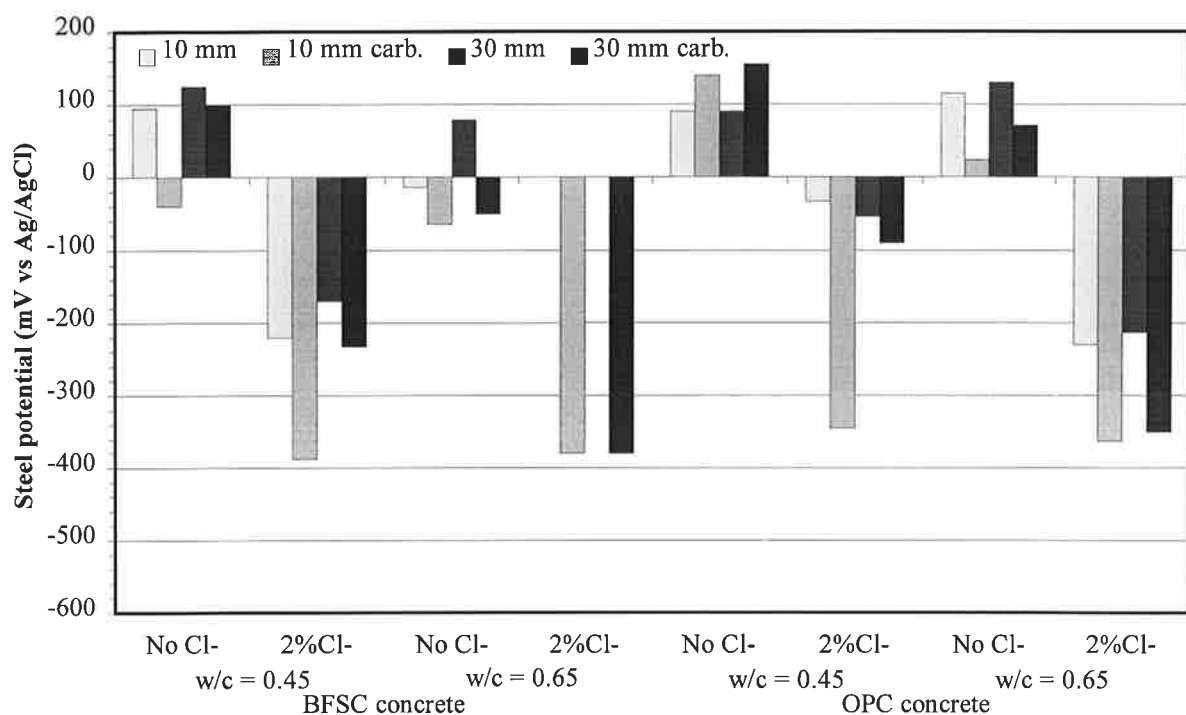
Figure 11 - Steel potential in specimens exposed at 80% R.H. and 20°C (average value days 514-1075).
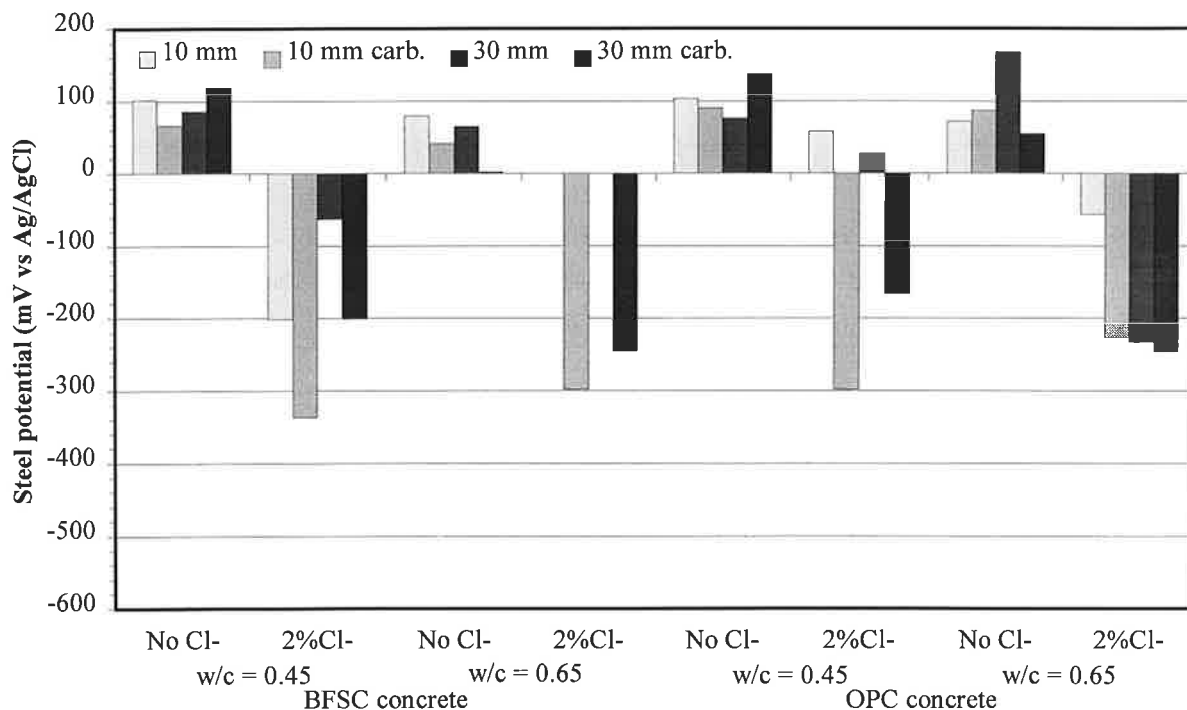
Figure 12 - Steel potential in specimens exposed at 80% R.H. and 40°C (average value days 1808-1837). Measurements were carried out when temperature of specimens was about 24°C.

The increase of temperature from 20°C to 40°C (Fig. 12) did not change significantly the average steel potential although a shift to more positive values can be observed (however, it should be realized that the actual temperature of the specimens when potential was measured was around 24°C, and thus lower than the exposure temperature).

Very negative potentials were measured on specimens exposed in the fog room (Fig. 13). Rebars in chloride contaminated concrete had potentials between -400 and -600 mV Ag/AgCl, the more negative values for the highest water to cement ratio (0.65). Potential was rather negative also for steel in chloride free concrete with w/c 0.65, while relatively positive potentials (higher than -100 mV) were measured in concrete with w/c 0.45.

The negative values for steel in concrete without chloride is likely due to lack of oxygen in the wet concrete and also to crevice corrosion onset under the coating (as observed by S. Fiore in some specimens [8]).

When the specimens were exposed outside, potentials increased slowly and reached values similar to those observed in specimens exposed to 80% R.H.: steel in chloride free concrete had potentials higher than 0 mV Ag/AgCl and potential of steel in 2% Cl⁻ concrete was between -400 and -100 mV Ag/AgCl. These changes in potential were not associated with significant changes in corrosion rate (as observed in chapter 3).

Hence, the major parameters influencing the corrosion potential were the moisture content and the presence of chlorides (which can induce pitting corrosion and also can influence the moisture content of concrete, see resistivity results later on).
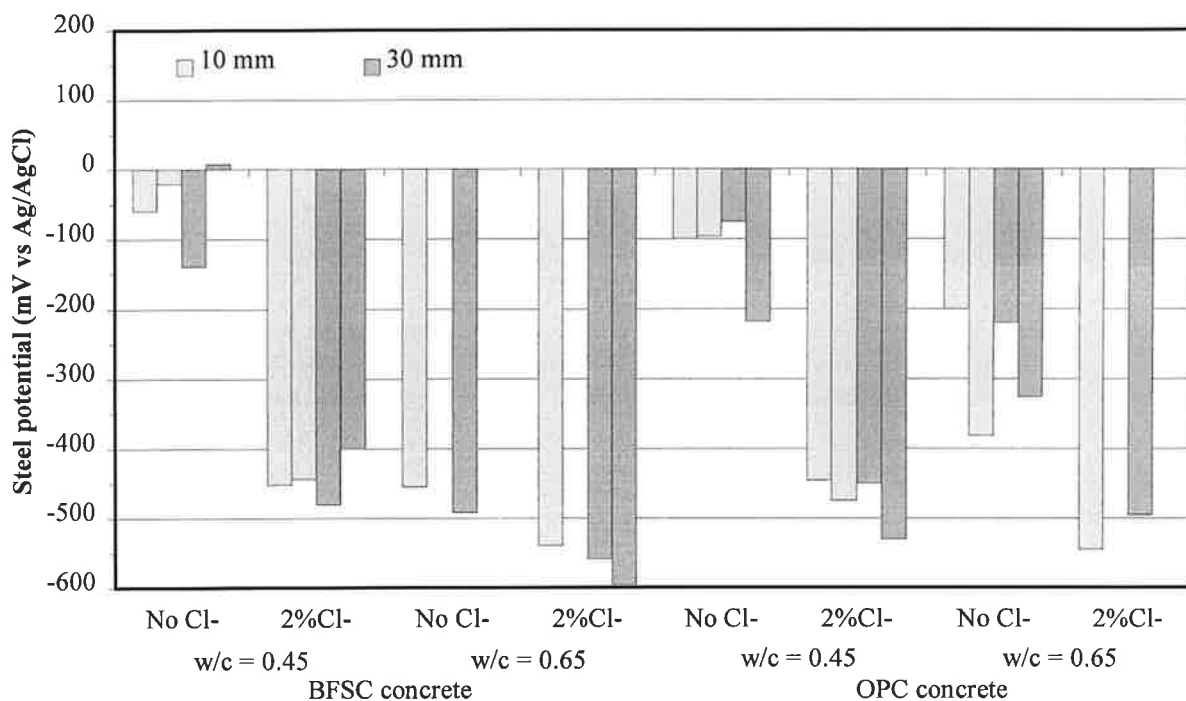
Figure 13 - Steel potential in specimens exposed in the fog room at 20°C (average value days 382-1165).
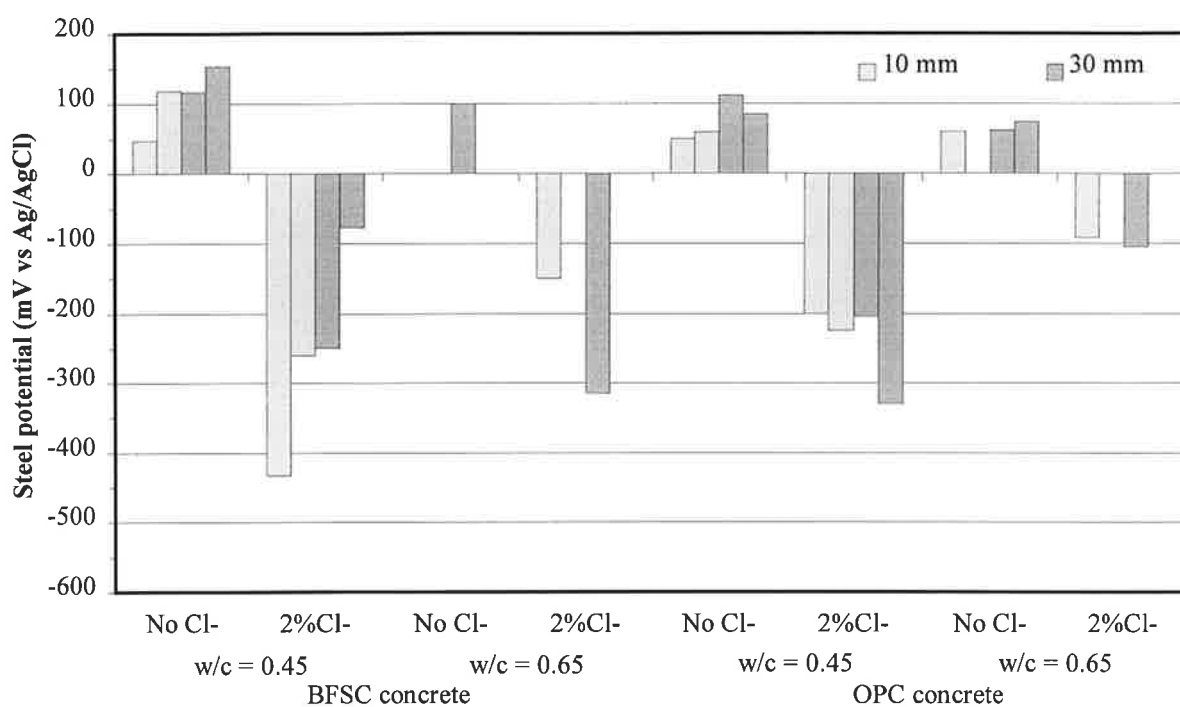
Figure 14 - Steel potential in specimens exposed outside after the fog room (average value days 1808-1837).
Measurements were carried out after the specimens were left for 12 hours at 20°C and 50% R.H.

The effect of relative humidity is reported in Figs. 15 and 16 (tests by S.Fiore [8]). A decrease of about 50-100 mV in steel potential was observed in all types of concrete by increasing the relative humidity from 75% to 95% (in steady conditions).
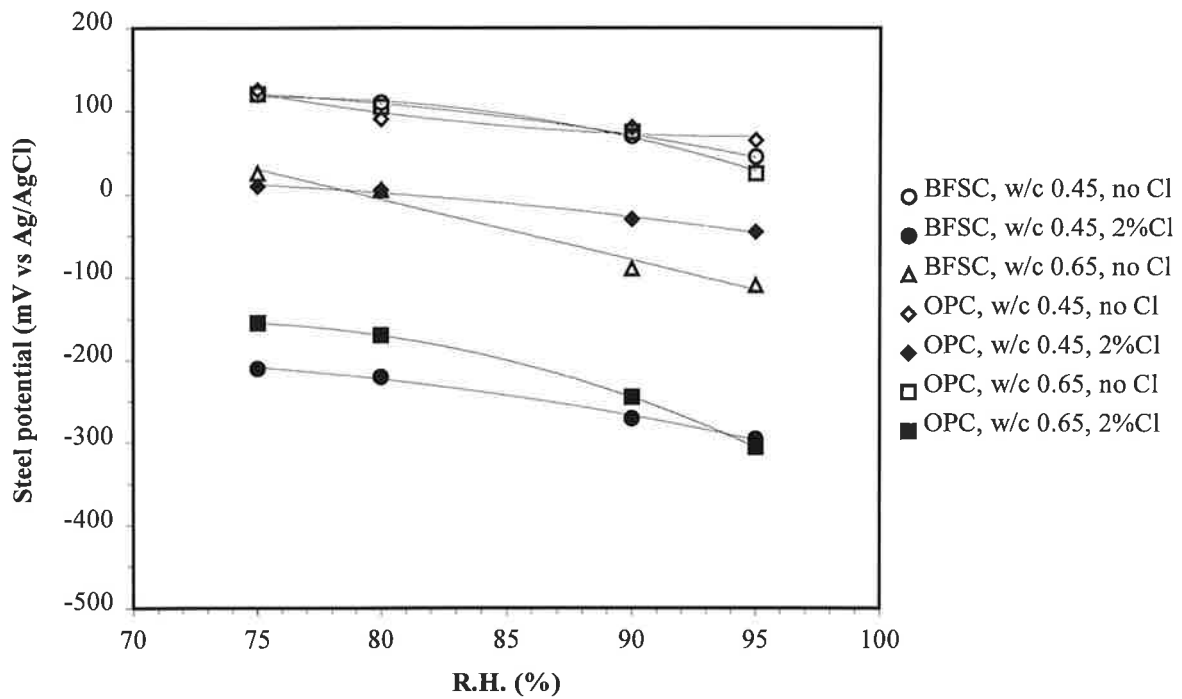
Figure 15 - Steel potential of rebars at a depth of 10 mm, during tests at different relative humidity (measurements carried out after a stable condition was reached).
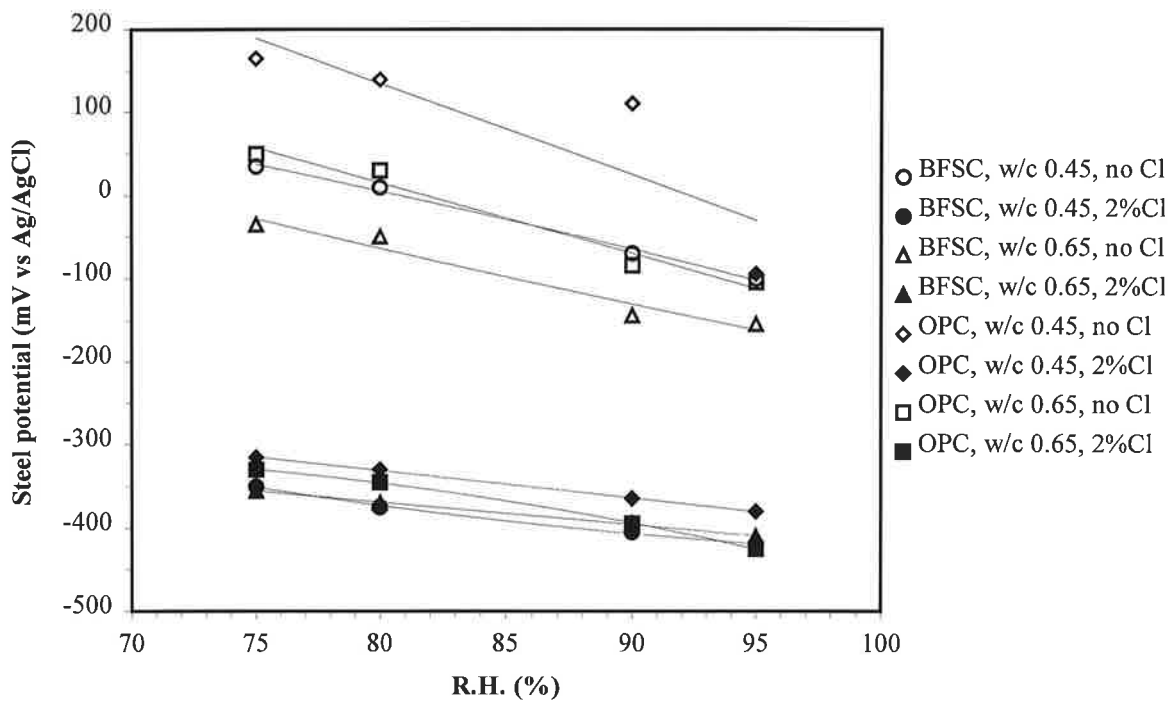
Figure 16 - Steel potential of rebars at a depth of 10 mm in specimens previously subjected to accelerated carbonation, during tests at different R.H. (measurements carried out after a stable condition was reached).

5. CONCRETE RESISTIVITY

The average values of resistivity of concrete during the different exposure periods are shown in Figs. 17-20. Resistivity ranged from 40 to 10000 Ω·m depending on concrete composition and the environment. The higher values were found for: BFSC concrete, the lower w/c ratio (0.45), chloride free concrete and dry environment.

At 80% R.H. and 20°C, resistivity of slag cement concretes varied between 500 and 6000 Ω·m, depending on w/c and chloride content (Fig. 17). Resistivity of OPC concrete showed a dependence on w/c and chloride content similar to BFSC concrete, but the values were about one order of magnitude lower (they ranged from 100 to 800 Ω·m, with only one exception).

Higher resistivity values were measured with the more superficial electrodes (10 mm), especially for specimens subjected to accelerated carbonation. Carbonation depths measured after five years on cubes exposed to the same conditions as the specimens (Table 2) are significantly higher than 10 mm in concretes subjected to accelerated carbonation. Therefore it is reasonable to suppose that resistivity measured with bars at 10 mm depth are representative for carbonated concrete. As far as specimens not subjected to accelerated carbonation treatment are concerned, maybe the measurement are some average of resistivity of carbonated and non carbonated concrete.

When temperature was increased to 40°C, resistivity of concrete decreased slightly in some specimens (Fig. 18).
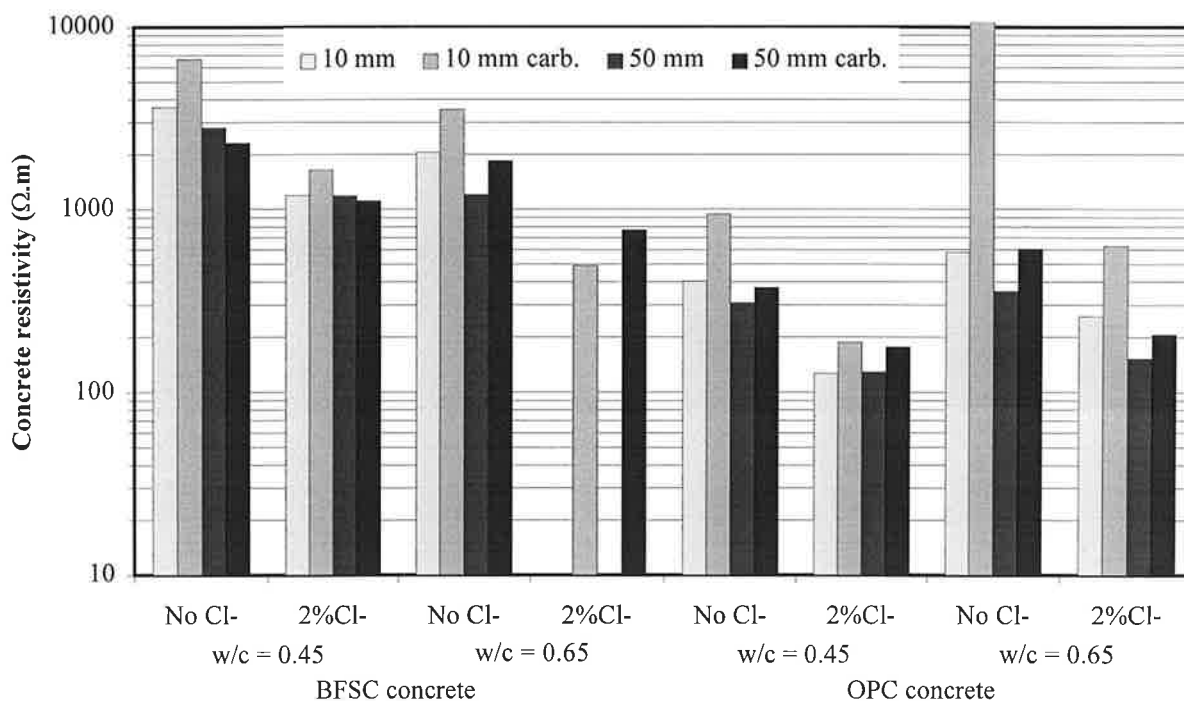
Figure 17 - Concrete resistivity in specimens exposed at 80% R.H. and 20°C (average value days 514-1075).
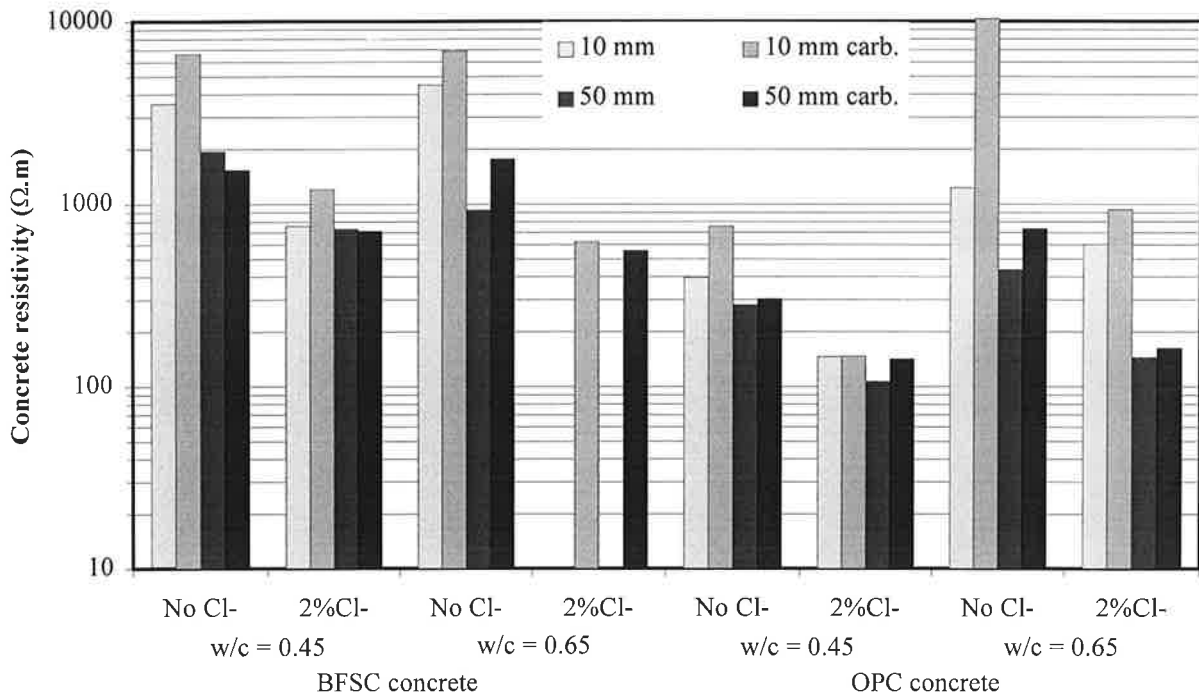
Figure 18 - Concrete resistivity in specimens exposed at 80% R.H. and 40°C (average value days 1808-1837). Measurements were carried out when temperature of specimens was about 38°C.
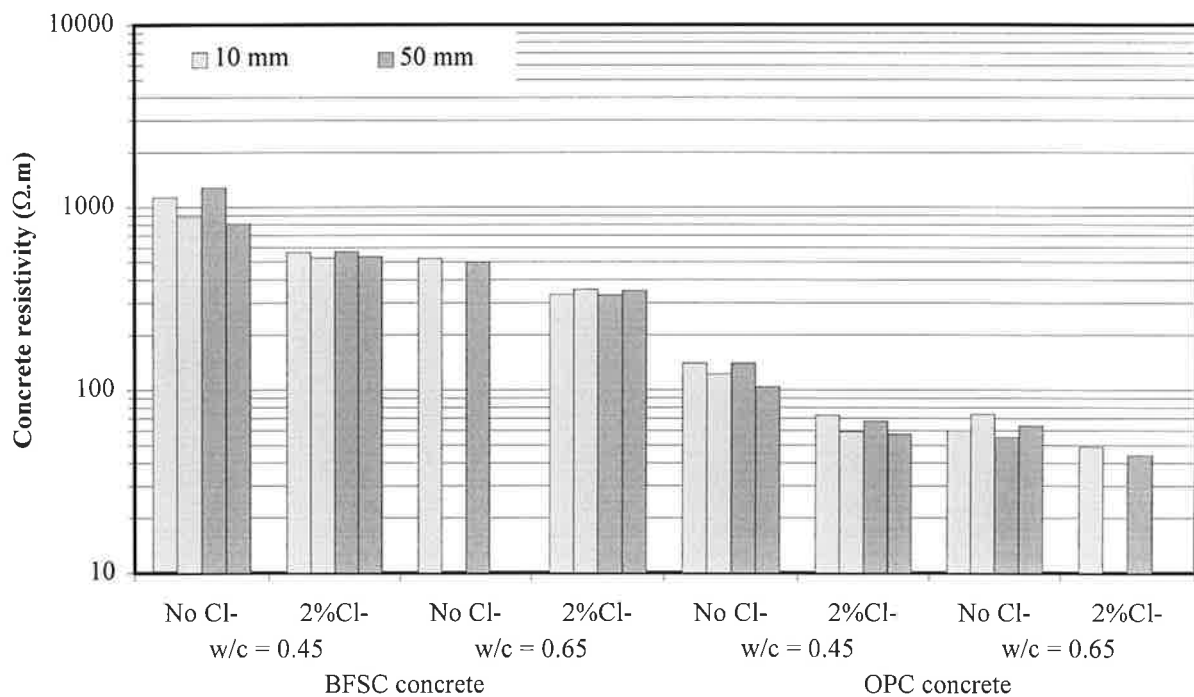
Figure 19 - Concrete resistivity in specimens exposed in the fog room at 20°C (average value days 382-1165).

In the fog room, resistivity of slag cement concrete varied between 300 and 1000 $\Omega \cdot$m (Fig. 19). Similarly to specimens at 80% R.H., resistivity of OPC concretes showed the same dependence on w/c and chloride content as BFSC concretes, but the absolute values were

about one order of magnitude lower (40 to 120 $\Omega\cdot$m). No differences between measurements at 10 mm and at 50 mm were observed (carbonation is not expected in this very wet condition). Changes in resistivity due to exposure of the specimens outside were negligible (Fig. 20), probably because a steady condition was not reached during the sixty days when resistivity was monitored, and/or the resistivity measured in embedded bars is not very sensitive to small moisture changes in the high R.H. range.

A.Mazzoni [7] and S.Fiore [9,17] analysed the results obtained in the first three years from a statistical point of view and showed that the major factors that influence concrete resistivity are: relative humidity, cement type and chloride content.

However, the effects of environment and concrete composition can be evaluated by studying their influence on basic parameters that influence electrical resistivity of concrete [2-4,18-26]:

- the pore solution composition, which depends on: cement type, mineral additions (PFA, BFSC, SF), chloride content, carbonation,

- the structure of hydrated cement paste, which depends on: w/c, curing, type of cement, mineral additions,

- the moisture content, which depends on: R.H., temperature, pore structure, chloride content,

- the temperature.

The effect of these parameters will be discussed with regard to the experimental results (conductivity, i.e. the inverse of resistivity, will be considered).
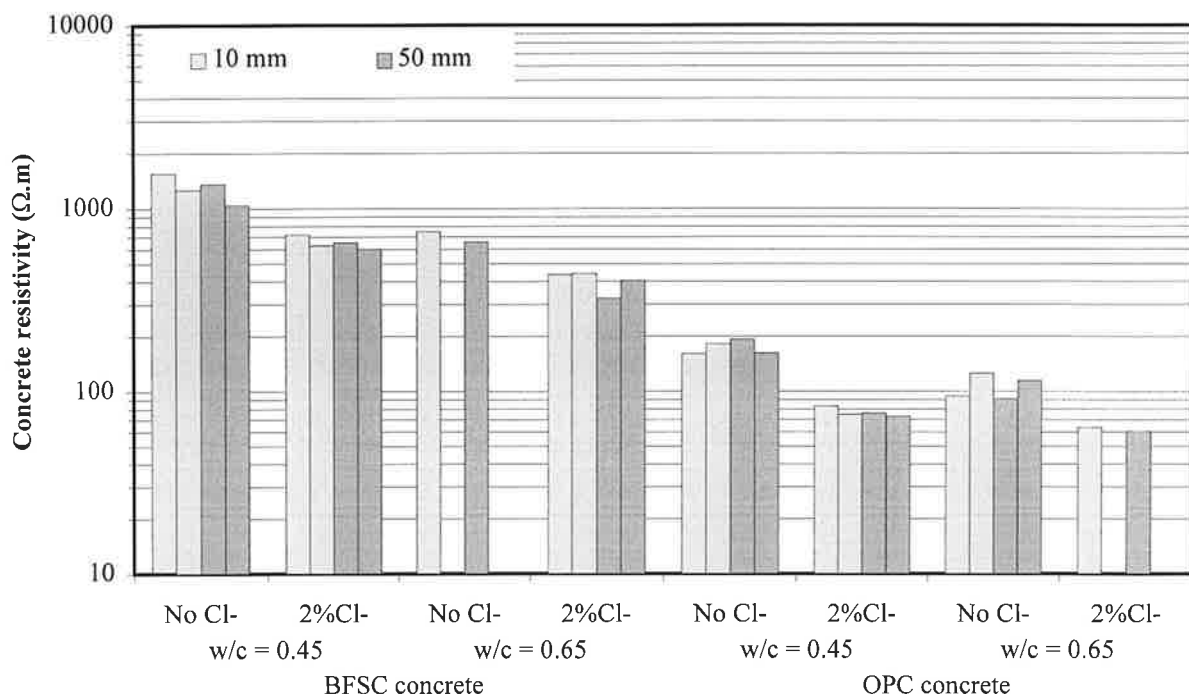
Figure 20 - Concrete resistivity in specimens exposed outside after the fog room (average value days 1808-1837). Measurements were carried out after the specimens were left for 12 hours at 20°C and 50% R.H.

5.1 *Pore solution composition*

Conductivity of concrete depends on the electrical conductivity of the solution contained in the pores of the hardened cement paste. The composition of the pore liquid in the concretes used for tests carried out at TNO is not known. However an estimation can be obtained from literature data.

The chemical composition of the pore solution depends on several factors [27-35]: cement type, w/c ratio, curing, chloride salt contamination, carbonation. In Table 3 the ionic concentrations measured by different researchers in the pore solution of cement pastes, mortars and concretes with mixes similar to those of specimens used at TNO are reported.

In chloride free concrete, ions that are present in higher concentration are hydroxyl (OH^-) and alkalis (Na^+ and K^+). Results from various authors are rather different and, also, ionic concentration in cement pastes are higher than in mortars and concretes. However, the use of BFSC resulted always in a reduction of ionic concentration. We can assume that the pore solution compositions of OPC and BFSC concretes with w/c 0.45 and without chloride are approximately the following:

• BFSC without chloride: 0.1M KOH + 0.1M NaOH,

• OPC without chloride: 0.3M KOH + 0.1M NaOH.

The addition of chloride bearing salts changes the chemical composition of pore solution depending also on the cation associated with the chloride anion, owing to chemical or physical binding of chloride and hydroxyl ions.

Table 3 - Ionic concentration measured in the pore solution extracted from cement pastes, mortars and concrete of OPC and 65-70%BFSC cement (n.a. = concentration not available).

Cement	Cl⁻	w/c	Age (days)	Sample	Source	$[OH^-]$	$[Na^+]$	$[K^+]$	$[Ca^{++}]$	$[Cl^-]$	$[SO_4^=]$
BFSC	no	0.45	28	paste	[28]	290	100	180	5	n.a.	n.a.
BFSC	no	0.5	28	mortar	[31]	107	61	66	<1	10	24
BFSC	no	<0.55	8 years	concrete	[35]	95	89	42	n.a.	5	8
BFSC	no	0.5	84	paste	[32]	355	n.a.	n.a.	n.a.	5	n.a
BFSC	0.4% (NaCl)	0.5	84	paste	[32]	457	n.a.	n.a.	n.a.	28	n.a
BFSC	1% (CaCl₂)	0.5	28	mortar	[31]	93	103	281	<1	89	6
OPC	no	0.45	28	paste	[28]	470	130	380	5	n.a.	n.a
OPC	no	0.5	28	mortar	[31]	391	90	288	<1	3	<0.3
OPC	no	0.5	28	paste	[27]	834	271	629	1	n.a.	31
OPC	no	0.5	192	mortar	[25]	251	38	241	<1	n.a	8
OPC⁽ᵃ⁾	no	0.5	84	paste	[32]	589	n.a.	n.a.	n.a.	2	n.a.
OPC⁽ᵇ⁾	no	0.5	84	paste	[32]	479	n.a.	n.a.	n.a.	3	n.a.
OPC⁽ᵃ⁾	0.4% (NaCl)	0.5	84	paste	[32]	741	n.a.	n.a.	n.a.	84	n.a.
OPC⁽ᵇ⁾	0.4% (NaCl)	0.5	84	paste	[32]	661	n.a.	n.a.	n.a.	42	n.a.
OPC	1% (CaCl₂)	0.5	28	mortar	[31]	62	90	161	<1	104	<0.3
OPC	1% (NaCl)	0.5	35	paste	[27]	836	978	660	1	517	72

[a] low C_3A content (7.7%).   [b] high C_3A content (14.3%).

Table 4 - Ionic conductance at infinite dilution in water at 25°C for ions relevant for pore solution [36].

Ion	H^+	K^+	Na^+	Ca^{++}	OH^-	$SO_4^=$	Cl^-	$CO_3^=$
Specific conductance (S·cm²/equivalent)	349.8	73.5	50.1	59.5	198.6	80	76.35	69.3

Furthermore, addition of sodium chloride results in an increase in OH⁻ concentration (and thus in pH), while addition of calcium chloride decreases the pH [30]. The compositions of the pore solution in concretes where 2% chlorides were added as $CaCl_2$ can be approximated by:

• BFSC with 2% chlorides: 0.05M KOH + 0.05M NaOH + 0.1M NaCl + 0.1M KCl

• OPC with 2% chlorides: 0.1M KOH + 0.05M NaOH + 0.1M NaCl + 0.1M KCl.

The (specific) conductance (measured for instance in $\Omega^{-1}m^{-1}$) of these solutions can be evaluated if the equivalent conductance of the different ions is known. In the literature, the equivalent ionic conductance of the ions present in the pore solution can be found in the condition of infinite dilution and at a temperature of 25°C (Table 4).

As the ionic concentration in the solution increases, the equivalent ionic conductivity changes from the value at infinite dilution. Figure 21 shows the variation of equivalent conductivity of KOH, NaOH, KCl and NaCl solutions as a function of concentration. Figure 22 shows the correspondent variation of specific conductivity.

Over the concentration range considered, changes in equivalent conductivity are not remarkable and, as a first approximation, can be neglected. Therefore the conductivities of the solutions that simulate the pore liquid of concrete have been evaluated using the equivalent ionic conductance at infinite dilution reported in Table 4.
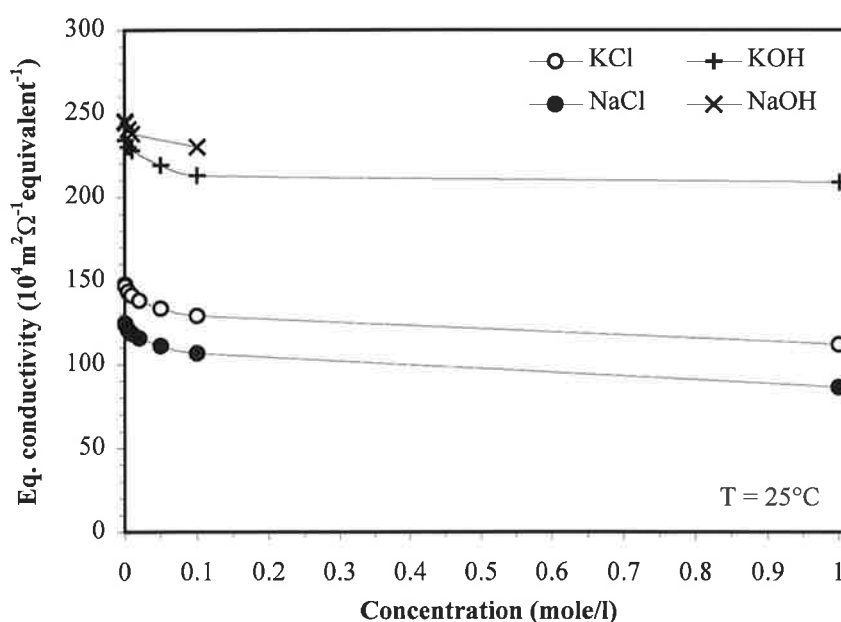
Figure 21 - Equivalent ionic conductivity of some solutions as a function of concentration.
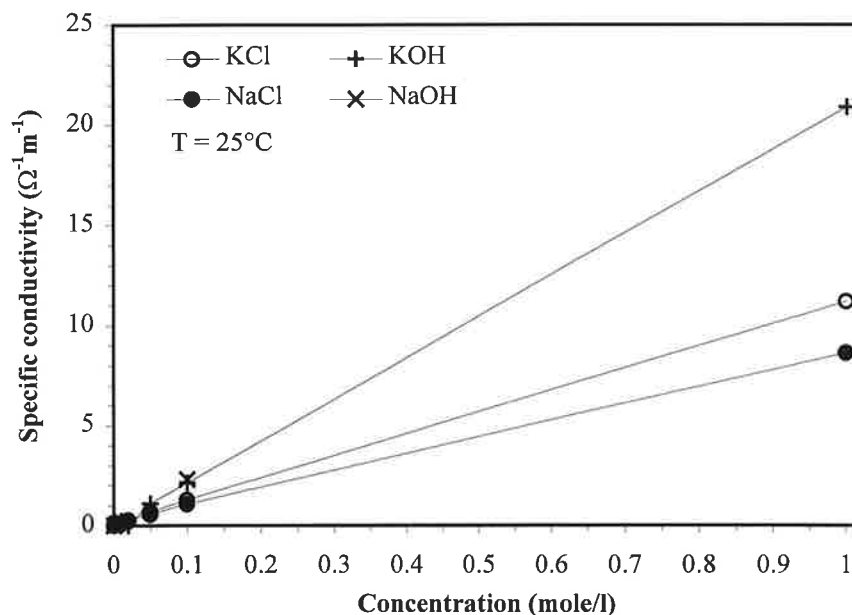
Figure 22 - Specific conductivity of some solutions as a function of concentration, calculated from equivalent conductivity values showed in Fig. 21.

The results are reported in Table 5 and they are compared with the conductivity values measured in the corresponding concretes, in different exposure conditions.

Even results in the fog room, where the moisture content of concrete is very high, show that conductivity of concrete is several orders of magnitude lower than the conductivity of a solution similar to the pore liquid (a small effect can also be attributed to the different temperatures for solution and concretes, as will be discussed below). The ratios between conductivity of pore solution and conductivity of concrete in the fog room is about 5000 for BFSC and about 1000 for OPC. The results on specimens exposed at 80% R.H. show a further decrease.

Table 5 - Comparison of conductivity $(\Omega^{-1} \cdot m^{-1})$ of concretes without chloride and water cement ratio 0.45 in different environments and conductivity calculated for solutions simulating their pore liquid composition.

Concrete Type	OPC, w/c 0.45		70%BFSC, w/c 0.45	
	No Cl⁻	2% Cl⁻	No Cl⁻	2%Cl⁻
Conductivity of simulating solution[1]:	10.7	6.7	5.2	5.4
Conductivity of concrete in:				
- 80% R.H. 20°C [2]	$2.7 \cdot 10^{-3}$	$8.3 \cdot 10^{-3}$	$2.9 \cdot 10^{-4}$	$8.9 \cdot 10^{-4}$
- fog room 20°C [3]	$7.6 \cdot 10^{-3}$	$1.5 \cdot 10^{-2}$	$9.9 \cdot 10^{-4}$	$1.8 \cdot 10^{-3}$

[1] Values calculated using equivalent conductivity at infinite dilution and 25°C.

[2] Average values of measurements at 10 mm on days 514-1075 in specimens not subjected to accelerated carbonation.

[3] Average values of measurements at 10 mm on days 382-1165.

Bürchler et al. [25] showed that the resistivity of pore solutions of OPC pastes and mortars (with w/c ratios between 0.4 and 0.75) ranged between 0.08 and 0.2 $\Omega \cdot m$ (i.e. conductivity varied between 5 and 12.5 $\Omega^{-1} \cdot m^{-1}$); the resistivities of the correspondent cement pastes and mortars were strongly influenced by R.H. and had values with the same order of magnitude of those presented for concrete in Table 5.

Table 5 shows that the addition of chloride ions as $CaCl_2$ does not increase significantly the conductivity of the pore solution (for OPC concrete the conductivity of the simulated pore solution even decreases), while conductivity of concretes with 2% chlorides is higher than that of the same concrete without chloride. This might be a consequence of the hygroscopic properties of this ion or also of changes in the interaction between cement paste and ions in the pore liquid (paragraph 5.2).

The differences found between simulating pore solution and concrete show a remarkable effect of hydrated cement paste microstructure and water content on conductivity.

5.2 Structure of cement paste

Measurements of concrete resistivity started 22 or 25 days after casting; thus, since no data are available during the first days, the influence of hydration of concrete can not be properly evaluated. However the increase of resistivity during the first 100 days of tests (see appendix A) suggests that an important role is played by the progressive hydration of cement paste and the changes in the pore structures (one month after casting, changes in the pore solution composition should be negligible [25] and hence they have no influence on resistivity). The higher resistivity of BFSC concrete is also a consequence of the lower porosity and finer microstructure.

The migration of ionic species through the concrete pore solution is rather different from that in a bulk solution. A first trivial cause is that the movement is restricted to the pore filled by water and thus only a small fraction of the total volume of concrete is available for movement of ions. In a wet concrete of medium quality the volume of pores filled by water can be approximately 10% of the total volume. This can justify a decrease of resistivity of about one order of magnitude with respect to that of a bulk solution. However, Table 4 shows that, even for wet concrete, conductivity is several orders of magnitude lower than for the pore solution.

A further influence of porosity is related to tortuosity of the pore structure of hydrated cement paste. In a bulk solution ions are allowed to move in the same direction as the external electrical field. In concrete this is no longer the case: by following the path available inside the pores, the ions will not always move in the direction of the electrical field but will also deviate from that, increasing the resistance to movement of ions and thus the overall resistivity of concrete (i.e. decrease its conductivity). Also other microstructural properties of cement paste, such as branching, roughness and connectivity of pores, are relevant (it has been suggested that the microstructure of hydrated cement paste can be described with the formalism of fractal geometry [37]).

Moreover the interaction between ions in the pore solution and the constituents of the cement paste (alumino-silicate-hydrate) should be considered. Chemical bonding and physical absorption or simply electrical interaction with the surface of pores can oppose to the movement of ions and therefore increase the resistivity. For instance Bürchler at al. [26] have investigated the dielectric properties of hardened cement paste and have suggested that the

formation of a double layer in the pore solution can influence the movement of ions near the cement paste surface.

5.3 *Moisture content*

Resistivity of concrete is associated with the electrical migration of ions in the aqueous solution contained in the pores of the cement paste. The amount of water available for this movement inside concrete depends on concrete porous structure and environmental conditions (R.H., temperature, wetting). In very low R.H. environments (i.e. <60%) water is only adbsorbed at the hydrated cement paste surface; the flow of ionic current is restricted to very thin layers of adsorbed water and strong interactions with the hydrated cement paste are expected. In environments with higher R.H., water can condense (starting from the small pores where capillary condensation can take place). Condensation increases the amount of pores filled by water, facilitating ionic movement and thus decreasing resistivity (i.e. increasing conductivity), although the resistivity of pore solution itself is expected to decrease owing to dilution [25].

The influence of moisture content on resistivity of concrete can be observed by comparing Figs. 17 and 19. In the fog room, where concrete is very wet, resistivity values 3-10 times lower were measured than in the 80% R.H. environment. S.Fiore [8] studied the relationship between the environment relative humidity and the resistivity of concrete, by exposing the specimens to environments at 20°C and R.H. increasing from 75% to 95% (measurements were carried out after a steady state was reached). The results of these tests, shown in Fig. 23, suggest a small increase in conductivity for the different types of concrete as the humidity of the environment increases in that range (a linear relationship was found). This variation is small compared to the differences in conductivity between the different types of concrete.
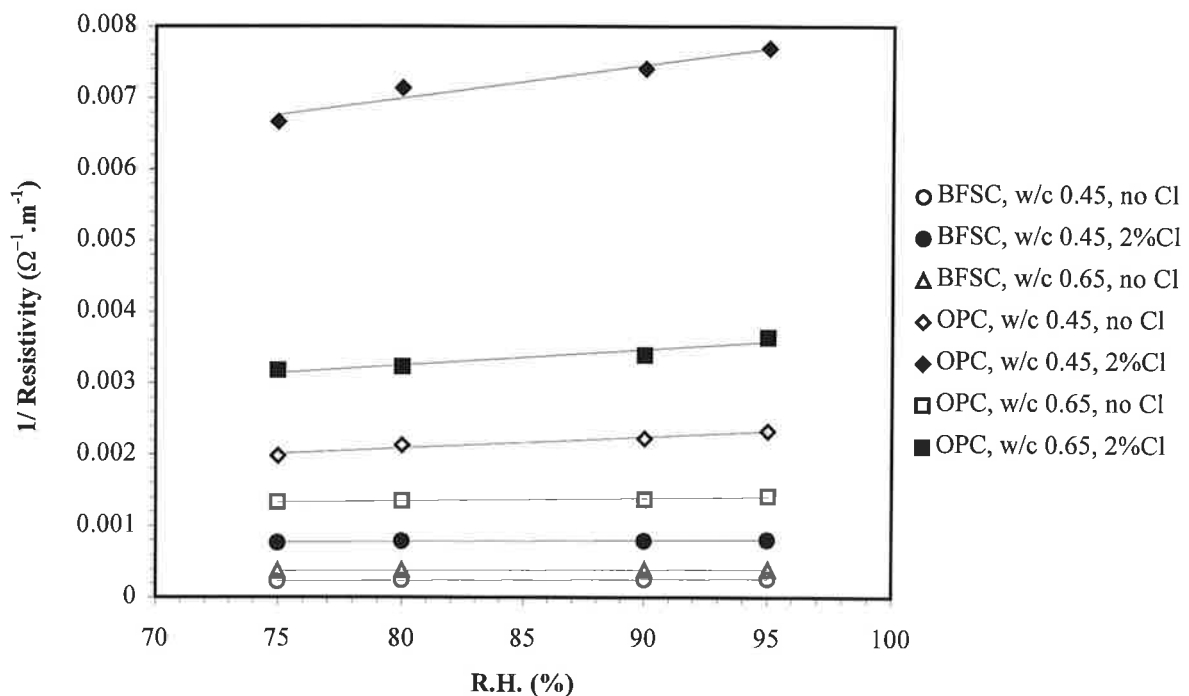
Fig. 23 - Conductivity of concrete (measured with bars at 10 mm depth and in steady state condition) as a function of relative humidity of the environment.
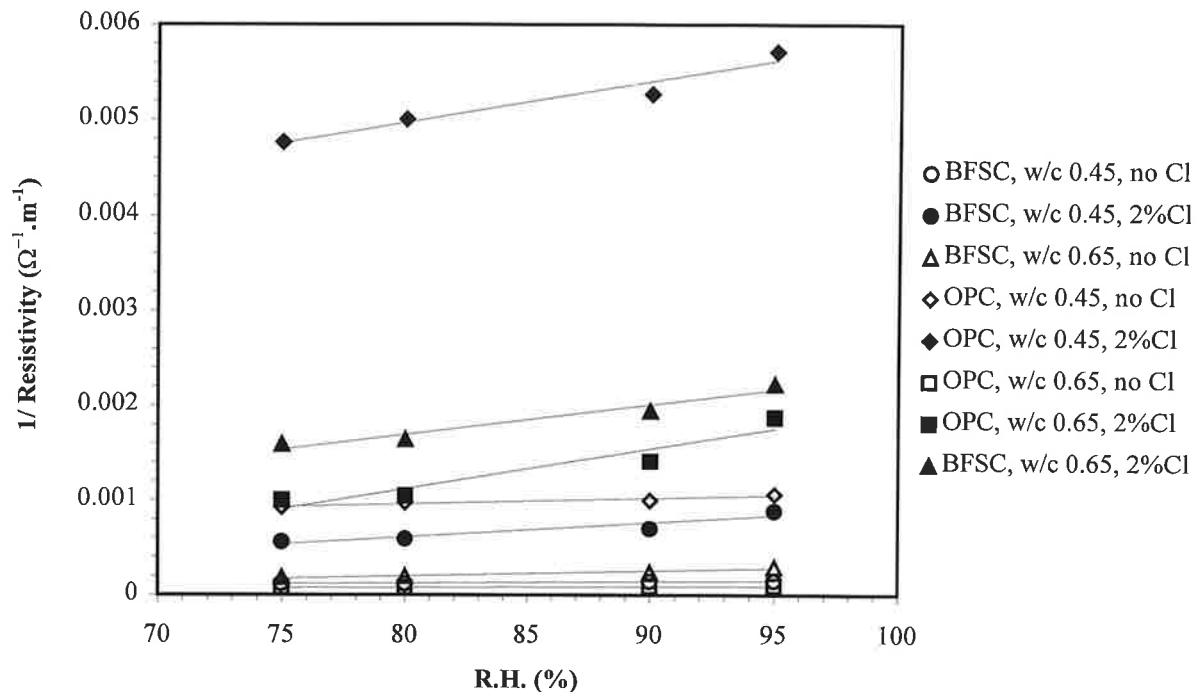
Fig. 24 - Conductivity of concrete in specimens subjected to accelerated carbonation (measured with bars at 10 mm depth and in steady state condition), as a function of relative humidity of the environment.

However, the values that can be extrapolated from these data to 100% R.H. are significantly lower than those that have been measured in the fog room (see for instance Table 5). This suggests that some pores are filled in the fog room (and remain so), which dry out in 80% R.H. and do not become refilled (up to 95%). Moreover, a very high resistivity increase would be expected if R.H. was further decreased, as shown in references [22,25,26] (this has been explained with the loss of continuity between the pores filled by water). Thus, the linear trend shown in Fig. 23 is likely to be true only in the range of temperature considered during the tests and significant deviations are expected both below and above this range.

Figure 24 shows that a behaviour similar to that in Fig. 23 was found also on specimens subjected to accelerated carbonation (results at a depth of 10 mm are shown), although owing to carbonation of concrete, lower values of conductivity were measured (according to the lower ionic concentration on pore solution [33]).

5.4 Temperature

Tests carried out by M.Scotto [9] showed the influence of temperature on the resistivity of concrete. For specimens exposed outside, resistivity of concrete was measured for about 60 days following natural variations of temperature. For specimens in the 80% R.H. room, the resistivity was measured while the temperature was decreasing from 40°C to 20°C.

Figures 25 and 26 show the relationships between concrete conductivity and temperature obtained during outside exposure in the specimens with BFSC and OPC concrete respectively. In each figure the same marker has been used for the two specimens with the same concrete composition and for measurements at 10 mm and 50 mm depth. A certain scatter of results is evident (due also to differences in the two specimens); however these data suggest an exponential relationship between conductivity and temperature.
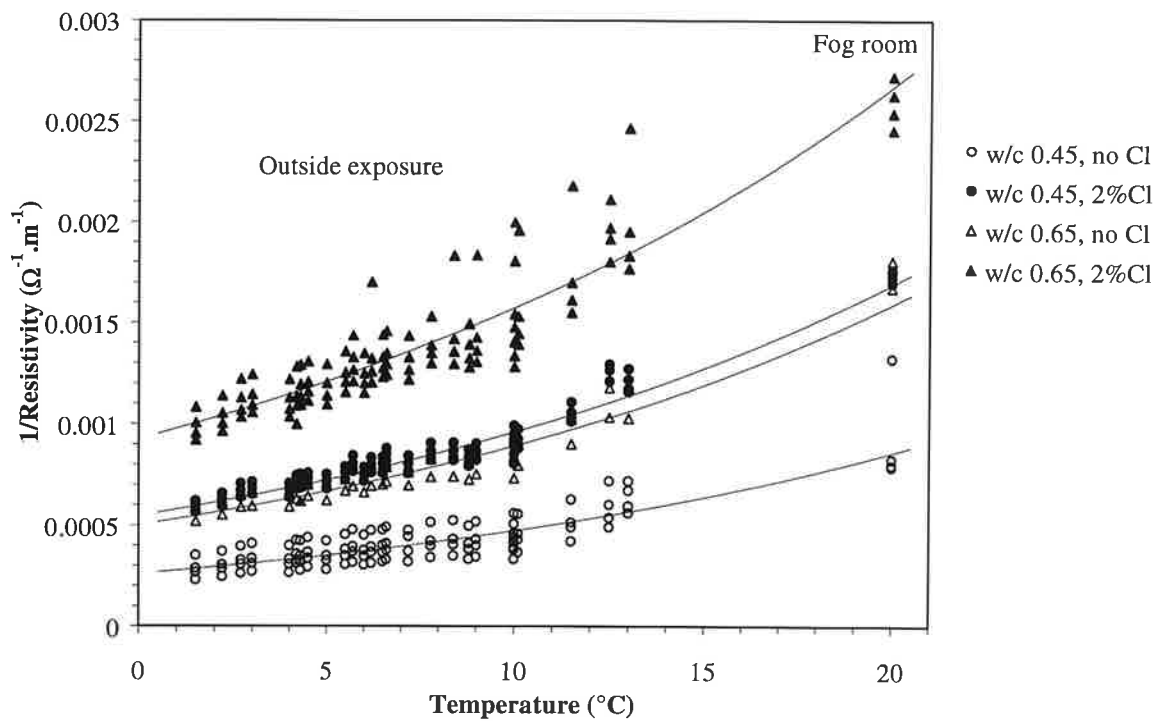
Figure 25 - Relationship between concrete conductivity and temperature in specimens with BFSC concrete exposed outside after three years in the fog room (measurements with electrodes at 10 mm depth).
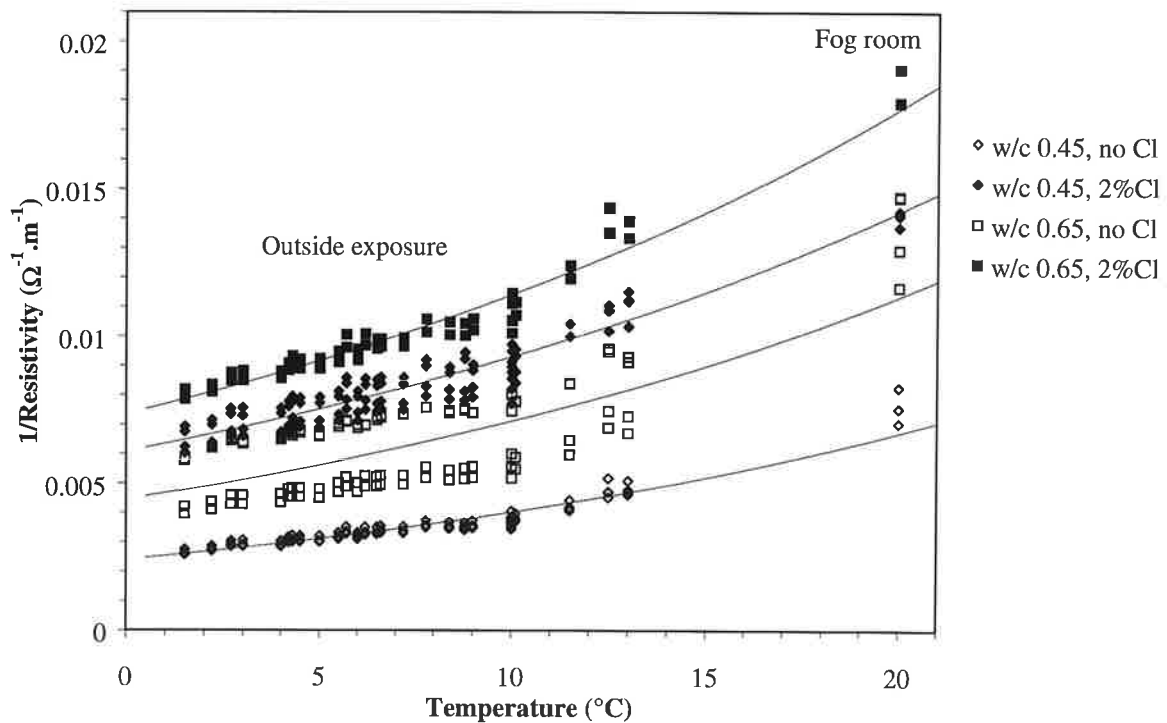
Figure 26 - Relationship between concrete conductivity and temperature in specimens with OPC concrete exposed outside after three years in the fog room (measurements with electrodes at 10 mm depth).

Measurements carried out during outside exposure with temperature ranging from 2 to 15°C are in good agreement with previous measurements in the fog room at 20°C. This results shows that a high humidity content was still in the concrete after about 60 days of outside exposure.

Figure 27 shows the results obtained during dynamic tests in which the specimens were slowly cooled from 40°C to 20°C. Also in this case the experimental data can be interpolated with exponential relationships.

Figure 28 compares results of specimens exposed outside and in the fog room with results of specimens exposed to 80% R.H. Conductivity is plotted on a logarithmic scale so that the supposed exponential relationships can be represented as linear trends.

The two series of data have different interpolating straight lines, even for the same type of concrete, the specimens exposed at 80% R.H. showing always lower values of conductivity. Nevertheless the slope of the linear trend seems to be the same in the different concretes and exposure conditions. Table 6 reports the parameters of the exponential interpolation:

$$\text{Conductivity} = A \cdot e^{B \cdot \text{Temperature}}$$

and shows that the coefficient B (i.e. the slope of the straight line in the semilogarithmic plot) ranges from 0.03 to 0.06; the lower values were measured in the dynamic tests at 80% R.H. These values are very similar to the ones calculated for the corrosion rate (paragraph 3.3). They suggest that the resistivity of concrete can double for every increase in temperature of 12 to 23°C (the former value is calculated for B=0.06, the latter for B=0.03).
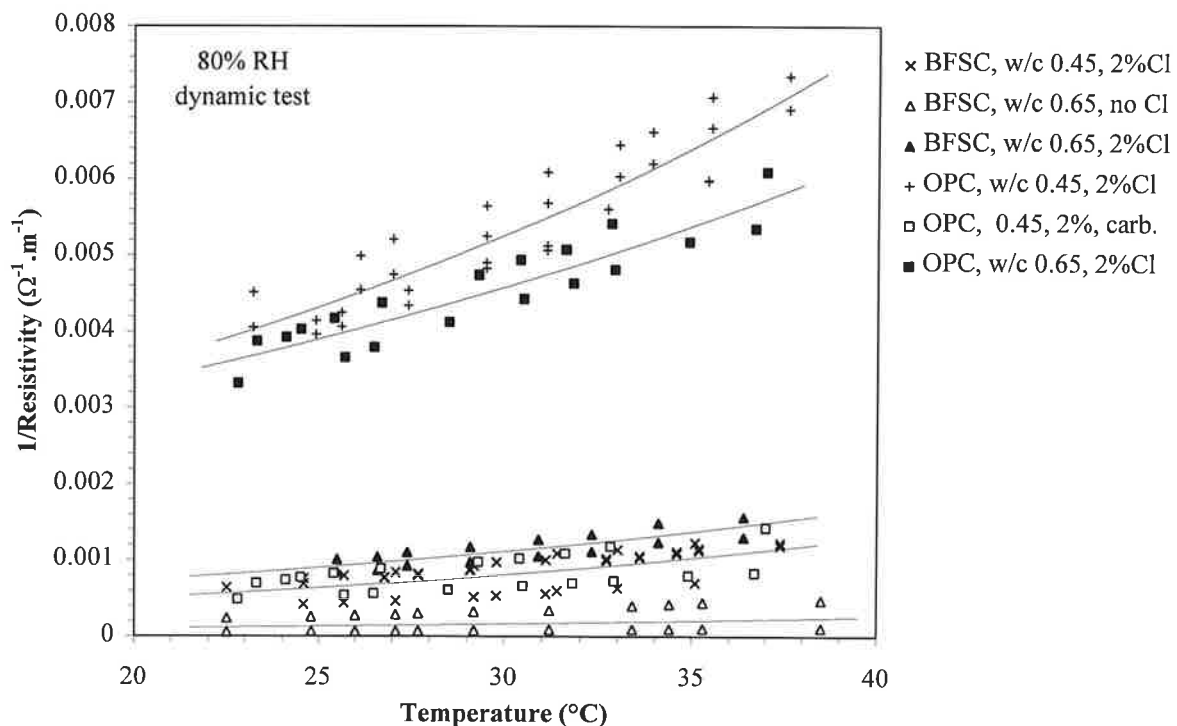
Figure 27 - Relationship between concrete conductivity and temperature in specimens exposed at 80% R.H. environment (measurements with electrodes at 10 mm depth).
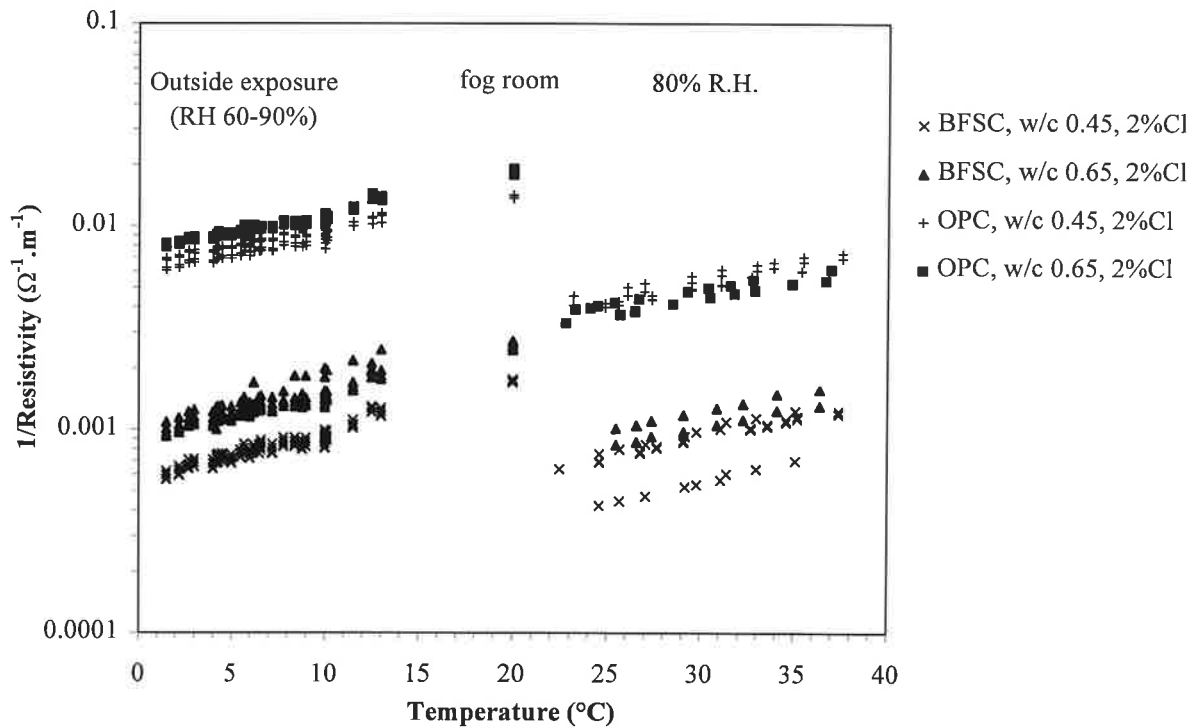
Figure 28 - Comparison of relationships between concrete conductivity and temperature found in specimens exposed outside and specimens in the 80% R.H. room (measurements with electrodes at 10 mm depth).

Table 6 - Interpolation of experimental data on concrete conductivity against temperature reported in Figs. 25-28 with an exponential relationship: Conductivity = $A \cdot e^{B \cdot Temperature}$.

Cement	w/c	Chloride	Outside exposure (T = 1-13°C)			Dynamic tests (T=20-40°C)		
			A	B	R^2	A	B	R^2
BFSC	0.45	0%	0.00026	0.0597	0.69			
BFSC	0.45	2%	0.00055	0.0565	0.93	0.0002	0.0479	0.44
BFSC	0.65	0%	0.00050	0.0578	0.91	0.00006	0.0319	0.37
BFSC	0.65	2%	0.00093	0.0529	0.82	0.0003	0.042	0.72
OPC	0.45	0%	0.0024	0.0513	0.93			
OPC	0.45	2%	0.0061	0.0425	0.86	0.0016	0.0393	0.86
OPC	0.65	0%	0.0045	0.0468	0.52			
OPC	0.65	2%	0.0074	0.0439	0.94	0.0017	0.0322	0.84

In order to investigate the variation in concrete conductivity with temperature, the influence of temperature on pore solution conductivity and composition and on the water content in the pores has been considered.

To evaluate the effect of temperature on the conductivity of pore solution, literature data have been reviewed. Usually an empirical formula is used for evaluating the variation of equivalent ionic conductivity (λ°_T, at infinite dilution) against temperature [38]:

$$\lambda^{\circ}_T = \lambda^{\circ}_{T^{\circ}}[1 + \alpha(T\text{-}T^{\circ}) + \beta(T\text{-}T^{\circ})^2 + ...]$$

where: $T^{\circ} = 25°C$.
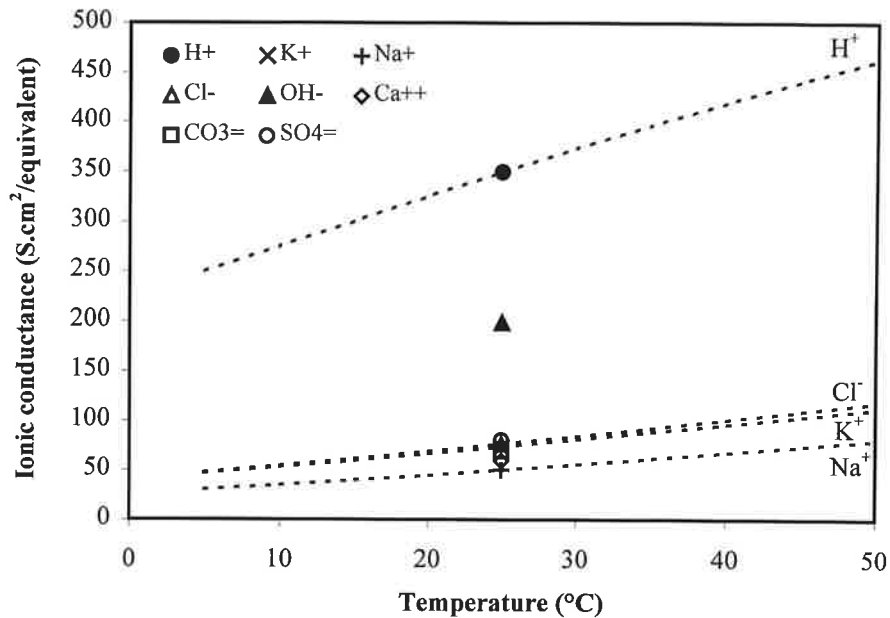
Figure 29 - Effect of temperature on the equivalent conductance of different ions [36].

In [36] a relationship up to the third power of temperature is proposed and the coefficients are given for H^+, Na^+, K^+ and Cl^- ions (in solutions). Figure 29 shows these relations. Despite the polynomial relation proposed, the data suggest in practice a linear trend, while resistivity shows a hyperbolic trend (Fig. 30). Unfortunately, no data are available concerning the hydroxyl ion (which has a high mobility and is very important in determining the conductivity of pore solution in alkaline concrete). Furthermore, the effect of temperature on the conductivity of a real solution can be different from the one predicted from the equivalent ionic conductivity at infinite dilution.
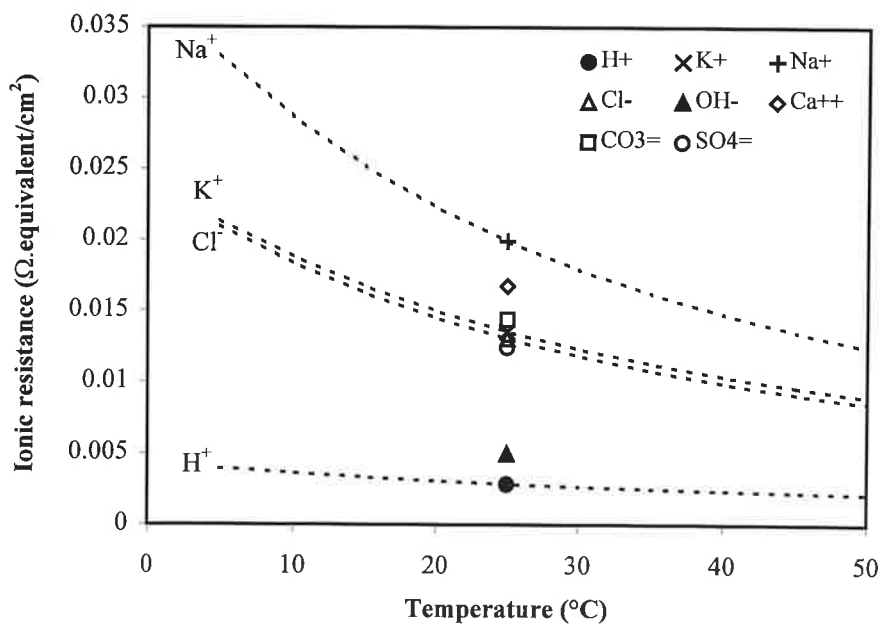
Figure 30 - Effect of temperature on the equivalent resistivity of different ions [36].
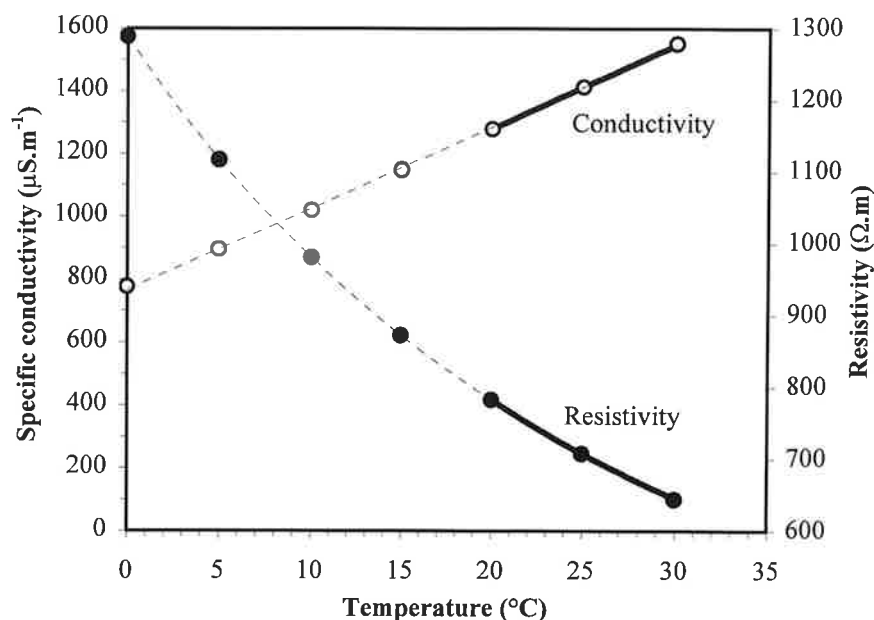
Figure 31 - Specific conductivity and resistivity of 0.01M KCl solution as a function of temperature (the dark lines refer to data from [37] and the markers to data from [39]).

Data in Fig. 29 concern equivalent conductivity at infinite dilution and thus do not take into account interactions between ions. In real solutions therefore a different correlation could apply. Figure 31 shows, as an example, data on the variation of specific conductivity and resistivity of a 0.01M KCl solution [39]. Also results shown in Fig. 31, suggest that conductivity of bulk solutions, in practice, is linearly correlated with temperature, although a small deviation can be observed.
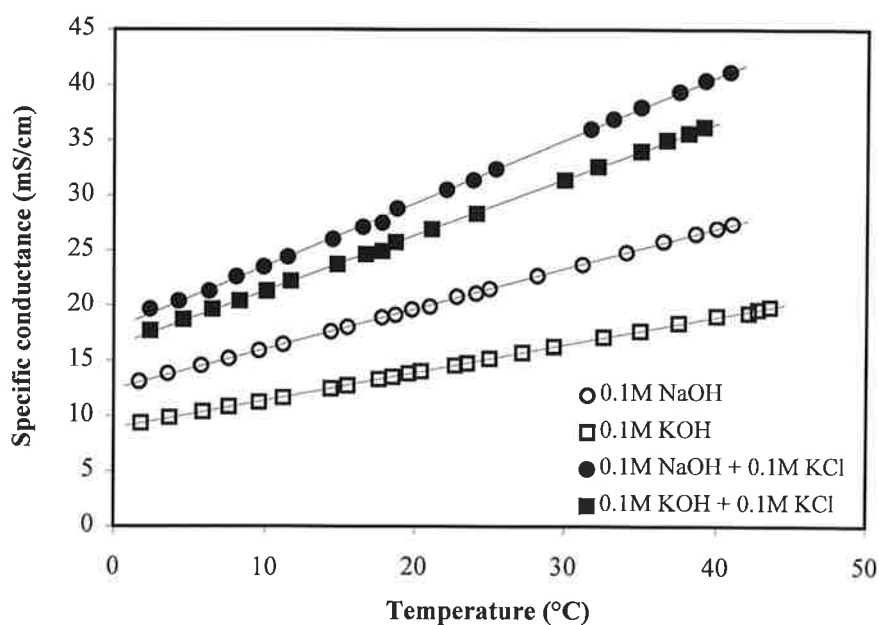
Figure 32 - Results of conductivity measurements in some alkaline solutions while they were heated from 1°C to 40°C.

Table 7 - Conductivity of BFSC and OPC concretes (X_{concr}) with w/c 0.45 compared with conductivity of solutions (X_{sol}) simulating their pore solutions.

Concrete:	BFSC, w/c 0.45, no Cl			OPC, w/c 0.45, no Cl		
Simulating pore solution:	0.1M KOH + 0.1M NaOH			0.3M KOH + 0.1M NaOH		
Temperature (°C)	X_{concr} ($\Omega^{-1} \cdot m^{-1}$)	X_{sol} ($\Omega^{-1} \cdot m^{-1}$)	X_{sol}/X_{concr}	X_{concr} ($\Omega^{-1} \cdot m^{-1}$)	X_{sol} ($\Omega^{-1} \cdot m^{-1}$)	X_{sol}/X_{concr}
1	$2.8 \cdot 10^{-4}$	2.2	7834	$2.5 \cdot 10^{-3}$	4.0	1577
5	$3.5 \cdot 10^{-4}$	2.4	6872	$3.0 \cdot 10^{-3}$	4.4	1429
10	$4.7 \cdot 10^{-4}$	2.7	5751	$4.0 \cdot 10^{-3}$	5.0	1245
15	$6.4 \cdot 10^{-4}$	3.0	4750	$5.1 \cdot 10^{-3}$	5.6	1071
20	$8.6 \cdot 10^{-4}$	3.3	3883	$6.7 \cdot 10^{-3}$	6.1	913

To further evaluate the effect of temperature on the conductivity of the pore solution, some experimental tests were carried out in solutions with compositions similar to concrete pore liquid: 0.1M KOH, 0.1M NaOH, 0.1M KOH + 0.1M KCl and 0.1M NaOH + 0.1M KCl (the last two in order to simulate the effect of chloride ions). The conductivity of these solutions was measured while they were slowly heated from 1°C to 40°C. Results (Fig. 32) show again a linear relationship between conductivity and temperature.

Table 7 compares the variations of conductivity in BFSC and OPC concretes without chlorides and in the solutions that have been assumed to simulate their pore solution, as a function of temperature. Conductivity of concrete has been evaluated with the exponential relationships of Table 6 (data in the fog room were considered); conductivity of pore solution has been calculated using the linear relationships of Fig. 32 applied to the simulating solution reported in paragraph 5.1.

The ratio between conductivity of concrete and conductivity of the simulating pore solution varies significantly with temperature, showing that the changes in concrete are not proportional to the variations in the pore solution.

Therefore other factors, besides the pore solution composition, do affect the influence of temperature on conductivity of concrete.

There is some evidence [13] that temperature can affect the steady state composition of the pore solution. As temperature increased from 25 to 70°C, a decrease in hydroxyl ions concentration and an increase in chloride ion concentration (where these ions were mixed in) were observed in mortars made with a sulphate resistant cement and two portland cements with different C_3A content. These effects were stronger at temperatures higher than 40°C, but they were significant also from 25 to 40°C. The release of chloride ions at increasing temperature was attributed to instability of calcium chloro aluminate hydrate, while the decrease in the OH⁻ concentration in the uncontaminated mortar was attributed to instability of calcium sulpho-aluminate hydrate formed due to the reaction of gypsum, added to regulate the setting time of cement, with C_3A.

A change in the pore solution composition will also change the concrete conductivity. However, this effect should be very small, at least in the range of temperature considered in the tests shown in Figs. 25-28 and for the relatively short duration of those tests.

A further parameter that influences concrete conductivity is the water content in the pores, especially with regard to large ones. In fact, for a certain level of moisture content and a fixed temperature, water inside the large pores will be only partially condensed on the pore walls. As a first approximation, it can be assumed that when the temperature changes during short term tests, the total water content in the concrete pores does not change. Therefore a temperature variation can bring about a change in the condensed water content. Namely, if the temperature decreases, the condensed water content is expected to increase. This can increase the water layer thickness through which ion transport can occur and, therefore, can increase the overall conductivity of concrete.

However even this effect is expected to be negligible both for tests in the fog room and at 80% R.H. In fact if we consider for instance the OPC concrete with w/c 0.45 and no chloride mixed in, we can assume that the total porosity is around 12% and that at 80% R.H. about half of the pores (6% of volume of concrete) are filled with water; consequently concrete contains roughly 60 l/m^3 of condensed water. In equilibrium conditions, the remaining volume of pores (6%) should be filled with air at 80% R.H. Since the density of saturated water vapour at 40°C is 0.051 kg/m^3, the amount of evaporated water in the air-filled pores is:

$$0.051 \text{ kg/m}^3 \times 80\% \times 6\% = 0.0025 \text{ kg/m}^3 = 2.5 \text{ g/m}^3$$

where 80% is the R.H. and 6% the volume of pores filled by air. This water content is indeed negligible with regard to the mass of water already present in the pores and thus, even if all of this vapour would condense, the consequence on water content would be negligible also on a microscopical scale.

A further effect that could be responsible for the exponential relationships observed between concrete conductivity and temperature is the interaction between ions and the cement paste. In fact, the influence of temperature on the interaction between ions and hydrated cement paste (discussed in paragraph 5.2) can be expected. Unfortunately, no experimental evidence is available on the effect of temperature on this interaction.

6. CORRELATIONS AND MECHANISMS OF CORROSION CONTROL

Several works have shown good correlations between corrosion rate of steel and concrete conductivity or steel potential respectively [1-3,22,24,40]; these were explained with some models describing mechanisms that could control corrosion in carbonated and chloride contaminated concrete [1,3].

6.1 *Corrosion rate and conductivity*

Several authors [1-4] have suggested a linear relationship between corrosion rate and conductivity of concrete. For instance, Fig. 33 shows the relationship found by Glass et al. [1] in carbonated mortar with 0.4% chloride by cement weight. Results refer to a single specimen and resistivity changes were obtained by changing the humidity of the environment. Although a certain scatter is evident, a clear correlation was found. Similar results were found by Feliu et al. [3] and Alonso et. al. [24].

Polder et. al [2] applied different techniques for measuring both resistivity of concrete and corrosion rate of steel in concretes with various compositions and exposed to a marine environment. They obtained a linear relationship, but the correlation was dependent on the concrete cover, as shown in Fig. 34. The influence of concrete may be related to the chloride content at the rebar depth, as more dense concrete (with slag or fly ash) contained lower chloride contents at the bar depth, as compared to the OPC mixes. In fact, complicated three-way relationships exist between chloride penetration rate, resistivity and corrosion rate. For fixed exposure time, concrete with high resistivity has a lower penetration rate [42].
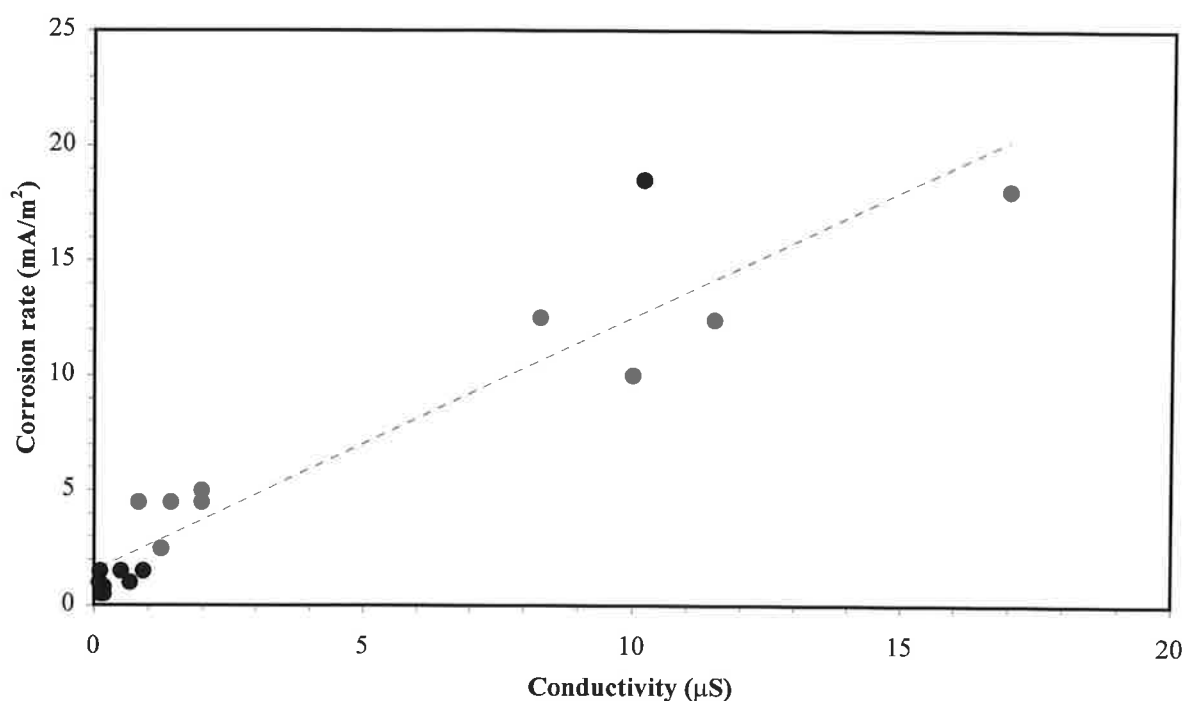
Figure 33 - Relationship between mortar conductivity and corrosion rate obtained on steel exposed to carbonated mortar containing 0.4% chloride [1].
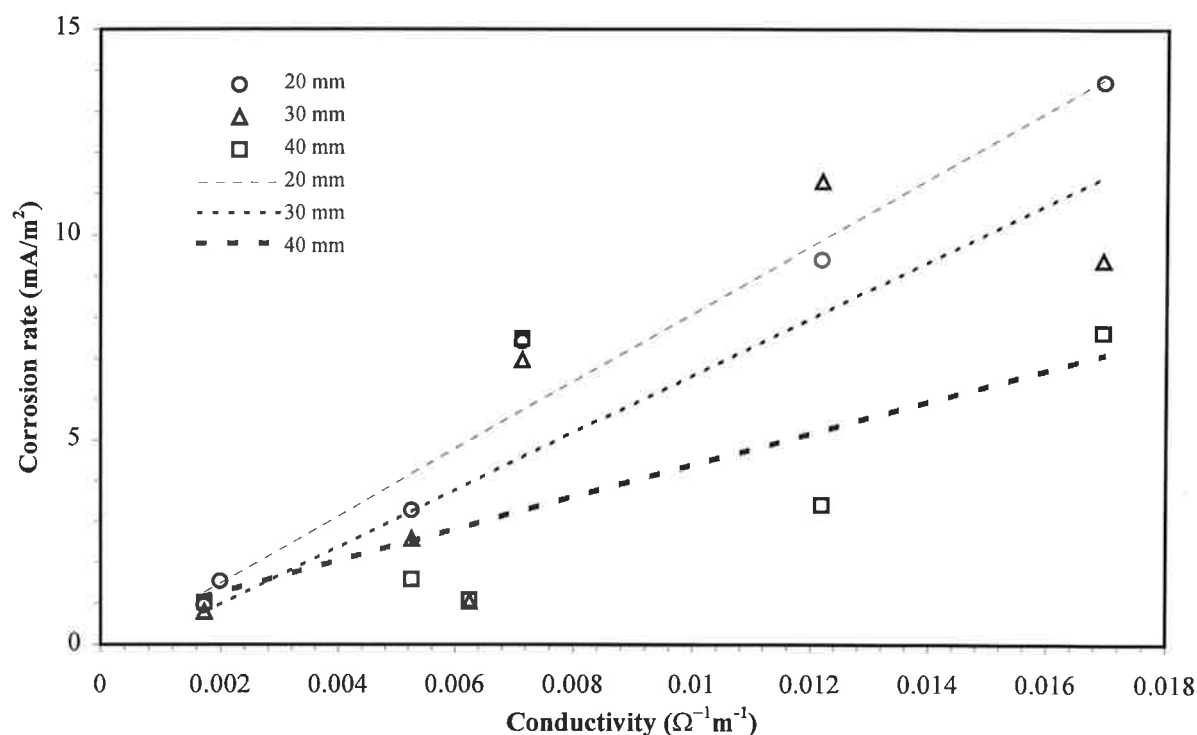
Figure 34 - Relationship between concrete conductivity and corrosion rate of steel in marine exposed reinforced concrete blocks [2].

Previous analyses of the experimental work carried out at TNO (see reports [4-9]) showed some linear relationships between concrete conductivity and corrosion rate, at least within single specimens. However the fitting straight lines were different (both in slope and in position) as a function of the concrete composition (type of cement, w/c, chloride content) and the exposure conditions. Here an attempt will be made to study these relationships and to find out the influential factors.

Corrosion rate of each specimen has been plotted in Figs. B1-B8 (appendix B) against conductivity of concrete measured on the same day. Each figure refers to a fixed concrete mix and reports all the results obtained during the five years of testing on the four specimens exposed to different environments (80% R.H., fog room, outside). Only conductivity measured with bars embedded at 10 mm depth and corrosion rate measured on rebars at 10 mm are reported.

It is clearly evident that a relationship valid for all types of concrete cannot be found (when comparing different figures, it should be observed that scales of axes are not the same). Even when the concrete composition is constant (i.e. when a single figure is considered) the experimental data do not show a common trend, although specimens with chloride show a lower scatter (see for instance Figs. B.2 and B.4) so that a certain correlation is suggested.

If single specimens are considered, more reliable relationships can be found. Some specimens show a very good linear correlation, such as B1 (Fig. B.2), D1 and D2 (Fig. B.4). For other specimens the scatter is higher but a reasonable interpolation of results can be obtained, especially in those specimens where the corrosion rate is higher than 1-2 μm/year.
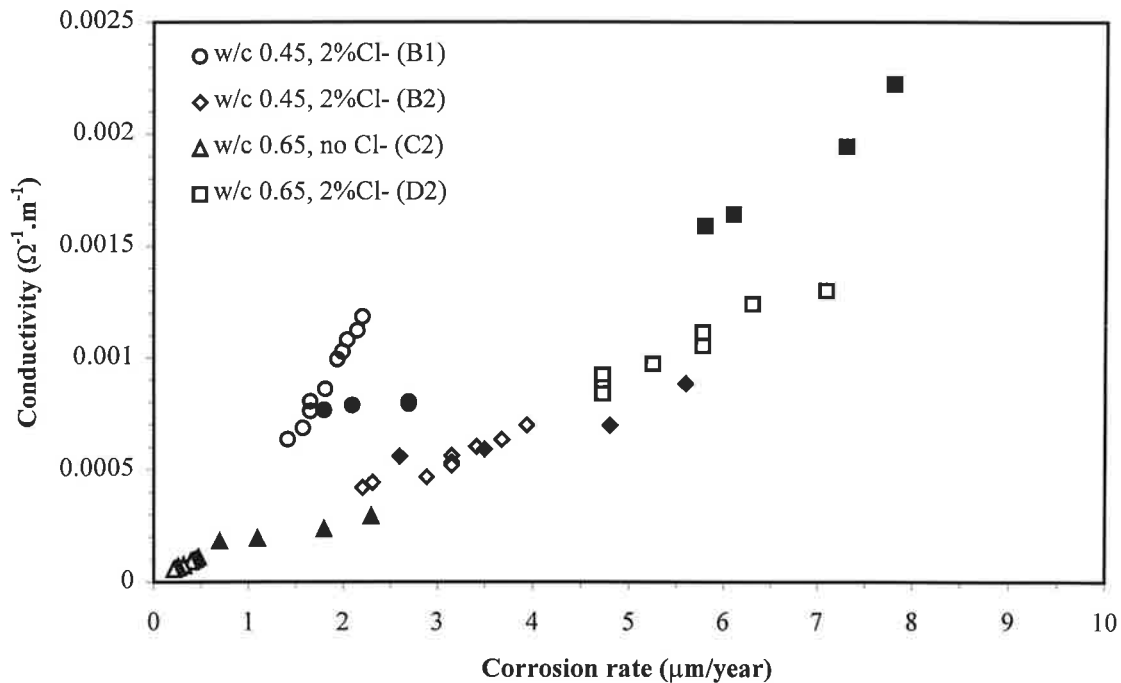
Figure 35 - Conductivity of concrete against corrosion rate of steel (measurements at 10 mm) during dynamic cooling tests from 40°C to 20°C at 80% R.H. [9] (white markers) and tests at R.H. ranging from 75% to 95% [8] (black markers) in some specimens with BFSC concrete.

Fig. 35 reports the relationships between conductivity and corrosion rate found in BFSC concretes during tests where the relative humidity was increased from 75% to 95% [8] (temperature was constant at 20°C and measurements were carried out in stable conditions) and during dynamic cooling tests [9] where the temperature decreased from 40°C to 20°C (R.H. was 80%). Only the specimens on which dynamic cooling tests were performed are reported. Each type of marker refers to a single specimen (hence also to a particular type of concrete); black markers show the results of tests at different R.H. and the white ones the results of cooling tests at 80% R.H. Only measurements at 10 mm are reported.

A linear correlation between corrosion rate and conductivity of concrete can be observed in this figure. Furthermore, results from different types of tests (i.e. varying R.H. or temperature) are in good agreement, especially when the same specimen is considered. However in some cases (for instance, specimen D2) a significant difference can be observed; with this regard, it should be realised that tests at different R.H. values were carried out at an age of about three years, while dynamic cooling tests were carried out about two years later.

Fig. 36 reports the relationships found in OPC concretes during the same tests. The overall correlation in this case is much less clear than the one observed for BFSC concretes; however when a single specimen and a single type of test is considered, a good linear correlation arises. The results of the two types of test are in good agreement only for specimen H2; for specimens F2 and H1 they are shifted, although the slope of the curve is roughly constant in the two series of results on the same specimen.
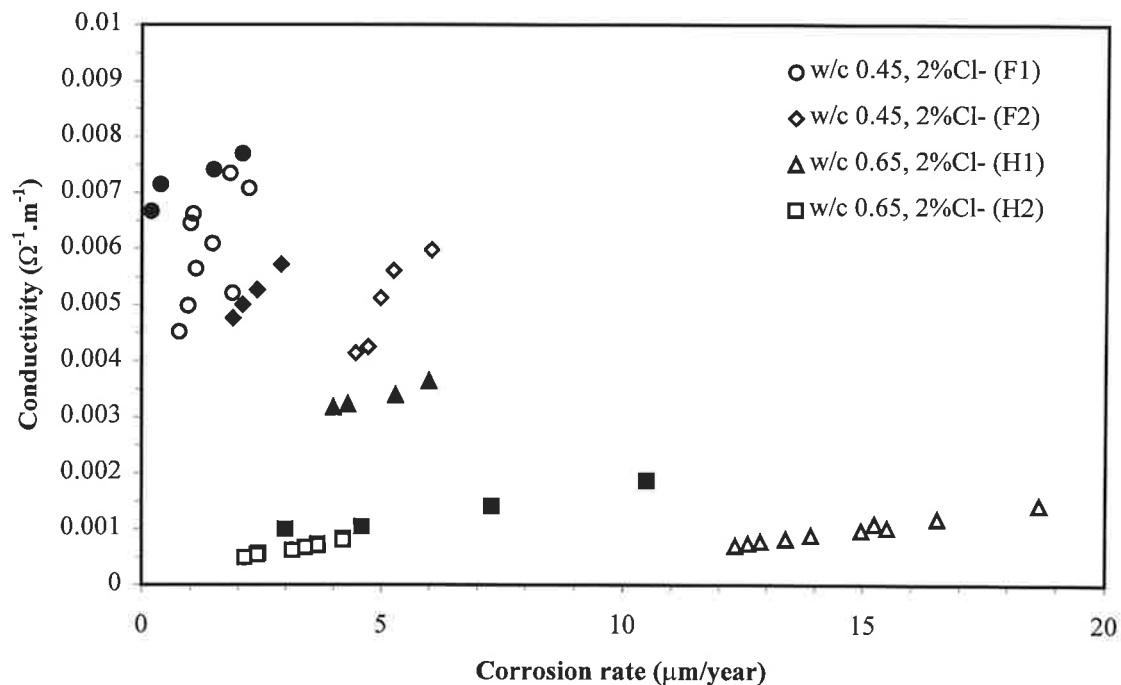
Figure 36 - Conductivity of concrete against corrosion rate of steel (measurements at 10 mm) during dynamic cooling tests from 40°C to 20°C at 80% R.H. [9] (white markers) and tests at R.H. ranging from 75% to 95% [8] (black markers) in some specimens with OPC concrete.

As a matter of fact, Figs. 35 and 36 suggest that, during short term tests, the relationship between corrosion rate and conductivity in a well identified specimen is quite linear. In order to understand why this does not apply also to long term tests (appendix B) or to tests carried out at different times, the "history" of each specimen must be considered.

Fig. 37 shows the relationships found on specimen B1 (BFSC concrete, w/c 0.45 and 2% chloride) during different types of tests. Measurements at 80% R.H. and 20°C (increased to 40°C after five years) show a linear correlation. The higher values of both corrosion rate and conductivity were measured during the first year; in the following four years corrosion rates lower than 3 μm/year and conductivities around 0.01 $\Omega^{-1} \cdot m^{-1}$ were measured. Data from short term tests are within the scatter of long term results, although they move along different straight lines. Anyway the changes in corrosion rate and conductivity were very low during these short term tests.

Fig. 38 refers to specimen B2, which had the same composition of B1, but after 1 year was subjected to accelerated carbonation. The results before the carbonation treatment show a linear trend quite similar to that found on specimen B1 during the first year (the fitting line is only slightly shifted to lower values of conductivity). After the accelerated carbonation treatment, the relationship between corrosion rate and conductivity changed, shifting towards lower values of conductivity and higher values of corrosion rate. Since phenolpthalein test on concrete cubes showed that the carbonation depth was higher than 10 mm (Table 2), this change can be attributed to carbonation of concrete. All the measurements carried out during the four years after carbonation occurred are in excellent agreement: whatever the cause of change in resistivity was (variation of temperature, R.H. or both), corrosion rate changed according to the same linear relationship.
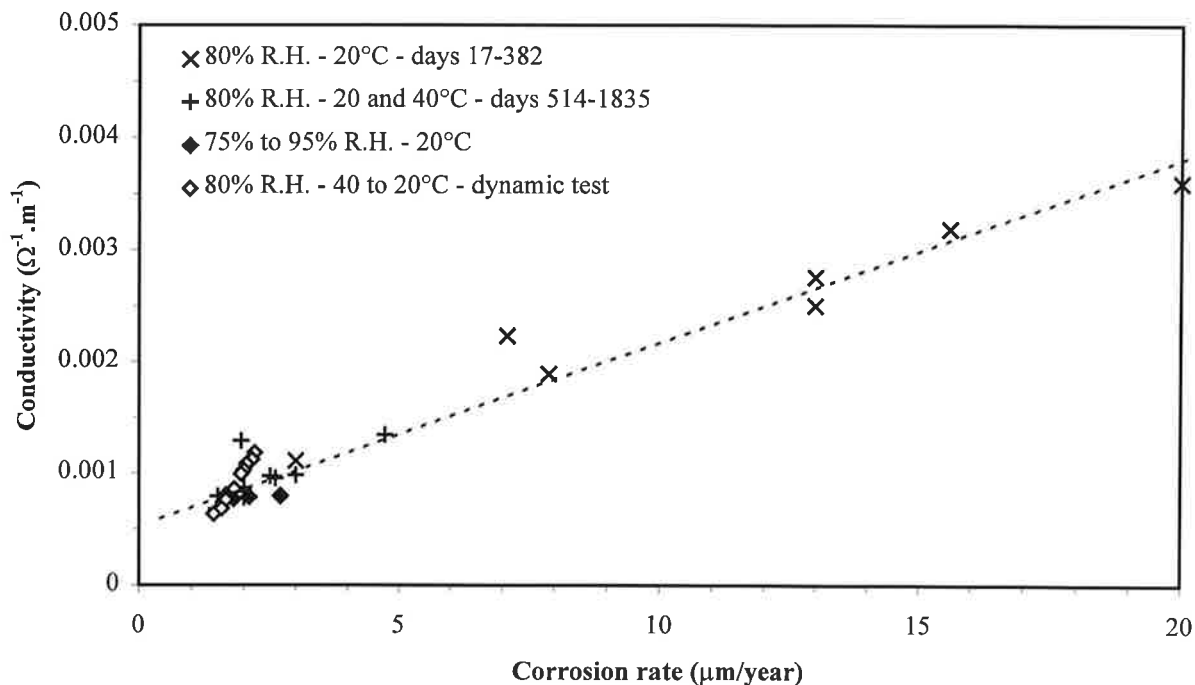
Figure 37 - Relationship between conductivity of concrete and corrosion rate of steel (measurements at 10 mm) in specimen B1 (BFSC cement, w/c 0.45, 2% Cl⁻) during different types of tests.
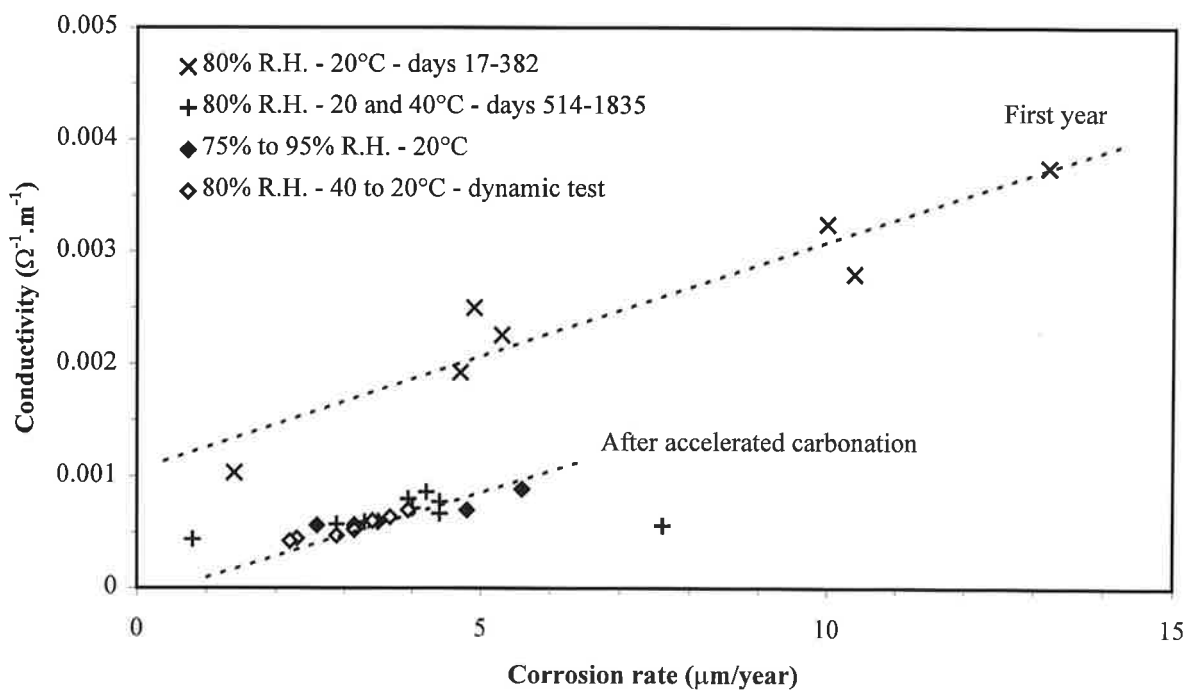
Figure 38 - Relationship between conductivity of concrete and corrosion rate of steel (measurements at 10 mm) in specimen B2 (BFSC cement, w/c 0.45, 2%Cl⁻, subjected to accelerated carbonation) during different types of tests.

Even in concrete with a higher w/c ratio and without chlorides (specimen C2, Fig. 39) carbonation changed the linear fitting curve, but again carbonation of concrete was the only factor that influenced the relationship. In this case the variation consisted in a remarkable change in the slope of the correlation line.

Also Fig. 40 (specimen D2: BFSC concrete, w/c 0.65, 2% chloride) shows the effect of carbonation (although in this case the results after accelerated carbonation are rather disperse).

Carbonation influenced the relationship between conductivity and corrosion rate also in steel embedded in OPC concretes with 2% chlorides, as shown in Figs. 41-43. In concrete with 0.45 water to cement ratio (specimen F1, Fig. 41), not subjected to accelerated carbonation, both corrosion of steel and concrete conductivity were very low after the first year (two higher corrosion values were measured, but they are probably influenced by experimental errors). However, even in this case, a different behaviour was observed during the first year of tests (most of the measurements were carried out during the first three months). This suggests that, at least in the presence of chloride, a stable condition was reached only after one year (this could be due to the slow drying out of concrete in the environment at 80% R.H. or also due to hydration of cement paste).

Specimen H1, with w/c 0.65 and 2% Cl⁻, shows three sets of linear relationships: one during the first year (similar to the other specimens), one during second and third year (and also during tests at different R.H. which were carried out in that period) and the third one during the fifth year (data of dynamic cooling tests, carried out in the fifth year, are in agreement although they are slightly shifted).
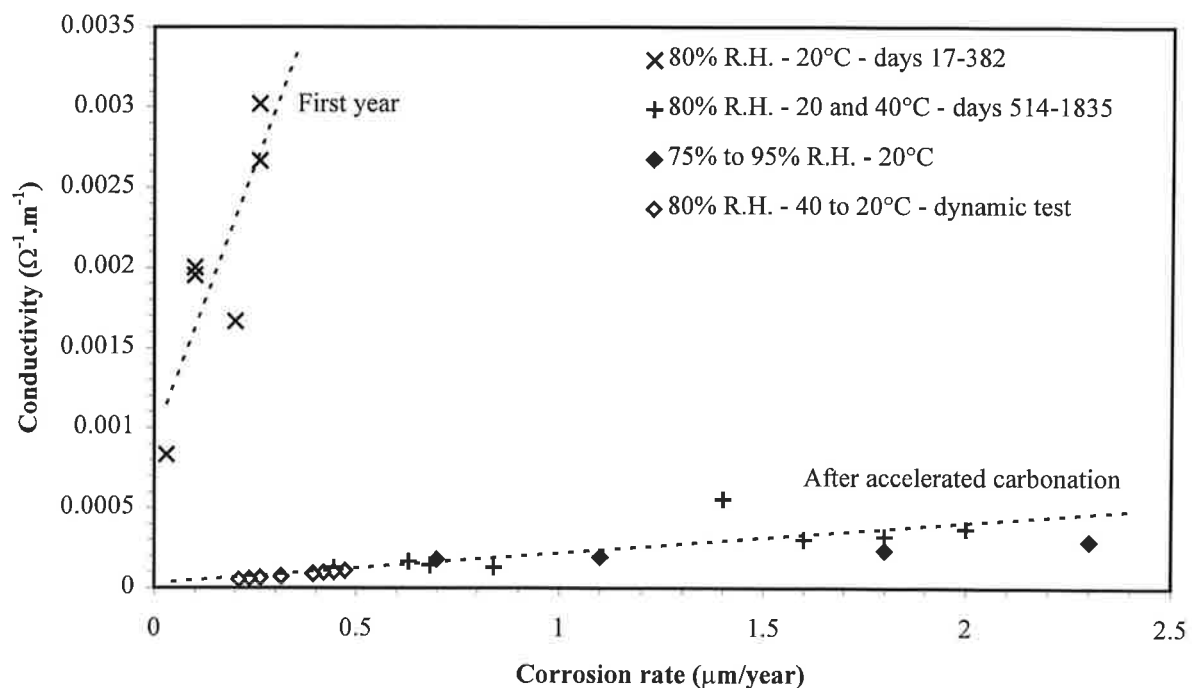
Figure 39 - Relationship between conductivity of concrete and corrosion rate of steel (measurements at 10 mm) in specimen C2 (BFSC cement, w/c 0.65, no Cl⁻, subjected to accelerated carbonation) during different types of tests.
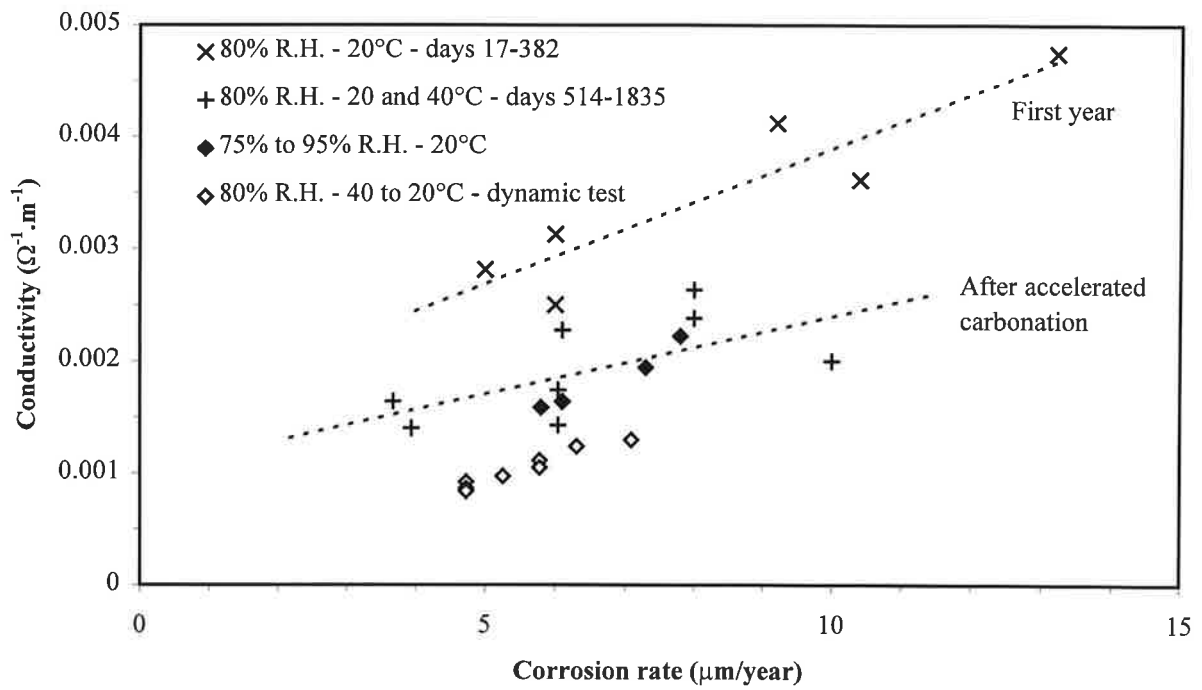
Figure 40 - Relationship between conductivity of concrete and corrosion rate of steel (measurements at 10 mm) in specimen D2 (BFSC, w/c 0.65, 2%Cl⁻, subjected to accelerated carbonation) during different types of tests.
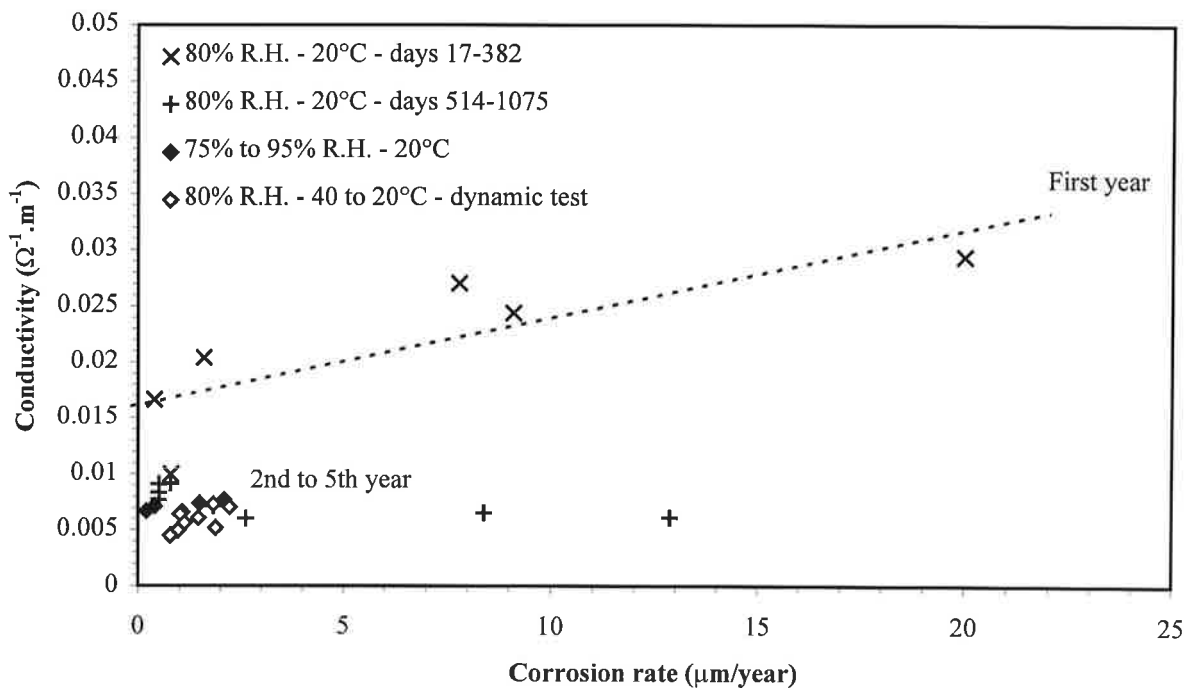
Figure 41 - Relationship between conductivity of concrete and corrosion rate of steel (measurements at 10 mm) in specimen F1 (OPC cement, w/c 0.45, 2%Cl⁻) during different types of tests.
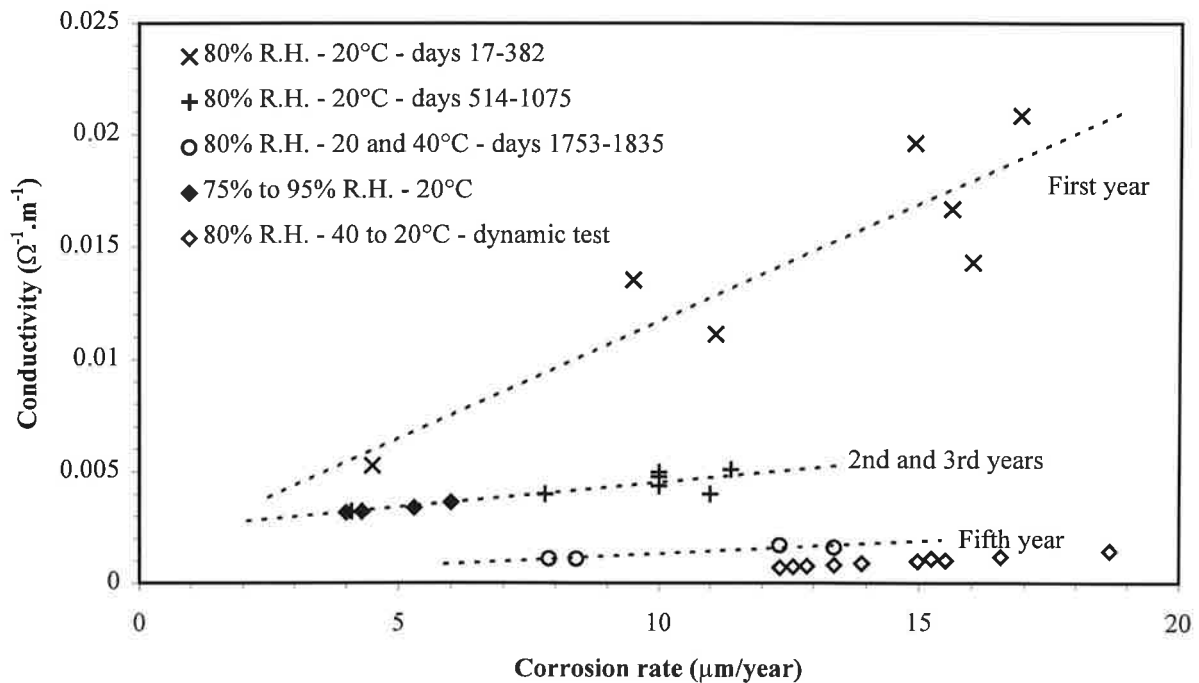
Figure 42 - Relationship between conductivity of concrete and corrosion rate of steel (measurements at 10 mm) in specimen H1 (OPC cement, w/c 0.65, 2%Cl⁻) during different types of tests.

This behaviour might suggest that carbonation of the external layer (10 mm) occurred between the third and the fifth year (this specimen was not subjected to accelerated carbonation). In fact, the relationship found after 5 years is rather similar to that found on specimen H2 (with the same type of concrete) after the accelerated carbonation treatment (Fig. 43).

The analysis of the time evolution of the relationship between corrosion rate and concrete conductivity (i.e. the inverse of resistivity) has shown that a general correlation applicable to all types of concretes and environments does not exist. Nevertheless, good linear correlations were found in homogeneous conditions (namely the same type of concrete, the same age, the same chloride content and carbonation conditions) regardless of the cause that changed both corrosion rate and conductivity (only temperature and R.H. have been considered here).

The absence of a generalized correlation show that the simple measure of resistivity of concrete cannot be used to evaluate the corrosion rate of the steel embedded in that concrete (although such an approach would be very useful, since concrete resistivity measurements are usually more easy to carry out than corrosion rate measurements).

However, the results of the tests discussed here suggest that the evaluation of corrosion rate through resistivity measurement might be successful to investigate in details the different parts of a single structure. In fact, provided that the structure is rather homogeneous as far as concrete composition and environmental exposure condition are concerned, the correlation between corrosion rate of steel and resistivity of concrete may be investigated in a small part of the structure and then a investigation covering larger parts of the structure can be carried out only with resistivity measurements.
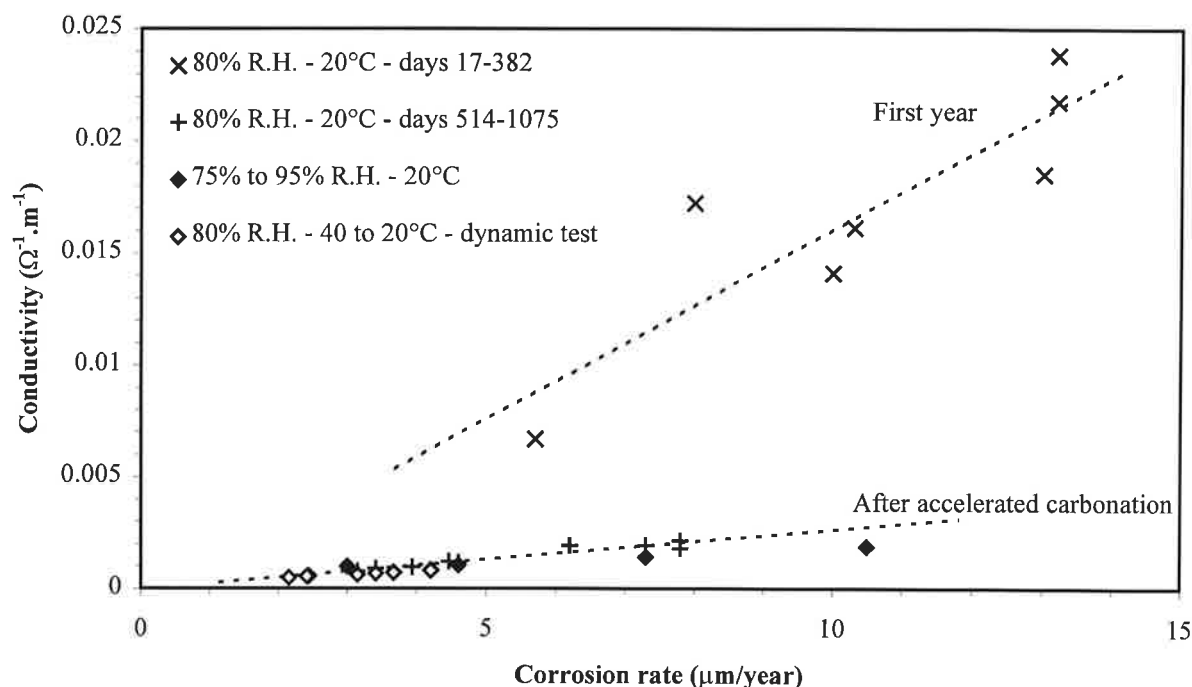
Figure 43 - Relationship between conductivity of concrete and corrosion rate of steel (measurements at 10 mm) in specimen H2 (OPC, w/c 0.65, 2%Cl⁻, subjected to accelerated carbonation) during different types of tests.

In the first part of this report, the influence of several factors on both corrosion rate and resistivity was discussed. The relationships found in this paragraph show that some of these parameters have a similar influence on corrosion rate and conductivity, so that their influence on corrosion rate can be assessed simply by studying their influence on conductivity (or resistivity). This seems to be the case of environmental factors such as temperature and R.H.: in fact, when the same specimen was considered, change in resistivity due both to temperature or R.H. variation brought about the same variation in corrosion rate (i.e. the fitting straight line was the same). This observation supports the idea that, once the correlation is known for a given structure, a more widespread analysis of the corrosion condition could be carried out mainly on the basis of resistivity measurement.

Nevertheless the limits of such an approach should be clear, since other parameters have different influences on corrosion rate and resistivity and therefore change also the relationship between them. These are: cement type, w/c ratio, carbonation and chloride content. In most of the practical application, these factors should be constant within a particular structure. However, if chloride penetration is the cause of corrosion, the situation becomes more complicated because chloride penetration and resistivity are related [42].

Cement type strongly influences the electrical resistivity of concrete, but it also affects the correlation of conductivity against corrosion rate. In particular, a resistivity of about one order of magnitude higher (for the same w/c and in the same conditions of exposure) can be found for BFSC concrete versus OPC concrete (paragraph 5), but these differences in resistivity not necessarily bring about similar differences in corrosion rate since the correlations between conductivity and corrosion rate can be different. Similarly, water to cement ratio influences concrete resistivity (the lower w/c, the higher the resistivity); however again water cement ratio affects the relationship between corrosion rate and

conductivity, and thus the increase of resistivity due to a higher w/c ratio cannot be applied to the relationship found for a certain w/c ratio in order to evaluate the changes in corrosion rate.

The results discussed above suggest that also the corrosion conditions of the rebars are likely to influence the correlation between corrosion rate and conductivity. No correlations can be found in passive steel in chloride free and non carbonated concrete. However, even when the steel is actively corroding (e.g. corrosion rate is higher than 2 μm/year) the same type of concrete can show different correlations during time, mainly due to carbonation. Also chloride penetration in carbonated concrete might have similar effects. This was not studied in the work carried out at TNO, since chloride was added to the mix; however, by comparing Fig. 39 (concrete without chlorides) with Figs. 38 and 40 (concretes with chlorides), a decrease in the slope of the straight line that correlates conductivity of concrete with corrosion rate can be expected in carbonated concretes with chlorides. This means that, for a certain value of conductivity of concrete, corrosion rate is lower in not carbonated concrete.

6.2 Corrosion potential and corrosion rate

It is well known that the corrosion potential of steel in concrete can be correlated to the probability of corrosion of steel (passive or active corrosion). As a matter of fact, inspection of structures is often based on potential mapping [4]. Some authors have also suggested that corrosion potential can be correlated to corrosion rate of rebars, at least under well defined conditions. For instance, Fig. 44 shows a linear relationship between potential and logarithm of corrosion rate found by Glass et al. [1] on a steel rebar embedded in carbonated mortar with 0.4% chloride by cement weight, by changing the humidity content of concrete. However other authors have found much less clear results (for instance Andrade et al. [23]).

Figs. B.9-B.16 (appendix B) show the relationships between corrosion potential and corrosion rate during measurements carried out at TNO. Each graph refers to a fixed concrete mix and reports results on the four specimens exposed to different environments (80% R.H., fog room, outside). Only data on rebars embedded at 10 mm depth are reported.

In general, specimens in chloride free concrete have potential values more positive than -100 mV vs Ag/AgCl and the corrosion rate is lower than 1 μm/year. The figures do not suggest any significant difference between specimens exposed to the fog room (series 3 and 4) and those exposed to 80% R.H., even for specimens subjected to accelerated carbonation (series 2). However, during some measurements on the specimens in the fog room, much more negative potential were measured (Figs. B.11, B13 and B.15). These potential values were always associated with higher corrosion rates (which were attributed to crevice corrosion [8]).

Corrosion potentials more negative than -100 mV vs Ag/AgCl were measured (with only few exceptions) on steel in chloride contaminated concretes, regardless of the cement type. Corrosion rate at these potential values was more than 1 μm/year; it reached values up to 100 μm/year (and even higher). Data on specimens exposed to the fog room are shifted towards higher corrosion rates with respect to those on specimens in the 80% R.H. room: at the same potential, corrosion rate is several times higher in the former (Appendix B, Figs. B.10, B12, B14, B.16).

Fig. 45 shows the relationship between corrosion potential and corrosion rate measured after about 3 years. The results from different types of concrete and environment are in good agreement, and suggest a linear trend in a semilogarithmic plot.
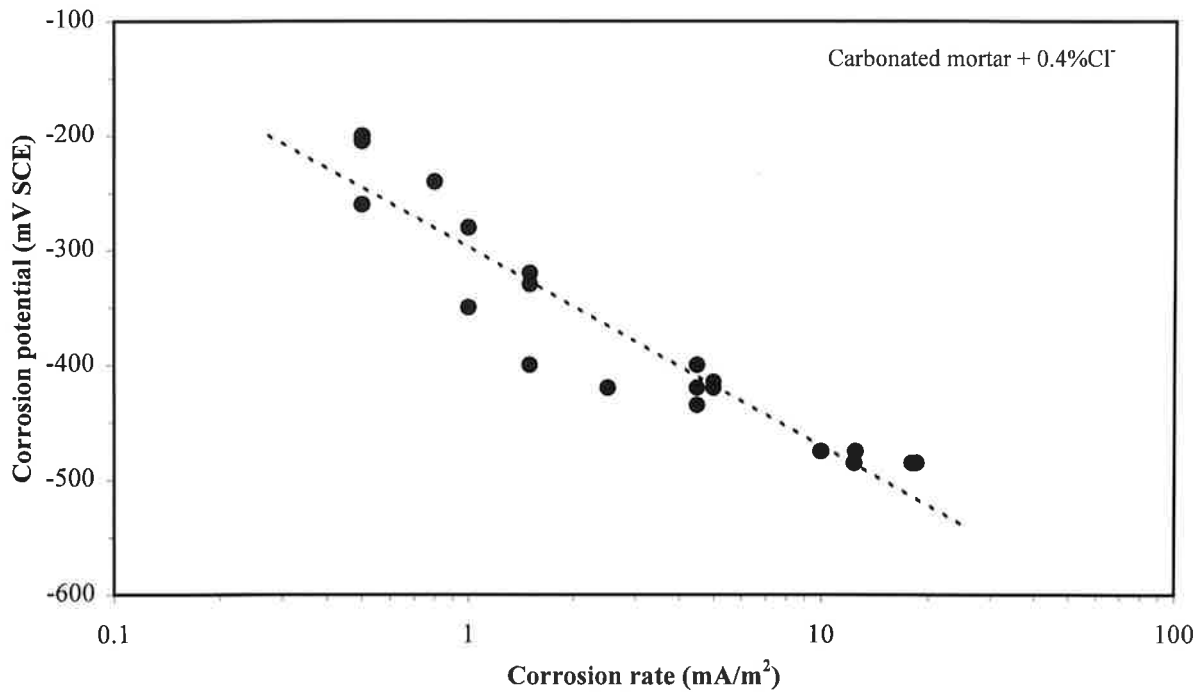
Figure 44 - Relationship between corrosion potential and corrosion rate obtained on steel exposed to carbonated mortar containing 0.4% chloride [1].
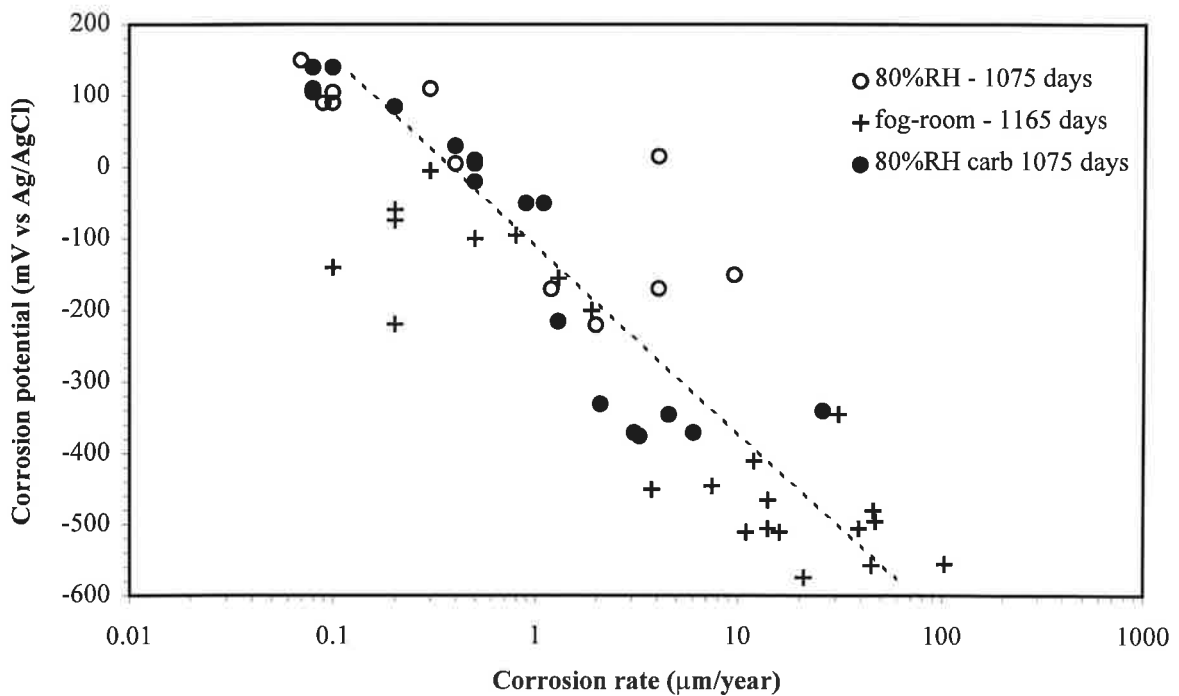
Figure 45 - Correlation between potential and corrosion rate of steel in all types of concrete exposed to the different environments (rebars at 10 mm depth have been considered).

When the potential of steel decreases from +100 mV Ag/AgCl to -600 mV the corrosion rate increases from about 0.1 µm/year to 100 µm/year. However scatter of result is not negligible: for a fixed potential the corrosion rate can change an order of magnitude.

6.3 Mechanisms of control of corrosion

Corrosion of steel in concrete is an electrochemical process which consists of anodic and cathodic reactions taking place at the steel surface (for instance, iron dissolution and oxygen reduction). Schematization in Fig. 46 show that circulation of current is required: electrons produced by the anodic process flow through the metal towards the cathodic site, and the electrical circuit is closed through concrete, where the current is transported by ions in the pore solution. The corrosion rate is proportional to the current flowing into the circuit (Faradays' law), and thus every process shown in Fig. 46 can control the corrosion rate, by limiting the current flux.

Depending on concrete properties and environment, different mechanisms of control of corrosion rate of steel in concrete have been proposed in the literature [1,3,10-12,15,41].

It is well known that, in contact with non carbonated and chloride free concrete, steel is in passive condition, namely its surface is protected by a passive layer that hinders the anodic reaction of ion dissolution to occur. Corrosion rate is therefore very low (of the order of <0.1 μm/year [15]) and the corrosion process is under anodic control. Fig. 47 shows a schematic Evans diagram for passive steel in concretes with different moisture content. By increasing the moisture content of concrete, the corrosion potential will shift to more negative values (following the shift of the cathodic curve due to lower oxygen content), but the corrosion rate will not change. In water saturated concrete, lack of oxygen takes the corrosion potential to very negative values where passivity of steel will be lost; however the corrosion rate is still negligible (low potential corrosion [15]).

Passivity can vanish in the presence of chloride ions or carbonation. Chloride ions penetration (above a threshold content [10-12]) into concrete can break the passive film and give rise to localized corrosion (pitting corrosion). The anodic process occurs where the passive film has been destroyed, whereas the cathodic reaction takes place on the still passive areas. Carbonation of concrete decreases the pH of the pore solution to values below those required for the stability of the passive film. Hence, a uniform attack can occur.

When steel is not passive (i.e. is "active"), the corrosion process is no more under anodic control and the corrosion rate is strongly influenced by moisture content.
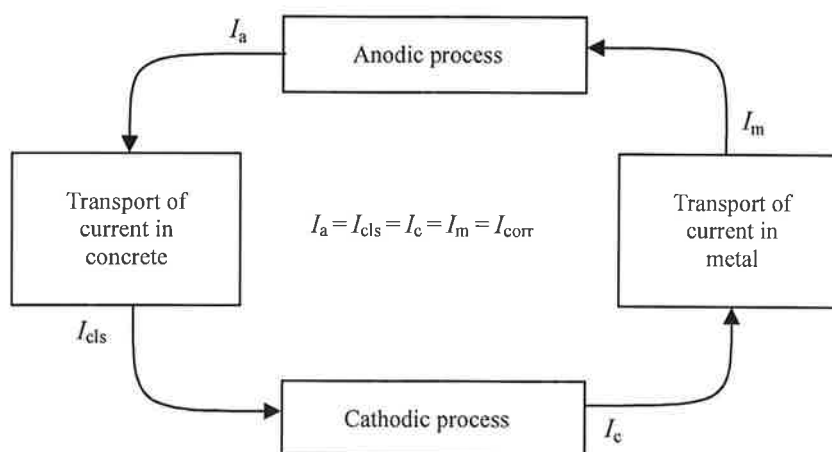
Figure 46 - Schematic illustration of the electrochemical mechanism of corrosion of steel in concrete [12].
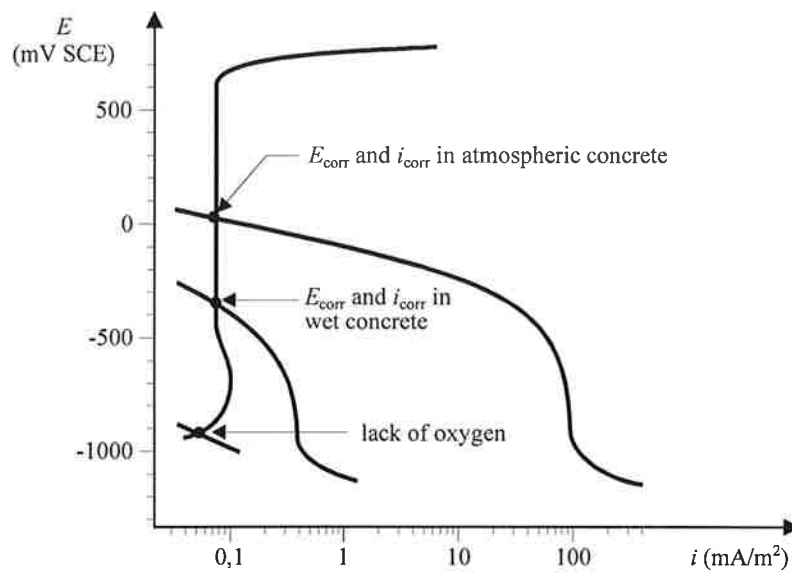
Figure 47 - Schematic representation of corrosion condition of passive rebars in concrete with different moisture contents [12].

In very wet concrete, corrosion rate can be depressed by lack of oxygen (cathodic control), in the same way as for passive steel. Vice versa, in drier environments it has been suggested that the resistivity of concrete can be the main influential factor on corrosion rate (resistive control) [3,15]. In fact, resistivity of concrete influences the ionic transport in the concrete pore solution by inducing an ohmic drop that reduces the driving voltage available for the corrosion process, as shown in Fig. 48.

Experimental results on carbonated mortars [1] showed that, in accordance with the resistive control, changes in resistivity in carbonated mortars gave rise also to changes in corrosion rate (Fig. 33); however also a correlation between corrosion rate and corrosion potential was found (Fig. 44).
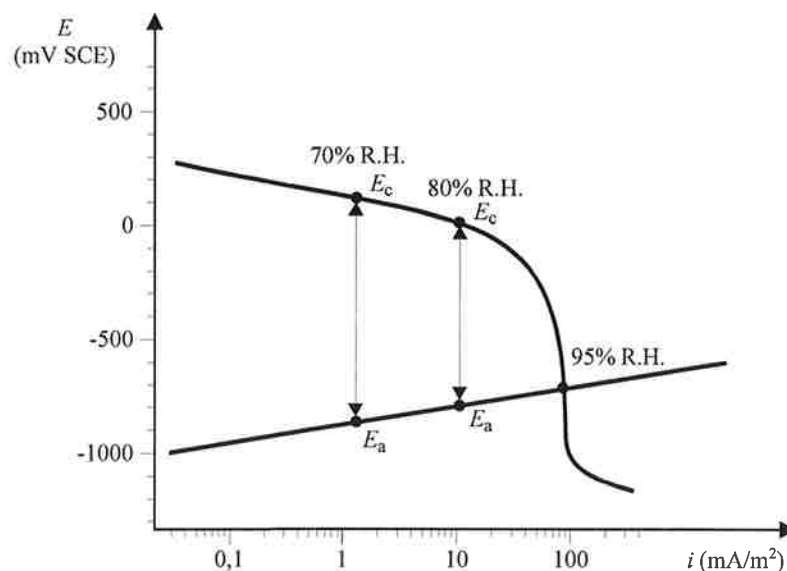
Figure 48 - Schematic representation of corroding steel in carbonated concrete with different moisture contents [12].
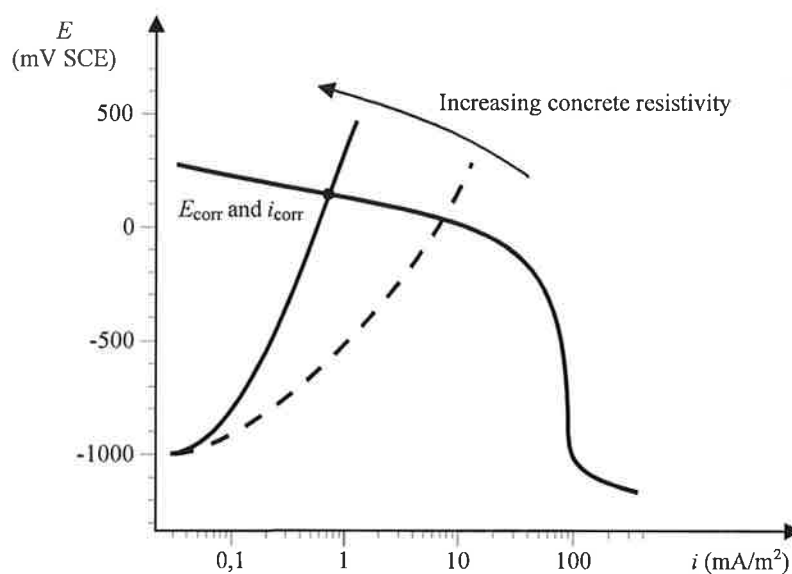
Figure 49 - Schematic representation of the "anodic resistance control" proposed by Glass et al. [1].

To explain the change in corrosion potential as a function of corrosion rate Glass et al. [1] suggested that the corrosion rate is under anodic control, i.e. the anodic reaction determines the corrosion rate, as shown in Fig. 49. However, to take into account also the influence of resistivity on the corrosion rate, they also suggested that the anodic reaction is controlled by resistivity of concrete. This mechanism was termed anodic resistance control.

The results of the experimental tests carried out at TNO and discussed in the previous chapters can be interpreted according to the controlling mechanisms just mentioned.

Different relationships between corrosion rate and conductivity have been observed for measurements during the first year (mainly during the first three months) with respect to measurements carried out in the following years, both in chloride free and in 2% chloride contaminated concrete.

During the early measurements higher corrosion rates and higher conductivity of concrete can be observed; a roughly linear relationship between conductivity and corrosion rate is evident both in chloride free concretes (Fig. 39) and in concretes with 2% chlorides (Figs. 37, 38, 40-43). The progressive decrease in concrete conductivity induced by hydration of cement paste induced a decrease in corrosion rate; in chloride free concrete, corrosion rate values typical of passive steel were reached (Fig. 39). Therefore a sort of resistive mechanism seems to influence corrosion rate in an early age of concrete. However, the analysis of the controlling mechanism is of much more interest in the long term, i.e. after passivation occurs or stable corrosion condition are reached, and thus only the data after the first year will be discussed.

Specimens with chloride free and non carbonated concrete showed that steel is passive, with corrosion rates lower than 1 μm/year and potential more positive than -50 mV Ag/AgCl (with the only exception of some specimens in the fog room where crevice corrosion occurred). The anodic passive control is confirmed by the very small influence of the exposure condition on corrosion rate and the absence of correlation between corrosion rate and resistivity of concrete. It is interesting to observe that also in BSFC concrete passivity is obtained, at positive potentials. Some authors have questioned this as a result of reduced substances on slag cement [43,44].

Cathodic control due to lack of oxygen was never observed even in very wet concrete of specimens exposed to the fog room; in fact, although some rather negative values of potential (up to -600 mV Ag/AgCl) were measured, these were always associated with high corrosion rates (Fig. 45).

As far as corroding steel is concerned, results presented in Figs. 38-43 show a strong relationship between resistivity (conductivity) of concrete and corrosion rate in specimens exposed to 80% R.H. Linear correlation is particularly evident for carbonated concrete, both without chlorides (Fig. 39) and with 2% chloride (Figs. 38, 43). In carbonated concrete without chlorides, this relationship was observed to apply quite well also for very low corrosion rates within 0.1 and 1 μm/years (Fig. 39). Also corrosion of steel in non carbonated concrete with 2% chlorides seems to be related to conductivity of concrete, as measurements during second and third years on specimen H1 (Fig. 42) suggest. However, often specimens with non carbonated concrete and 2% chlorides did not show large changes in both corrosion rate and conductivity (both had rather low values, as shown in Fig. 37 for BFSC concrete or in Fig. 41 for OPC concrete), and the correlation was not clear. In concrete contaminated with chloride and exposed to the fog room, corrosion rate was high, but poor correlations were found between corrosion rate and conductivity (App. B).

The good linear relationships found between corrosion rate and conductivity in carbonated concrete suggests that the corrosion process is controlled by resistivity. Furthermore, the relationships found also between corrosion rate and corrosion potential are in agreement with the anodic resistance control theory. For instance, specimen C2 showed a progressive decrease in corrosion rate and in concrete resistivity after the first year (and this gave rise to the linear relationship between corrosion rate and conductivity shown in Fig. 39). Meanwhile, also the corrosion potential increased with time (Fig. A.11, appendix A).
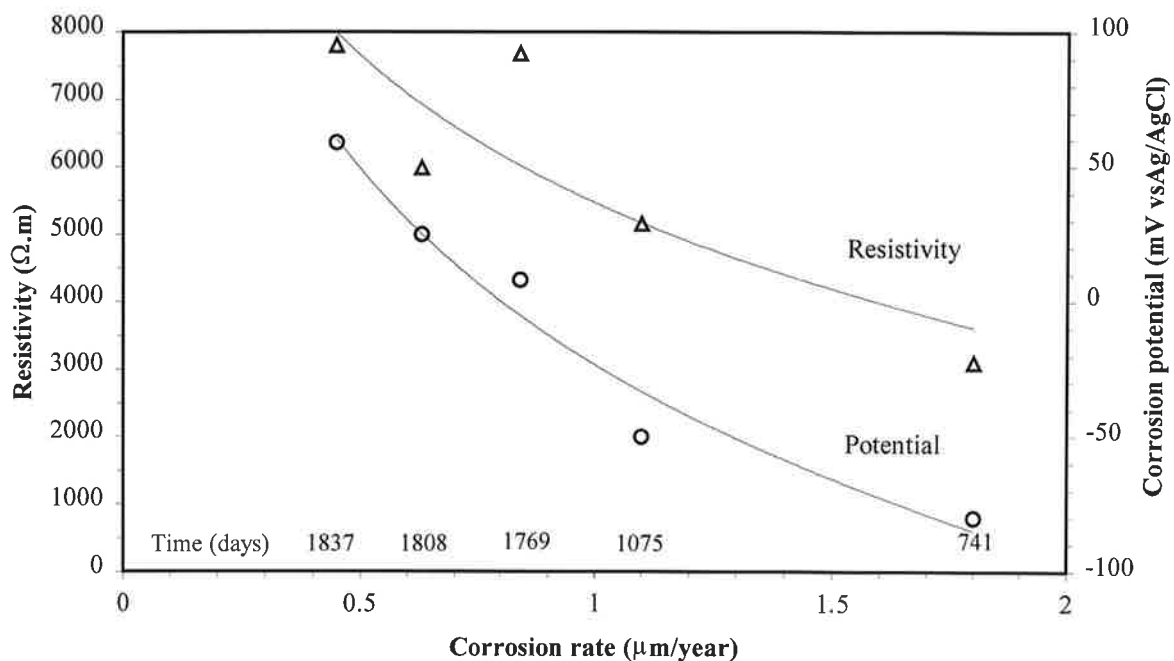
Figure 50 - Relationships between corrosion rate, resistivity of concrete and steel potential in specimen C2, after the accelerated carbonation treatment.

Fig. 50 reports concrete resistivity and corrosion potential against the corrosion rate, and shows that changes in concrete resistivity not only affect corrosion rate, but also the corrosion potential. Moreover, the corrosion potential values are quite positive, similar to those of passive steel in uncarbonated concrete. These observations support the idea that corrosion rate is under anodic resistive control. This has important consequences for the interpretation of measurements with the techniques commonly used for inspection of corrosion in reinforced concrete structure (namely, potential mapping and polarization resistance). High potential values and low corrosion rates of steel in carbonated concrete exposed to relatively dry environment (80% R.H.) might suggest that steel is passive (if no information about carbonation depth is available), and thus corrosion rate is under anodic passive control such as in alkaline concrete. Indeed, although from a practical point of view corrosion rate is anyway negligible, the quite different electrochemical conditions in carbonated concrete cannot be ignored. In fact, for anodic passive control, moisture changes do not influence corrosion rate, whereas for anodic resistance control, R.H. changes in the environment or wetting of concrete can decrease the resistivity and significantly increase the corrosion rate.

Corrosion of steel in concretes with 2% chloride but not carbonated is due to localized pitting corrosion, and therefore the control mechanism could be different with respect to the one observed on steel in carbonated concrete (where corrosion is uniform). Results in 80% R.H. environments, however, suggest again a certain correlation between corrosion rate and conductivity of concrete.

For specimens in the fog room resistivity of concrete is relatively low; however some relationships with the corrosion rate can still be found in specimens with chloride (appendix B). Fig. 51 compares specimens of BFSC concrete with w/c 0.45 and 2% chloride exposed to 80% R.H. (after accelerated carbonation, specimen, B2) and to fog room.
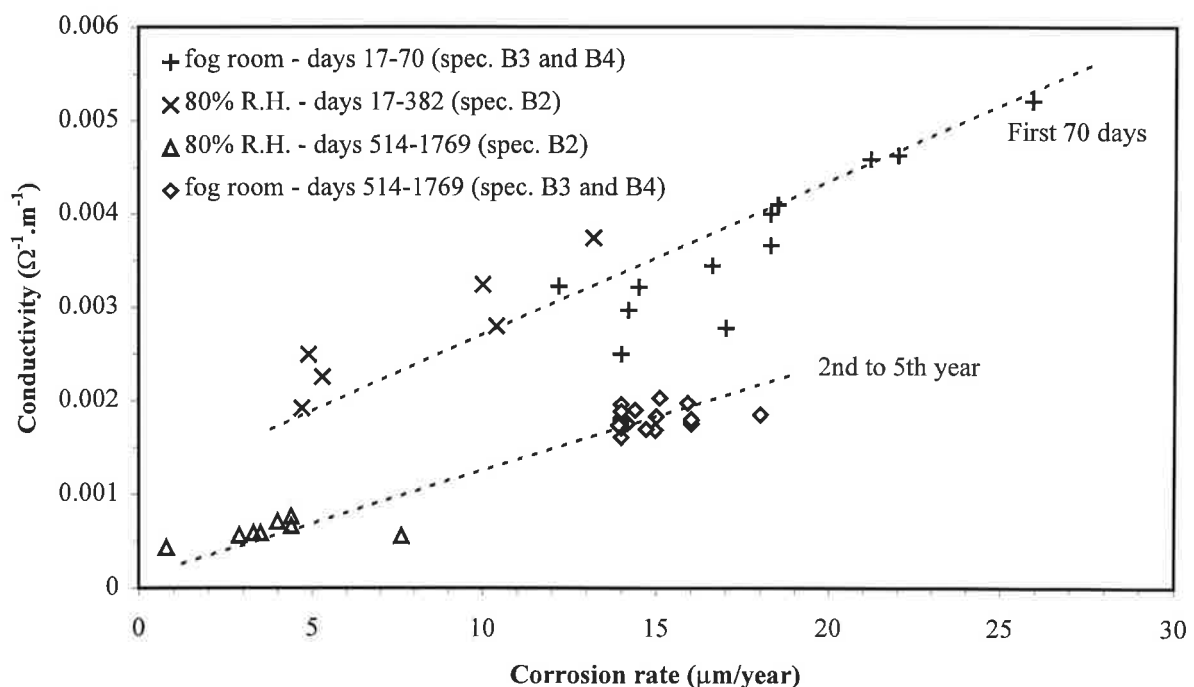
Figure 51 - Relationship between conductivity of concrete and corrosion rate of steel (measurements at 10 mm) in specimens with BFSC concrete, w/c 0.45, 2%Cl⁻ exposed to 80% R.H. and to fog room.

Apart from the first 70 days, results of specimens exposed to the fog room (B3 and B4) are quite concentrated and do not show any type of relationship; however they agree very well with the linear trend found on the specimen subjected to accelerated carbonation and exposed at 80% R.H. (see also Fig. 38). This suggests that the influence of concrete resistivity on the corrosion rate might be the same in the two conditions, at least in these three specimens with the same type of concrete (the fourth specimen, exposed to 80% R.H. but not to the carbonation treatment, had low corrosion rates and did not show any relationship on long term measurements, as shown in Fig. 37).

CONCLUSIONS

A general relationship between corrosion rate of steel and concrete resistivity, applicable to different types of concrete and environment, was not found during measurements on specimens with BFSC and OPC concrete exposed to wet (fog room) and semi-dry (80% R.H.) conditions. Nevertheless, good linear relationships were found for given specimens, when either temperature or R.H. of the environment were changed.

This correlation is quite complex, since it depends on several variables that influence both resistivity of concrete and corrosion rate of steel, which were systematically analyzed.

Moisture content in concrete had a strong influence on corrosion rate of steel and resistivity (or conductivity) of concrete. At 20°C, both corrosion rate and conductivity showed a linear dependence on R.H. during tests where the environment humidity ranged from 75% to 95% (corrosion rate was negligible, i.e. lower than 1 μm/year, in carbonated concrete without chlorides). In single specimens, a linear relationship was observed between corrosion rate of steel and conductivity of concrete when both varied owing to changes in relative humidity of the environment. Steel in concrete exposed to the fog room had significantly higher values of corrosion rate and conductivity, showing that specimens always maintained in wet conditions in the fog room had moisture contents much higher than those exposed for several years to 80% R.H., even when R.H. was increased up to 95% until a stable condition was reached. However, there was some evidence that, when other variables were constant, the relationship between corrosion rate and conductivity did not change.

Exponential dependence on temperature was found for conductivity of concrete, both on specimens exposed outside (with temperature ranging from 1 to 13°C) and on specimens cooling from 40 to 20°C at 80% R.H. Since the conductivity of a solution simulating the pore liquid was found to be linearly correlated with temperature, this behaviour is probably related to the physical or chemical interactions between ions and the cement paste. Also corrosion rate of steel showed and exponential dependence on temperature. Interpolation of experimental data of the different types of concrete showed that corrosion rate doubled for temperature increases ranging from 13 and 30°C, whereas conductivity of concrete doubled (i.e. resistivity halved) for temperature increases between 12 and 23°C. The relationship found between corrosion rate and conductivity when temperature changed was linear and coincided with the relationship found by changing the humidity of the environment.

The similar influence of temperature and R.H. on corrosion rate and conductivity in homogenous conditions, suggests that the effect of these variables on corrosion rate can be assessed by simply studying their influence on conductivity (or resistivity), once the relationship is known. However, other factors that affected both corrosion rate of steel and resistivity of concrete also altered the relationship between them.

Cement type strongly influenced the electrical resistivity of concrete: an increase of about one order of magnitude was observed comparing BFSC concrete to OPC concrete with the same mix and exposed to the same environment. A similar effect was brought about by water to cement ratio: the lower w/c, the higher the resistivity. However, it was shown that the variation in resistivity between concrete mixes with different types of cement or w/c ratio cannot be used to assess changes in the corrosion rate, since also the relationship between corrosion rate and conductivity changes.

This relationship also depends on the corrosion conditions of the rebars, and thus on the mechanisms that control corrosion. No correlation was found in passive steel in chloride free and non carbonated concrete, as expected in accordance to the anodic passive control of corrosion rate. Poor relationships were found in specimens with chloride contaminated concrete exposed to the fog room, where both corrosion rate and resistivity were rather constant during time. Conversely, good linear relationships were found in carbonated and/or chloride contaminated concrete exposed to 20°C at 75-95% R.H. and 20-40°C at 80%R.H., although the fitting line changed when carbonation occurred in chloride contaminated concrete. In these conditions also the steel potential was found to be related to corrosion rate (and thus also to resistivity of concrete) and results were in accordance with the anodic resistance control theory.

It was shown that simple measurements of resistivity of concrete are not sufficient to predict the corrosion rate of embedded steel. However, the good linear relationships found in given specimens suggest that similar correlations can be found in structures with homogeneous conditions, as far as concrete composition and environmental exposure are concerned. This has important implications for practice, since, provided the relationship between corrosion rate and concrete resistivity (or conductivity) has been studied in limited parts of the structure, resistivity mapping is likely to reveal spots with the highest corrosion rates.

The investigation regarding the influence of temperature also showed that the dependence of resistivity of concrete and corrosion on seasonal changes in temperature can be easily taken into account. Thus, corrosion rate and resistivity values measured at different temperatures can be "corrected" in order to refer to the same temperature (e.g. 20°C) so that a comparison is possible.

TNO Building and Construction Research
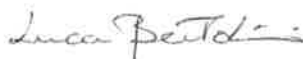
Dr. Luca Bertolini
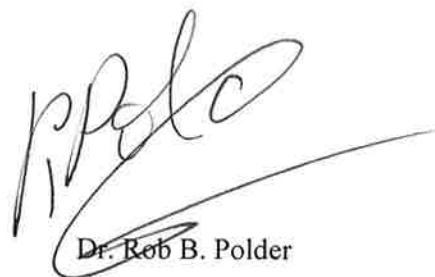
Dr. Rob B. Polder

Department of Building Technology

REFERENCES

1. G.K.Glass, C.L.Page, N.R.Short, "Factors affecting the corrosion rate of steel in carbonated mortars", Corrosion Science, **32**, 12, pp. 1283-1294, 1991.

2. P.B.Bamforth, M.Basheer, J.Chapman-Andrews, R.Cigna, M.I.Jafar, A.Mazzoni, E.Nolan, H.Wojtas, "Reinforcement corrosion and concrete resistivity - State of the art, laboratory and field results", in "Corrosion and Corrosion Protection of Steel in Concrete", Ed. R.N. Swamy, Vol. II, Sheffield Academic Press, Sheffield, pag. 1376-1381, 1994.

3. C.Alonso, C.Andrade, J.A.Gonzales, "Relation between resistivity and corrosion rate of reinforcements in carbonated mortar made with several cement types", Cement and concrete research, **8**, pp. 687-698, 1988.

4. COST 509, "Corrosion and protection of metals in contact with concrete", Draft final report, Heriot-Watt University, Edinburgh, Sept. 1-3, 1996.

5. M.Valente, R.B.Polder, R.Cigna, T.Valente, "Experimental investigation of concrete resistivity and corrosion rate of reinforcement in atmospheric conditions", TNO report BI-91-173, TNO Building and construction materials, Delft, december 1991.

6. A.Tondi, R.B.Polder, R.Cigna, "Concrete resistivity and corrosion rate of reinforcement in atmospheric concrete after one year", TNO report 93-BT-R0170, TNO Building and construction materials, Delft, March 1993.

7. A.Mazzoni, R.B.Polder, R.Cigna, "Concrete resistivity and corrosion rate of reinforcement in atmospheric conditions after two years", TNO report 94-BT-R1472, TNO Building and construction materials, Delft, December 1993.

8. S.Fiore, R.B.Polder, R.Cigna, "Corrosion rate of reinforcement and concrete resistivity of three years old concrete specimens in wet and semy dry climates", TNO report 94-BT-R1655, TNO Building and construction materials, Delft, December 1994.

9. M.Scotto di Carlo, R.B.Polder, R.Cigna, "Corrosion rate of reinforcement and concrete resistivity of five years old concrete specimens exposed to different temperatures", TNO report 96-BT-R1624/01, TNO Building and construction materials, Delft, December 1996.

10. "Corrosion of steel in concrete", Report of RILEM Technical Commiteee 60-CSC, P.Schiessl ed., Chapmann and Hall, 1988.

11. CEB, "Durable concrete structures", bulletin d'information n. 183, 1992.

12. P.Pedeferri, L.Bertolini, "La corrosione delle armature nel calcestruzzo e negli ambienti naturali", McGraw Hill Italia, Milano, 1996.

13. M.Maslehuddin, C.L.Page, Rasheeduzzafar, A.I. Al-Mana, "Effect of temperature on pore solution chemistry and reinforcement corrosion in contaminated concrete", in "Corrosion of reinforcement in concrete structures", Eds. C.L.Page, P.B.Bamforth, J.Figg, SCI, London, pp. 67-75, 1996.

14. W.Lopez, J.A.Gonzales, "Influence of temperature on the service life of rebars", Cement and concrete research, **23**, pp. 368-376, 1993.

15. H.Arup, "The mechanisms of the protection of steel by concrete", chapter 10 of: "Corrosion of reinforcement in Concrete construction", Ed. A.P.Crane, Ellis Horwood limited, pag. 151-157, 1983.

16. A.F.Baker, "Potential mapping techniques", Seminar on corrosion in concrete - Monitoring, surveying, and control by cathodic protection, London press center, 13 May 1986.

17. S.Fiore, R.B.Polder, R.Cigna, "Evaluation of the concrete corrosivity by means of resistivity measurements", in "Corrosion of reinforcement in concrete structures", Eds. C.L.Page, P.B.Bamforth, J.Figg, SCI, London, pp. 273-282, 1996.

18. O.Gjorv, O.Vennesland, "Electrical resistivity of concrete in the oceans", OTC, paper 2803, Houston, 1977.

19. H.W.Whittington, J.McCarter, M.C.Forde, "The conduction of electricity through concrete", Magazine of concrete research, **3**, No. 114, March, 1981.

20. R.B.Polder, M.B.G.Ketelaars, "Electrical resistance of blast furnace slag cement and ordinary portland cement concretes", Proc. Int. Conf. "Blended cement in construction", Ed. R.N.Swamy, Elsevier, pp. 401-415, 1991.

21. C.C.Naish, "Concrete inspection: interpretation of potential and resistivity measurements", Proc. "Corrosion of reinforcement in concrete", Eds. C.L.Page, K.W.J.Treadaway, P.B.Bamforth, Elsevier, pp. 314-332, 1990.

22. W.Lopez, J.A.Gonzales, "Influence of the degree of pore saturation on the resistivity of concrete and the corrosion rate of steel reinforcement", Cement and concrete research, **23**, pp. 368-376, 1993.

23. C.Andrade, J.Sarria, C.Alonso, "Statistical study on the simultaneous monitoring of rebar corrosion rate and internal relative humidity in concrete structures exposed to the atmosphere", in "Corrosion of reinforcement in concrete structures", Eds. C.L.Page, P.B.Bamforth, J.Figg, SCI, London, pp. 233-242, 1996.

24. S.Feliu, J.A.Gonzales, S.Feliu Jr., C.Andrade, "Relationship between conductivity of concrete and corrosion of reinforcing bars", British corrosion journal, **24**, 3, pp. 195-198, 1989.

25. D.Bürchler, B.Elsener, H.Böhni, "Electrochemical resistivity and dielectrical properties of hardened cement paste and mortar", in "Corrosion of reinforcement in concrete structures", Eds. C.L.Page, P.B.Bamforth, J.Figg, SCI, London, pp. 283-293, 1996.

26. W.Elkey, E.J.Sellevold, "Electrical resistivity of concrete, in "Corrosion of reinforcement - Field and labortory studies for modelling and service life", Ed. K.Tuutti, University of Lund, Report TVBM-3064, p. 303-334, February 1995.

27. C.L.Page, Ø.Vennesland, "Pore solution composition and chloride binding capacity of silica fume cement pastes", Materiaux et constructions, **16**, 91, 1983.

28. J.A.Larbi, A.L.A. Fraay, J.M.J.M.Bijen, "The chemistry of the pore solution of silica fume-blended cement systems", Cement and concrete research, **20**, pp. 506-516, 1990.

29. J.Tritthart, "Chloride binding in cement - I. Investigations to determine the composition of porewater in hardened cement", Cement and concrete research, **19**, p. 586-594, 1989.

30. J.Tritthart, "Chloride binding in cement - II. The influence of the hydroxide concentration in the pore solution of hardened cement paste on chloride binding", Cement and concrete research, **19**, p. 586-594, 1989.

31. R.B.Polder, "Chloride in cement-sand mortar - A. Expression experiments", TNO report BI-86-21, april 1986.

32. W.R.Holden, C.L.Page, N.R.Short, "The influence of chlorides and sulphates on durability", chapter 9 of: "Corrosion of reinforcement in Concrete construction", Ed. A.P.Crane, Ellis Horwood limited, pag. 143-150, 1983.

33. G.Sergi, "Corrosion of steel in concrete: cement matrix variables", PhD Thesis, University of Aston, Birmingham, 1986.

34. P.Sanberg, "Pore solution chemistry in concrete", in "Corrosion of reinforcement - Field and laboratory studies for modelling and service life", Ed. K.Tuutti, University of Lund, Report TVBM-3064, p. 161-170, February 1995.

35. R.B.Polder, R.J.Walker, C.L.Page, "Electrochemical desalination of cores from a reinforced concrete coastal structure", Magazine of concrete research, **47**, 173, p. 321-327, 1995.

36. P.Perry, "Chemical engineers handbook", McGraw Hill, 1963.

37. M.Kriechbaum, G.Degovics, P.Laggner, J.Tritthart, "Investigations on cement pastes by small-angle X-ray scattering and BET: the relevance of fractal geometry", Advances in cement research, **6**, No. 23, July, p. 93-101, 1994.

38. G.Bianchi, T.Mussini, "Fondamenti di elettrochimica: teoria e applicazione", Masson Editore, Milano, 1993.

39. CRISON conductimeter, Manual of instructions.

40. J.A.Gonzales, C.Andrade, "Corrosion of reinforcing bars in carbonated concrete", British corrosion journal, **15**, p. 135, 1980.

41. C.Andrade, M.C.Alonso, J.A.Gonzales, S.Feliu, "Similarity between atmospheric / underground corrosion and reinforced concrete corrosion", Proc. "Corrosion of reinforcement in concrete", Eds. C.L.Page, K.W.J.Treadaway, P.B.Bamforth, Elsevier, pp. 314-332, 1990.

42. R.B.Polder, "Chloride diffusion and resistivity testing of five concrete mixes for marine environment", Proc. RILEM int. Workshop on "Chloride penetration into concrete", St. Remy les Chevreuses, October 15-18, 1995.

43. D.E.Macphee, H.T.Cao, "Theoretical description of impact of blast furnace slag (BFS) on steel passivation in concrete", Magazine of concrete research, **45**, 162, p. 63-69, 1993.

44. R.B.Polder, R.F.M.Bakker, Discussion on the paper "Theoretical description of impact of blast furnace slag (BFS) on steel passivation in concrete", Magazine of concrete research, **46**, 167, p. 151-154, 1994.

APPENDIX A

Corrosion rate of steel, resistivity of concrete and steel potential against time
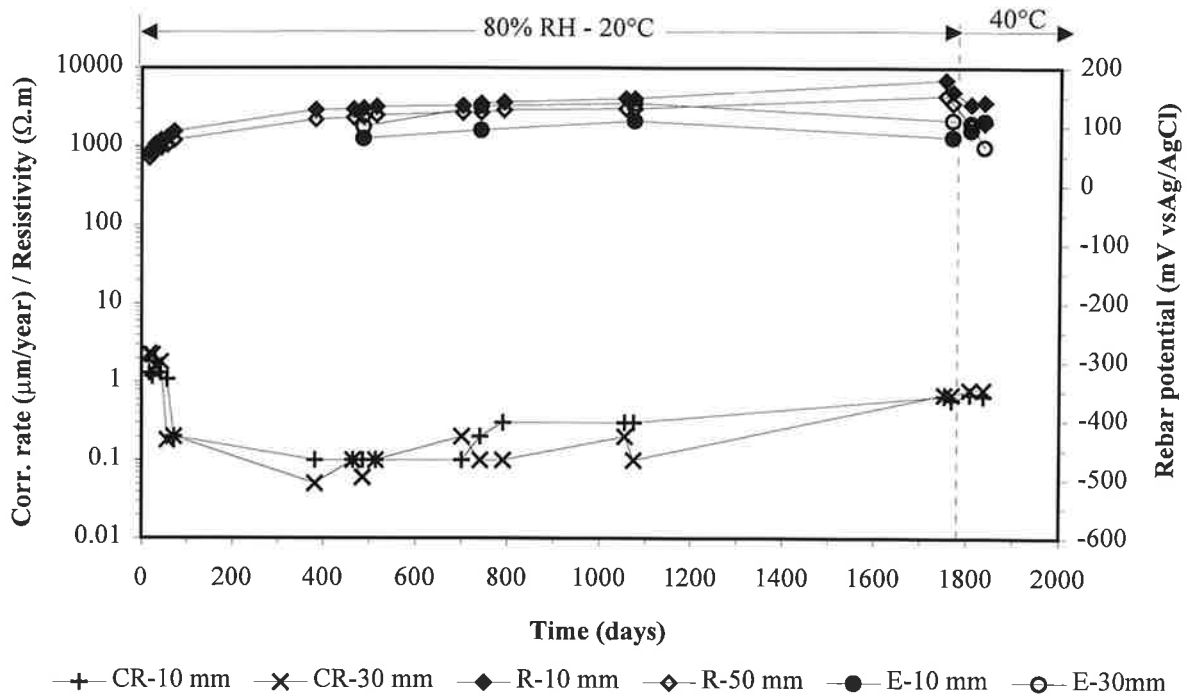
Figure A.1 - Corrosion rate of steel (CR), resistivity of concrete (R, measured with two-point method) and steel potential (E) against time in specimen *A1* (BFSC cement, w/c 0.45, no Cl⁻), exposed in the 80% R.H. room.
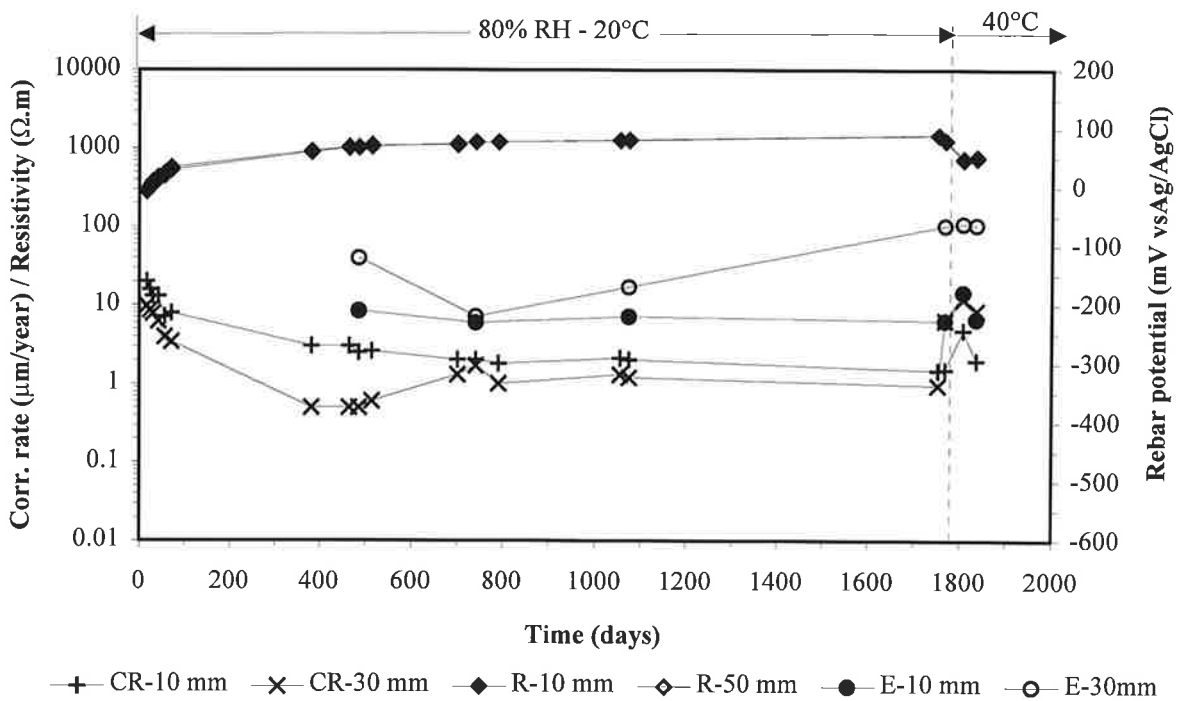
Figure A.2 - Corrosion rate of steel (CR), resistivity of concrete (R, measured with two-point method) and steel potential (E) against time in specimen *B1* (BFSC cement, w/c 0.45, 2% Cl⁻), exposed in the 80% R.H. room.
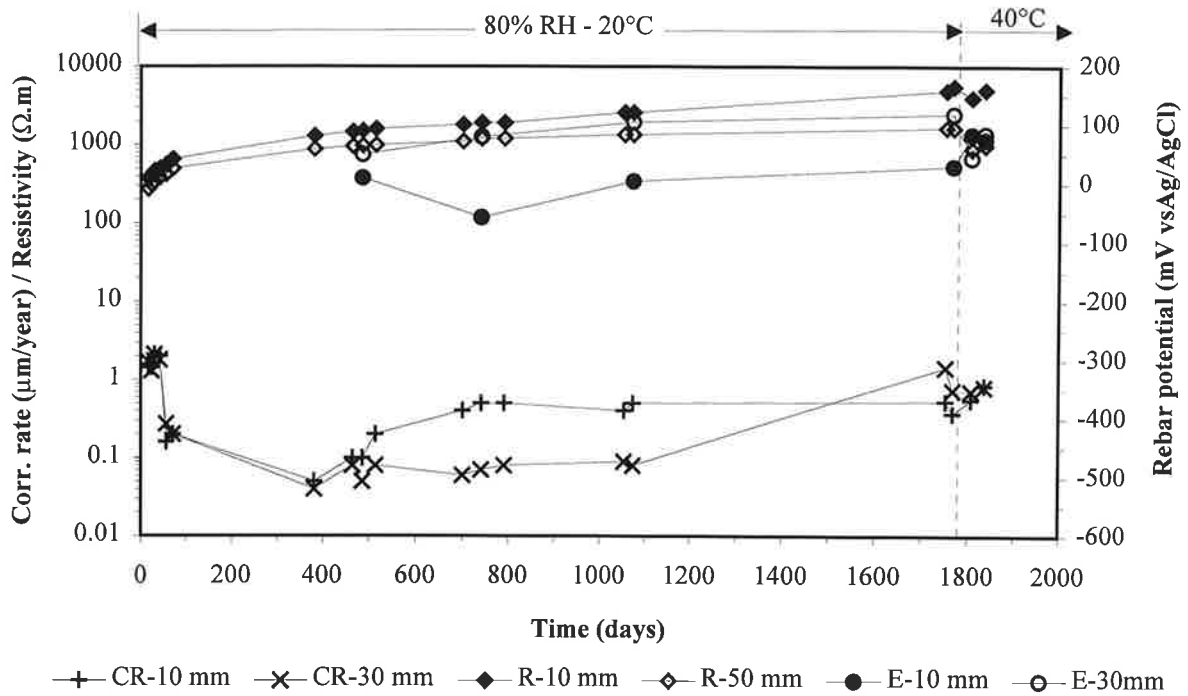
Figure A.3 - Corrosion rate of steel (CR), resistivity of concrete (R, measured with two-point method) and steel potential (E) against time in specimen *C1* (BFSC cement, w/c 0.65, no Cl⁻), exposed in the 80% R.H. room.
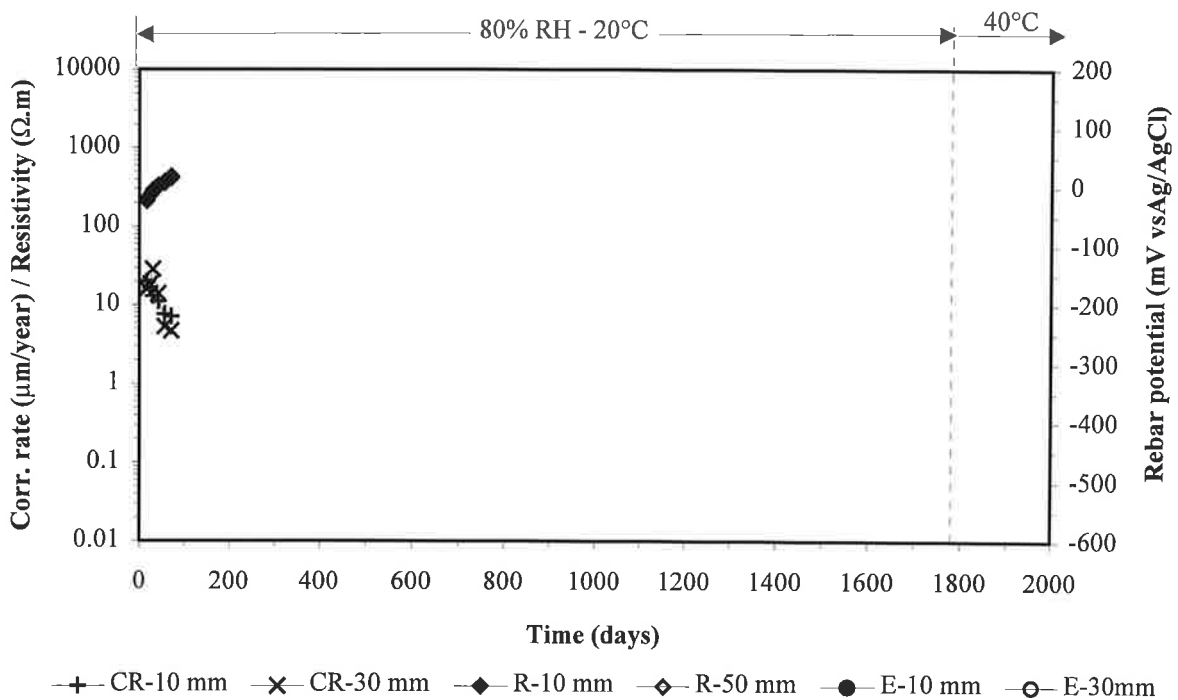
Figure A.4 - Corrosion rate of steel (CR), resistivity of concrete (R, measured with two-point method) and steel potential (E) against time in specimen *D1* (BFSC cement, w/c 0.65, 2% Cl⁻), exposed in the 80% R.H. room.
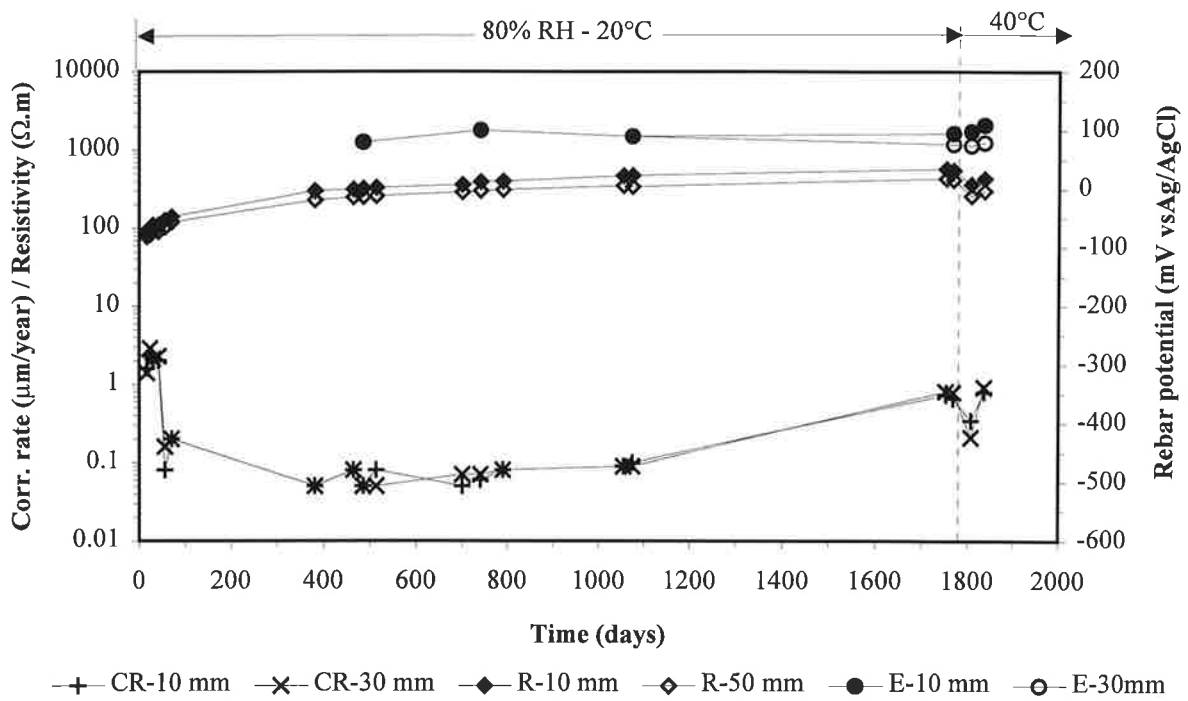
Figure A.5 - Corrosion rate of steel (CR), resistivity of concrete (R, measured with two-point method) and steel potential (E) against time in specimen *E1* (OPC cement, w/c 0.45, no Cl⁻), exposed in the 80% R.H. room.
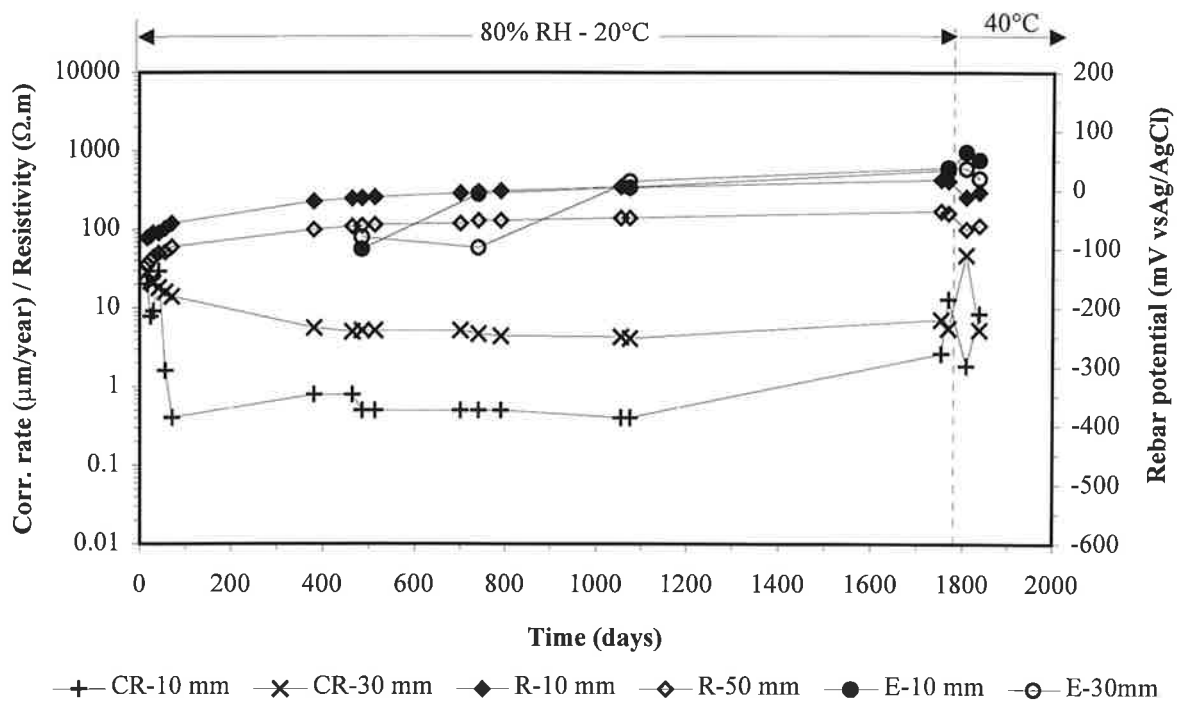
Figure A.6 - Corrosion rate of steel (CR), resistivity of concrete (R, measured with two-point method) and steel potential (E) against time in specimen *F1* (OPC cement, w/c 0.45, 2% Cl⁻), exposed in the 80% R.H. room.
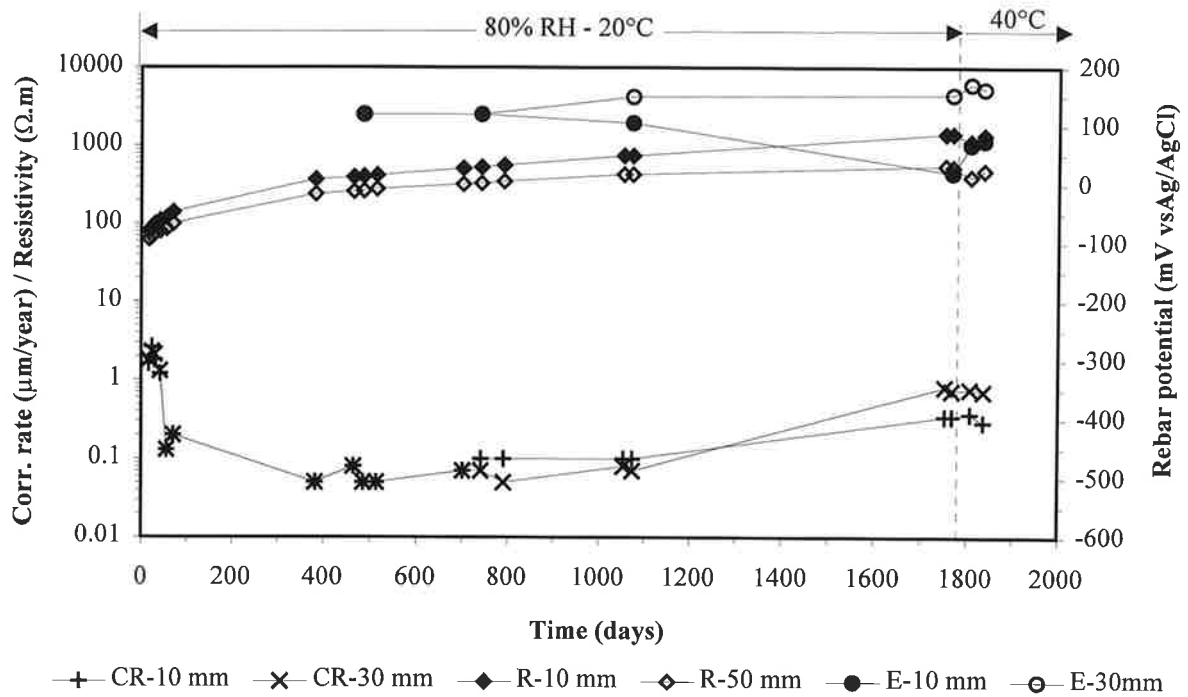
Figure A.7 - Corrosion rate of steel (CR), resistivity of concrete (R, measured with two-point method) and steel potential (E) against time in specimen *G1* (OPC cement, w/c 0.65, no Cl⁻), exposed in the 80% R.H. room.
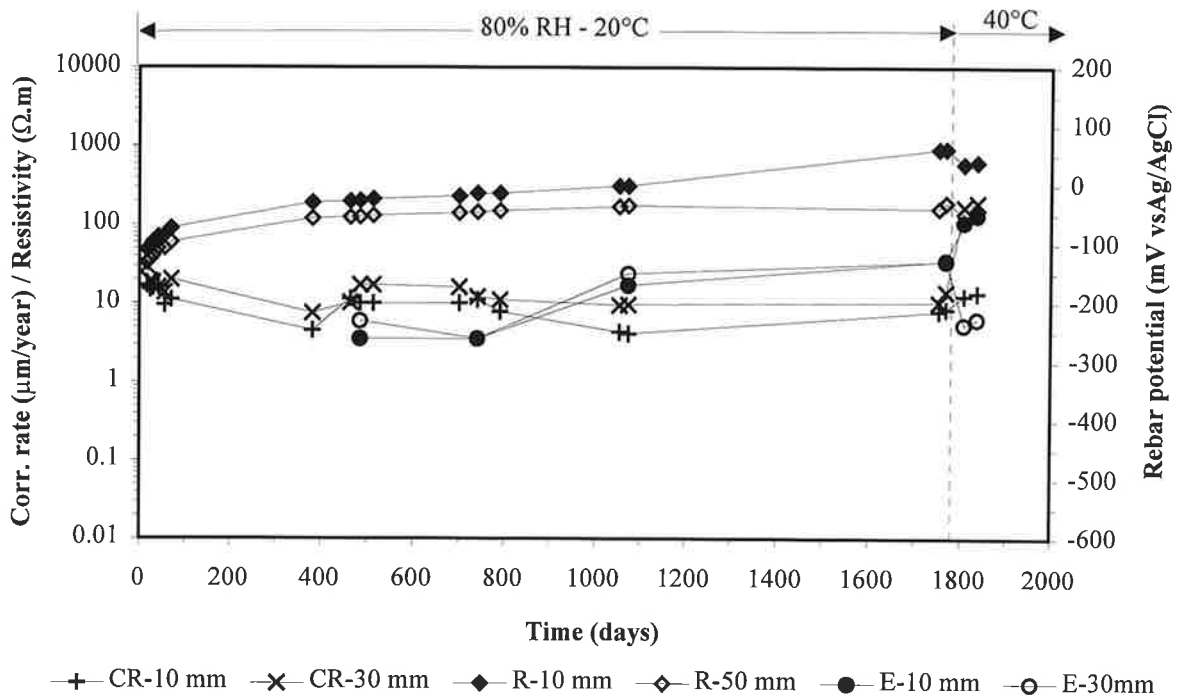
Figure A.8 - Corrosion rate of steel (CR), resistivity of concrete (R, measured with two-point method) and steel potential (E) against time in specimen *H1* (OPC cement, w/c 0.65, 2% Cl⁻), exposed in the 80% R.H. room.
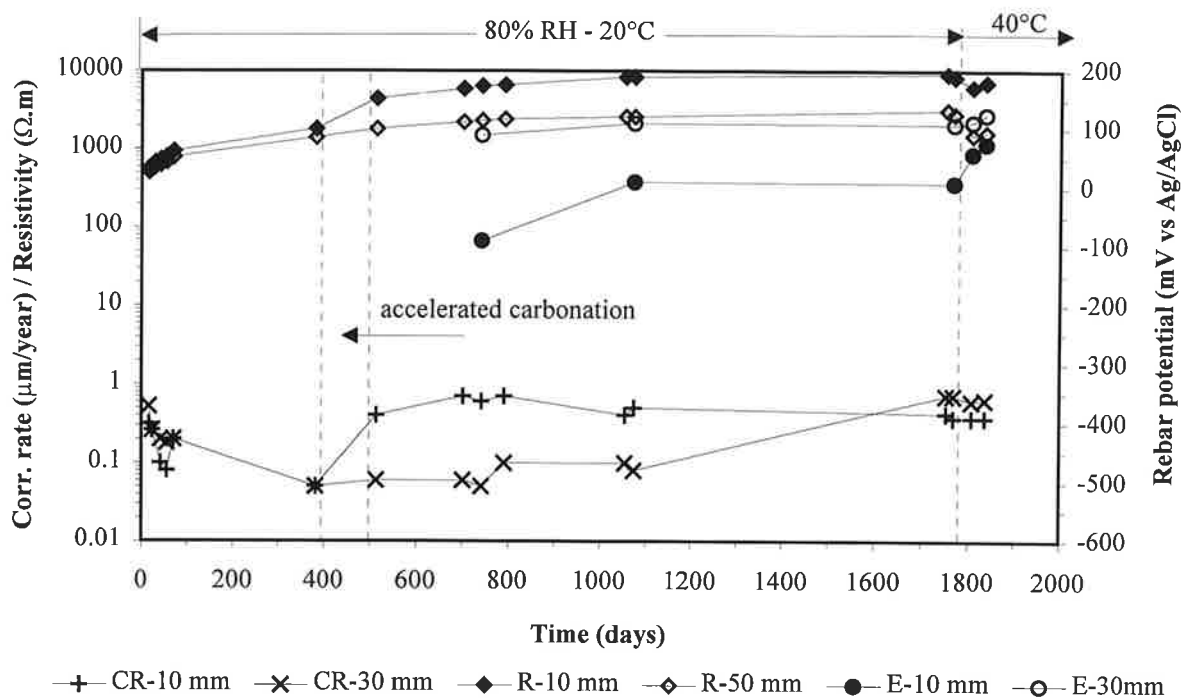
Figure A.9 - Corrosion rate of steel (CR), resistivity of concrete (R, measured with two-point method) and steel potential (E) against time in specimen *A2* (BFSC cement, w/c 0.45, no Cl⁻), exposed in the 80% R.H. room. Specimen subject to accelerated carbonation.
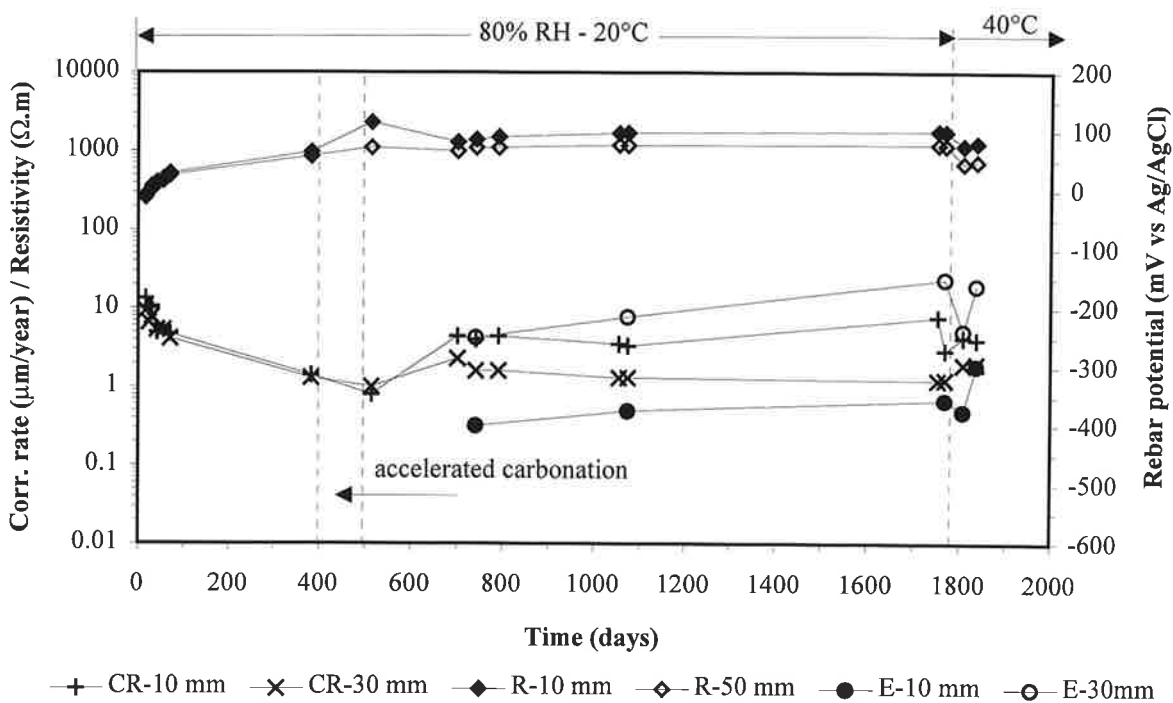
Figure A.10 - Corrosion rate of steel (CR), resistivity of concrete (R, measured with two-point method) and steel potential (E) against time in specimen *B2* (BFSC cement, w/c 0.45, 2% Cl⁻), exposed in the 80% R.H. room. Specimen subject to accelerated carbonation.
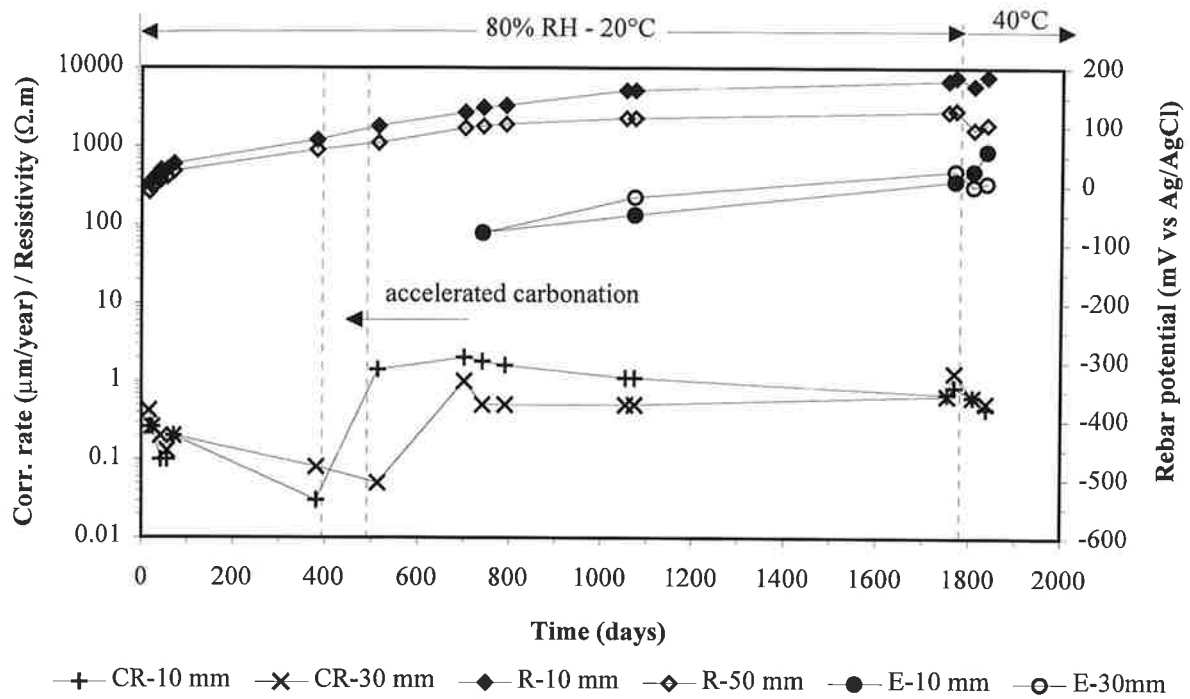
Figure A.11 - Corrosion rate of steel (CR), resistivity of concrete (R, measured with two-point method) and steel potential (E) against time in specimen *C2* (BFSC cement, w/c 0.65, no Cl⁻), exposed in the 80% R.H. room. Specimen subject to accelerated carbonation.
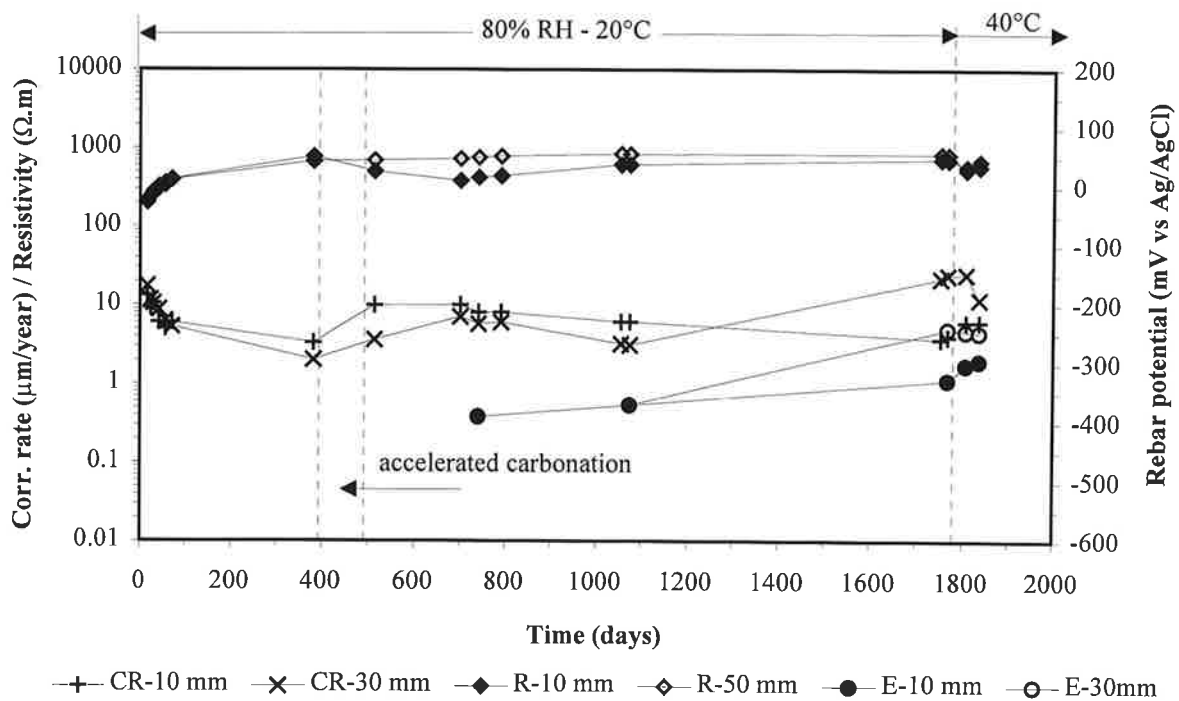
Figure A.12 - Corrosion rate of steel (CR), resistivity of concrete (R, measured with two-point method) and steel potential (E) against time in specimen *D2* (BFSC cement, w/c 0.65, 2% Cl⁻), exposed in the 80% R.H. room. Specimen subject to accelerated carbonation.
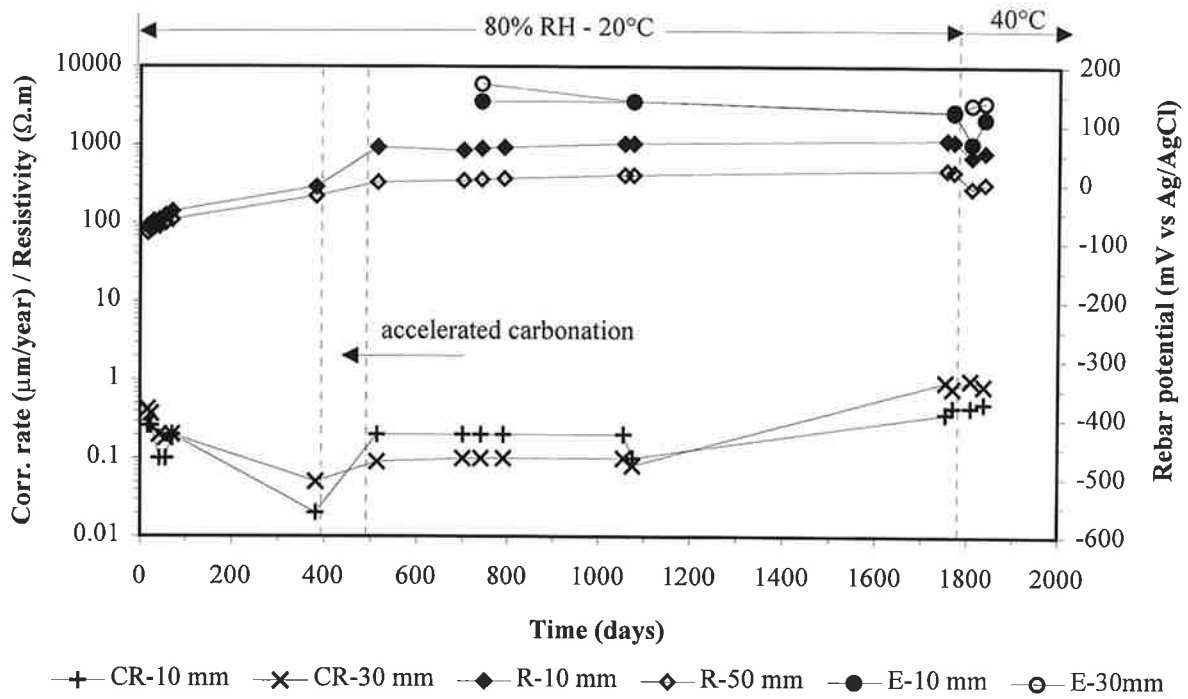
Figure A.13 - Corrosion rate of steel (CR), resistivity of concrete (R, measured with two-point method) and steel potential (E) against time in specimen *E2* (OPC cement, w/c 0.45, no Cl⁻), exposed in the 80% R.H. room. Specimen subject to accelerated carbonation.
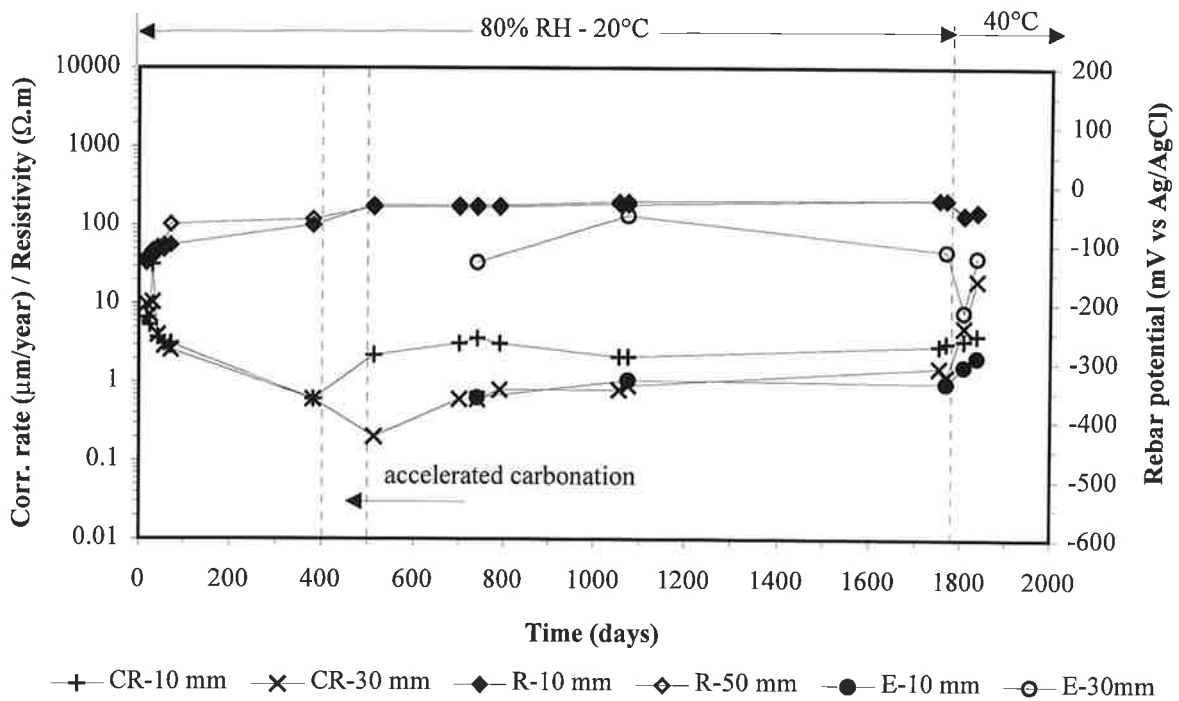
Figure A.14 - Corrosion rate of steel (CR), resistivity of concrete (R, measured with two-point method) and steel potential (E) against time in specimen *F2* (OPC cement, w/c 0.45, 2% Cl⁻), exposed in the 80% R.H. room. Specimen subject to accelerated carbonation.
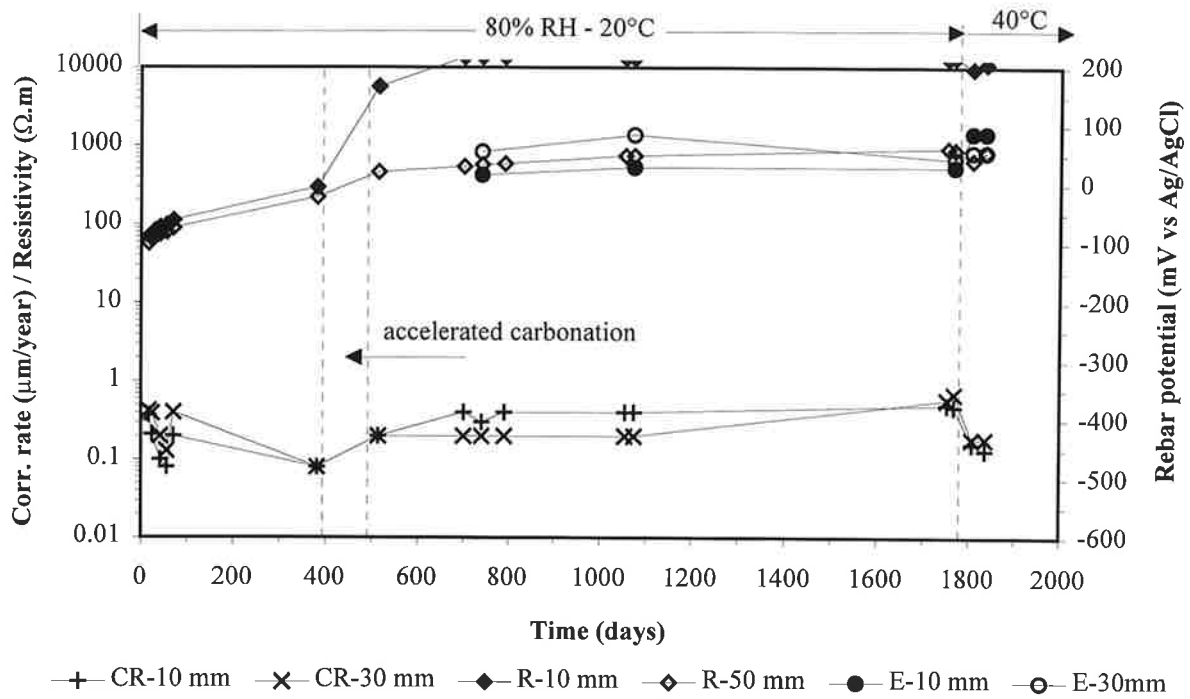
Figure A.15 - Corrosion rate of steel (CR), resistivity of concrete (R, measured with two-point method) and steel potential (E) against time in specimen *G2* (OPC cement, w/c 0.65, no Cl⁻), exposed in the 80% R.H. room. Specimen subject to accelerated carbonation.
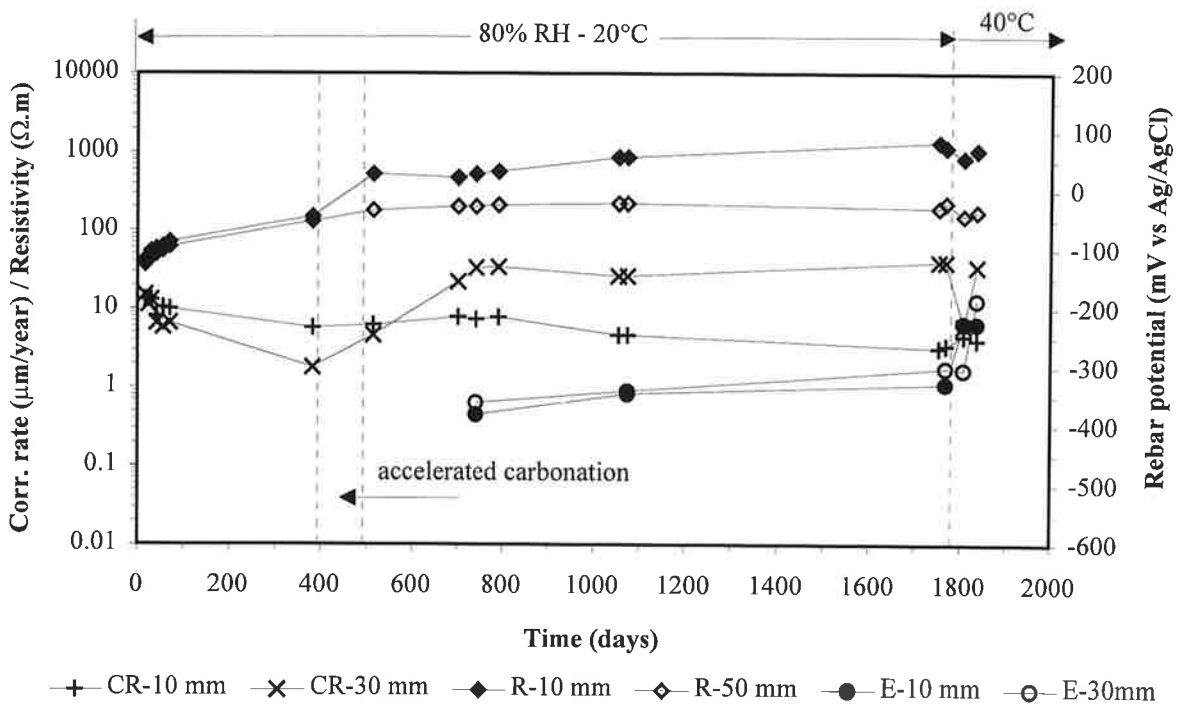
Figure A.16 - Corrosion rate of steel (CR), resistivity of concrete (R, measured with two-point method) and steel potential (E) against time in specimen *H2* (OPC cement, w/c 0.65, 2% Cl⁻), exposed in the 80% R.H. room. Specimen subject to accelerated carbonation.
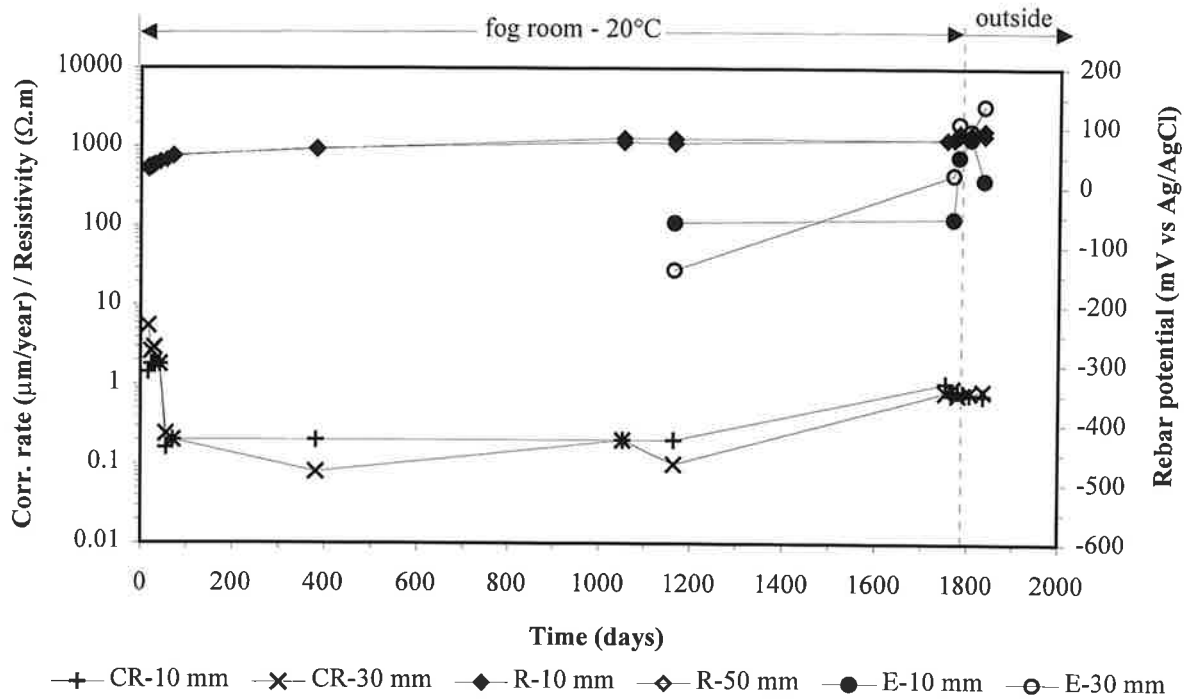
Figure A.17 - Corrosion rate of steel (CR), resistivity of concrete (R, measured with two-point method) and steel potential (E) against time in specimen *A3* (BFSC cement, w/c 0.45, no Cl⁻), exposed in the fog room and outside.
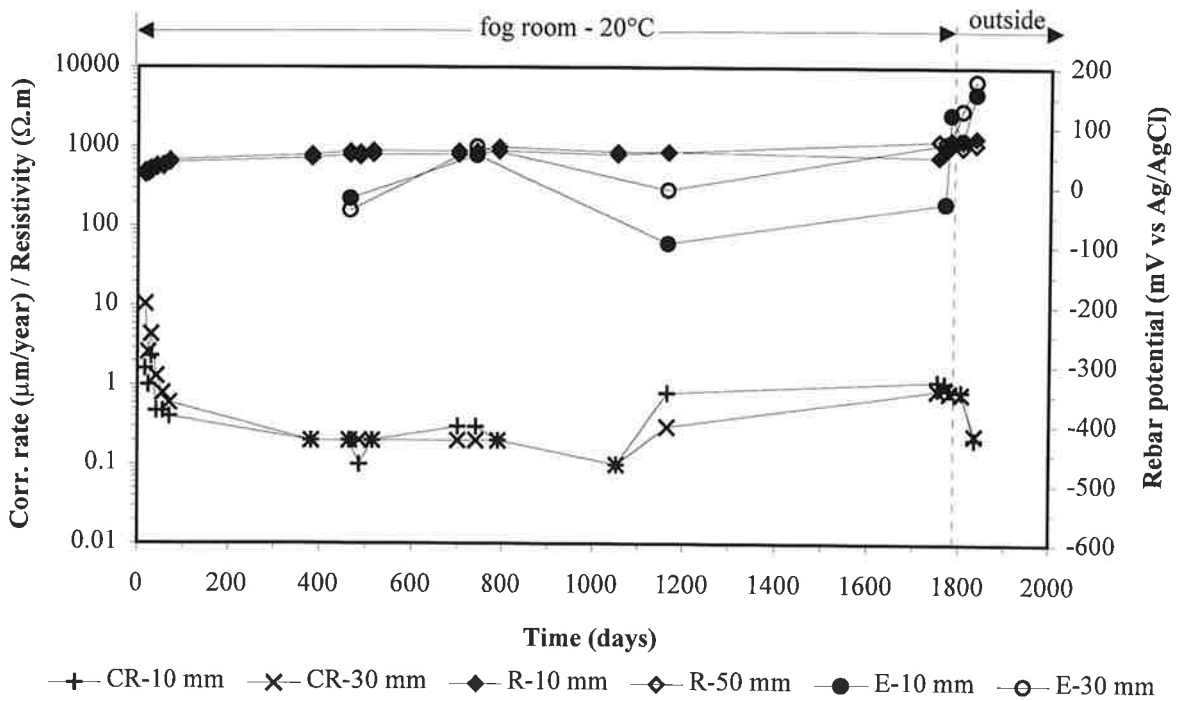
Figure A.18 - Corrosion rate of steel (CR), resistivity of concrete (R, measured with two-point method) and steel potential (E) against time in specimen *A4* (BFSC cement, w/c 0.45, no Cl⁻), exposed in the fog room and outside.
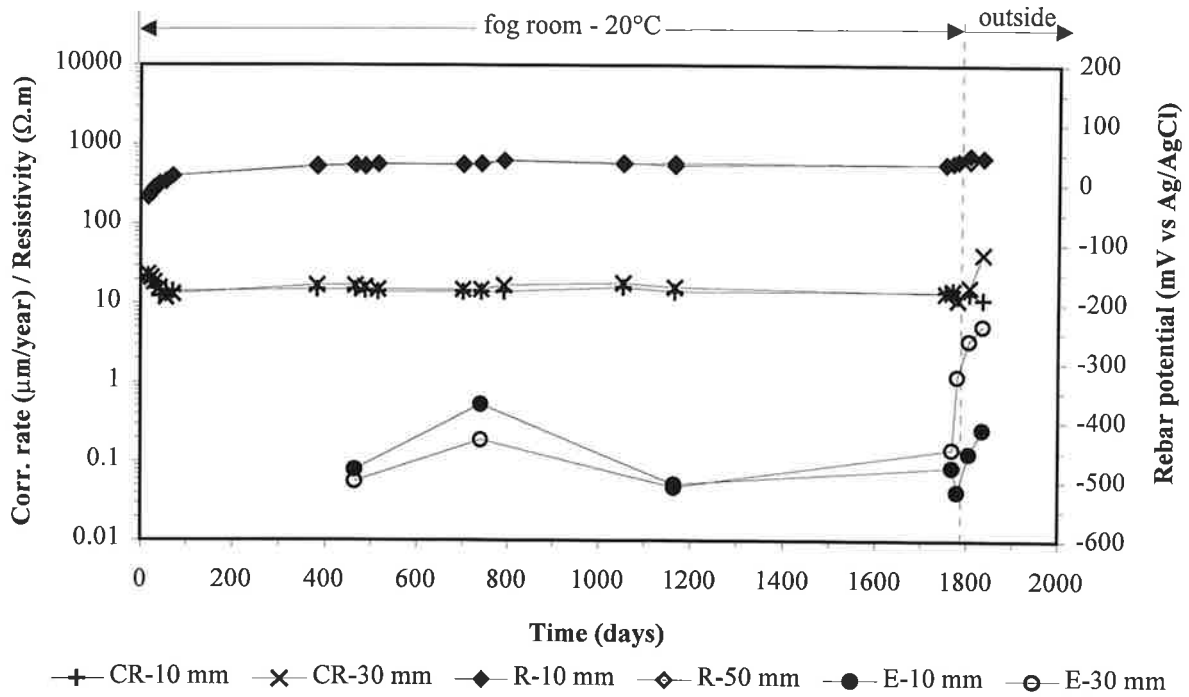
Figure A.19 - Corrosion rate of steel (CR), resistivity of concrete (R, measured with two-point method) and steel potential (E) against time in specimen *B3* (BFSC cement, w/c 0.45, 2% Cl⁻), exposed in the fog room and outside.
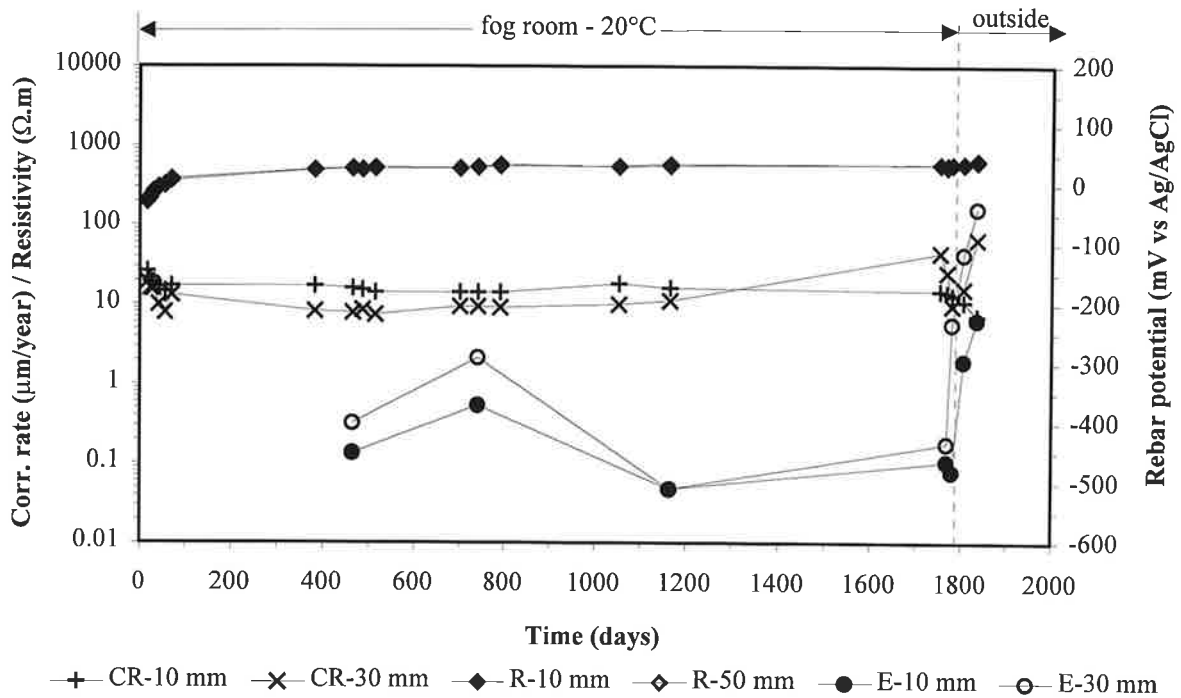
Figure A.20 - Corrosion rate of steel (CR), resistivity of concrete (R, measured with two-point method) and steel potential (E) against time in specimen *B4* (BFSC cement, w/c 0.45, 2% Cl⁻), exposed in the fog room and outside.
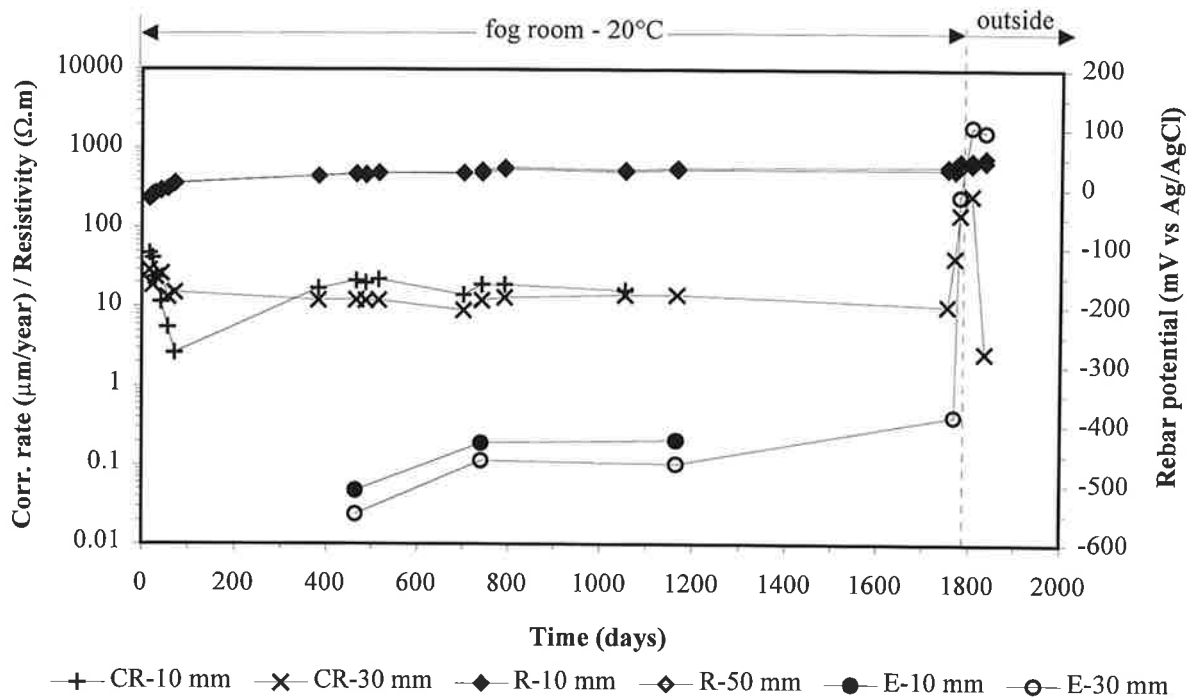
Figure A.21 - Corrosion rate of steel (CR), resistivity of concrete (R, measured with two-point method) and steel potential (E) against time in specimen *C3* (BFSC cement, w/c 0.65, no Cl⁻), exposed in the fog room and outside.
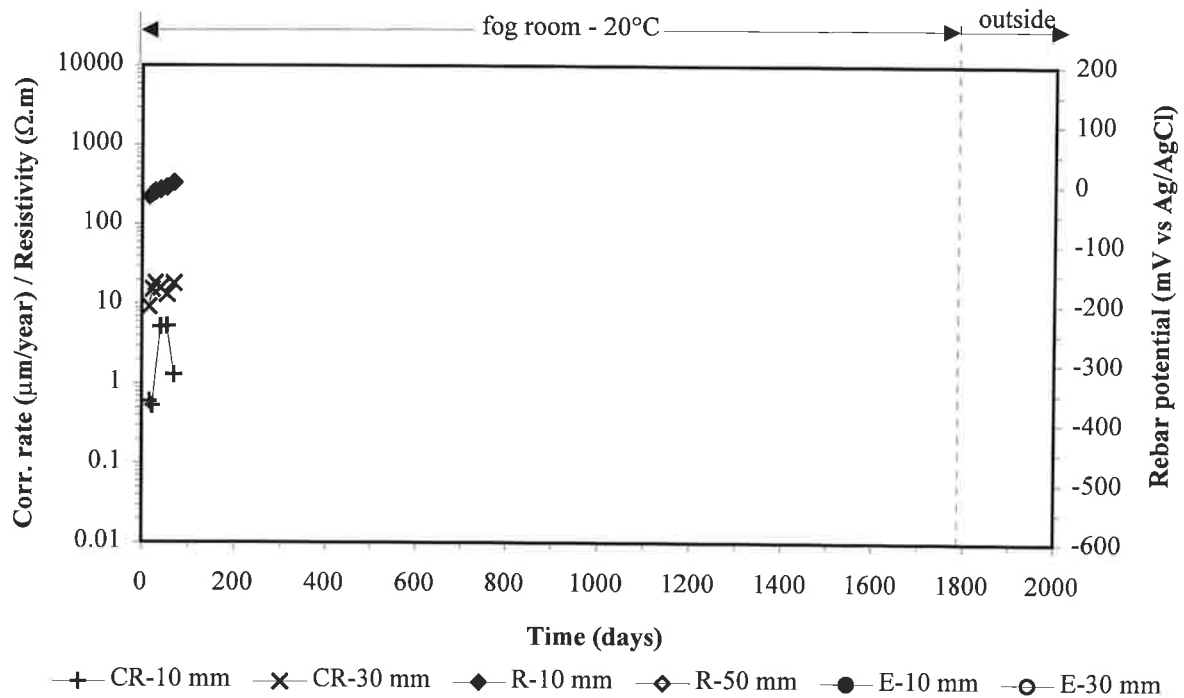
Figure A.22 - Corrosion rate of steel (CR), resistivity of concrete (R, measured with two-point method) and steel potential (E) against time in specimen *C4* (BFSC cement, w/c 0.65, no Cl⁻), exposed in the fog room and outside.
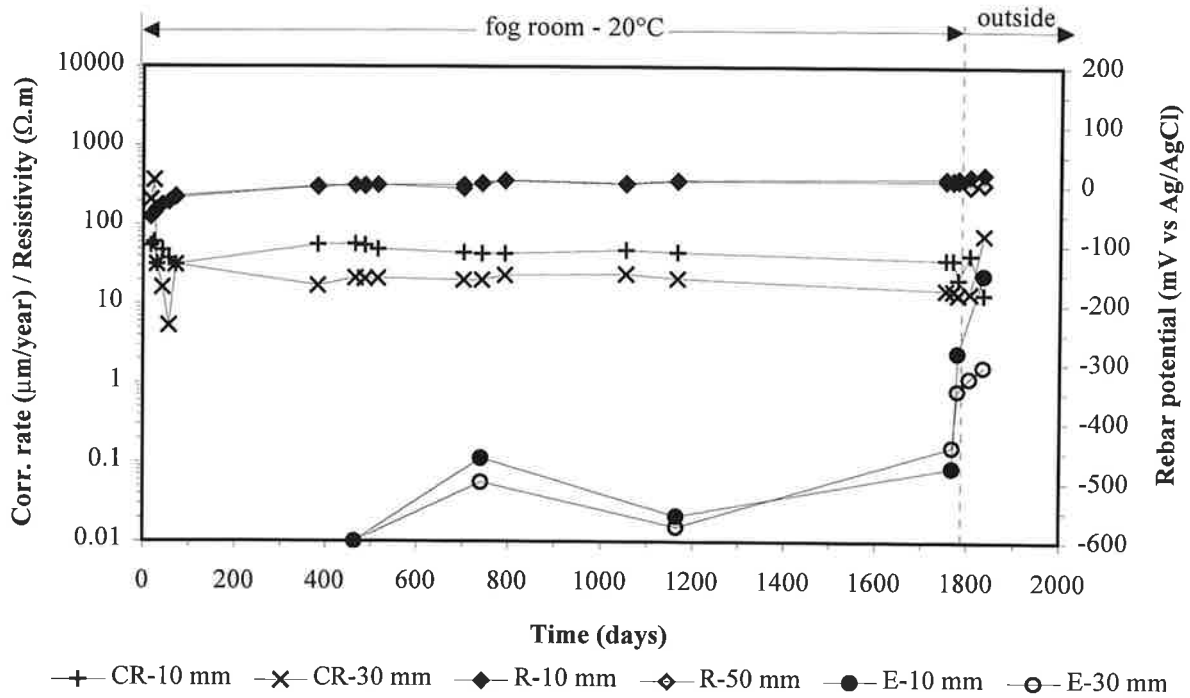
Figure A.23 - Corrosion rate of steel (CR), resistivity of concrete (R, measured with two-point method) and steel potential (E) against time in specimen *D3* (BFSC cement, w/c 0.65, 2% Cl⁻), exposed in the fog room and outside.
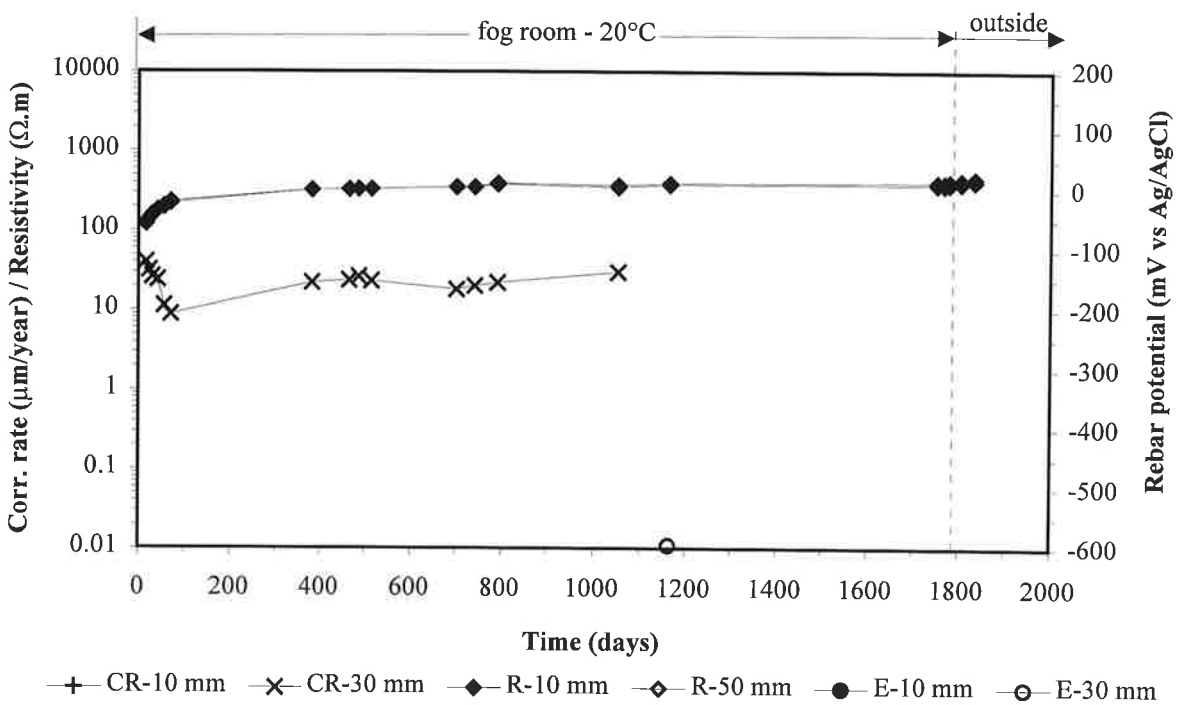
Figure A.24 - Corrosion rate of steel (CR), resistivity of concrete (R, measured with two-point method) and steel potential (E) against time in specimen *D4* (BFSC cement, w/c 0.65, 2% Cl⁻), exposed in the fog room and outside.
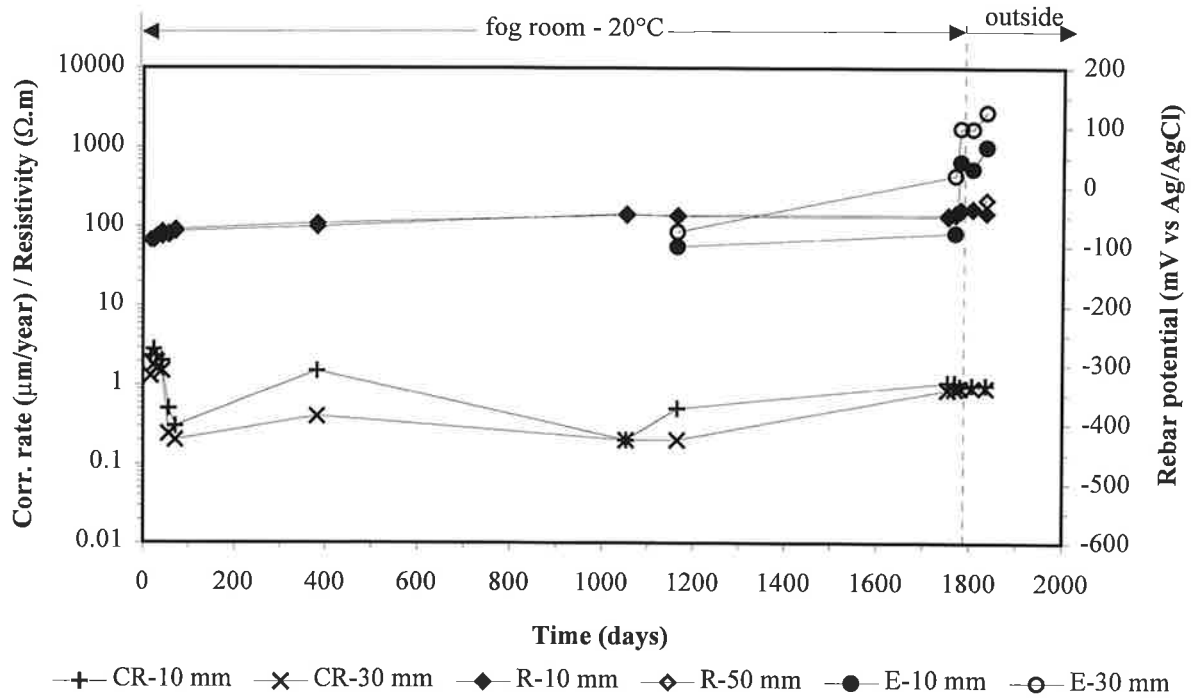
Figure A.25 - Corrosion rate of steel (CR), resistivity of concrete (R, measured with two-point method) and steel potential (E) against time in specimen *E3* (OPC cement, w/c 0.45, no Cl⁻), exposed in the fog room and outside.
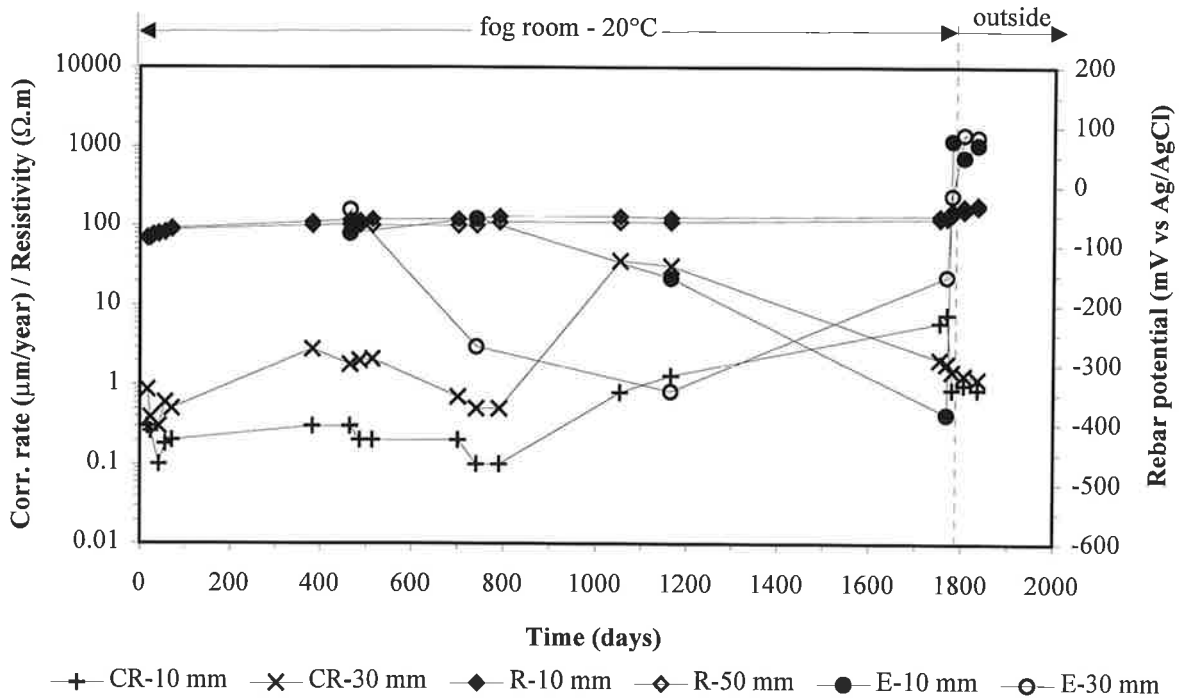
Figure A.26 - Corrosion rate of steel (CR), resistivity of concrete (R, measured with two-point method) and steel potential (E) against time in specimen *E4* (OPC cement, w/c 0.45, no Cl⁻), exposed in the fog room and outside.
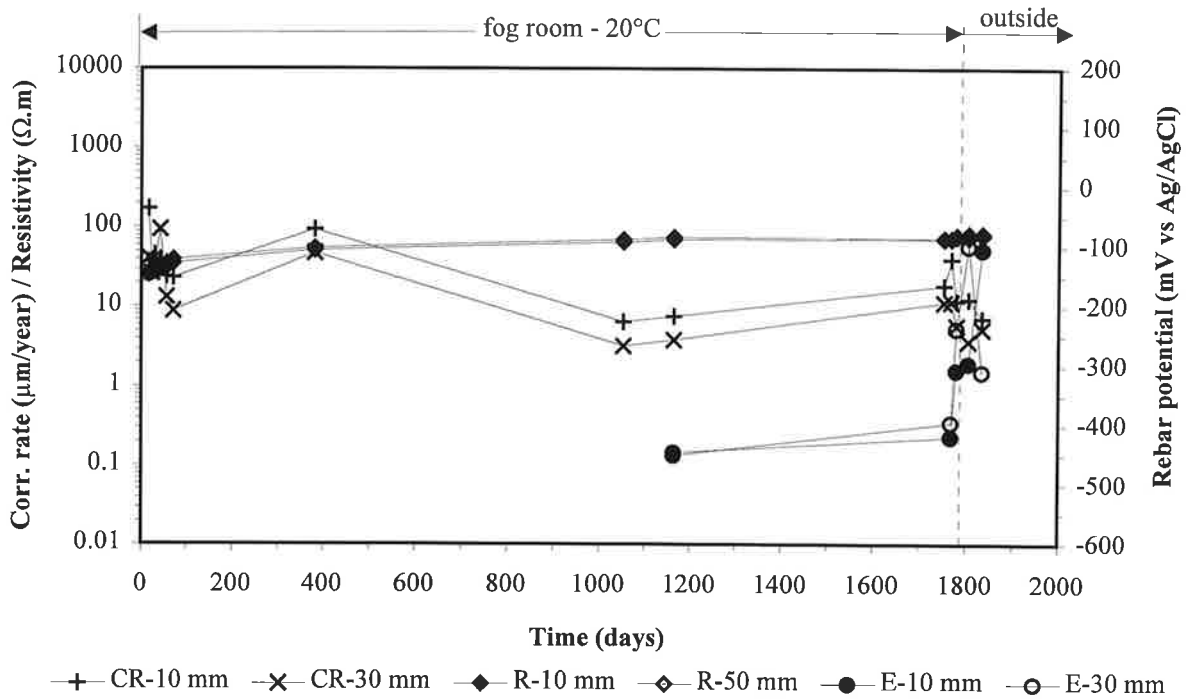
Figure A.27 - Corrosion rate of steel (CR), resistivity of concrete (R, measured with two-point method) and steel potential (E) against time in specimen *F3* (OPC cement, w/c 0.45, 2% Cl⁻), exposed in the fog room and outside.
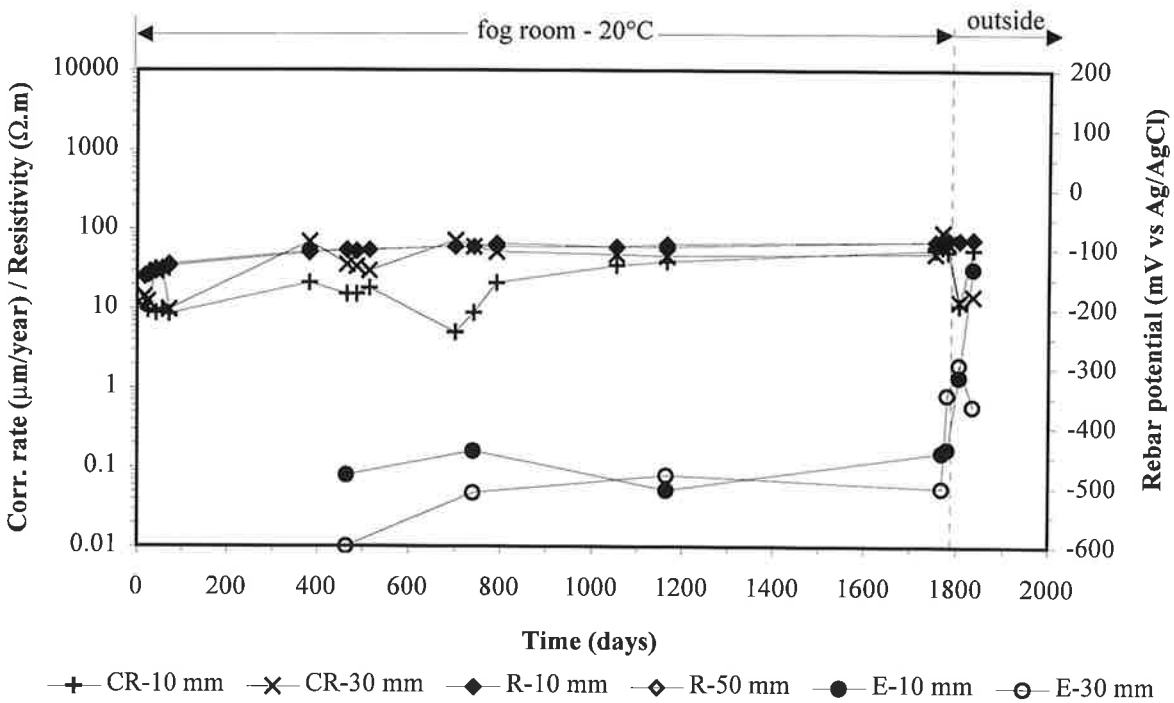
Figure A.28 - Corrosion rate of steel (CR), resistivity of concrete (R, measured with two-point method) and steel potential (E) against time in specimen *F4* (OPC cement, w/c 0.45, 2% Cl⁻), exposed in the fog room and outside.
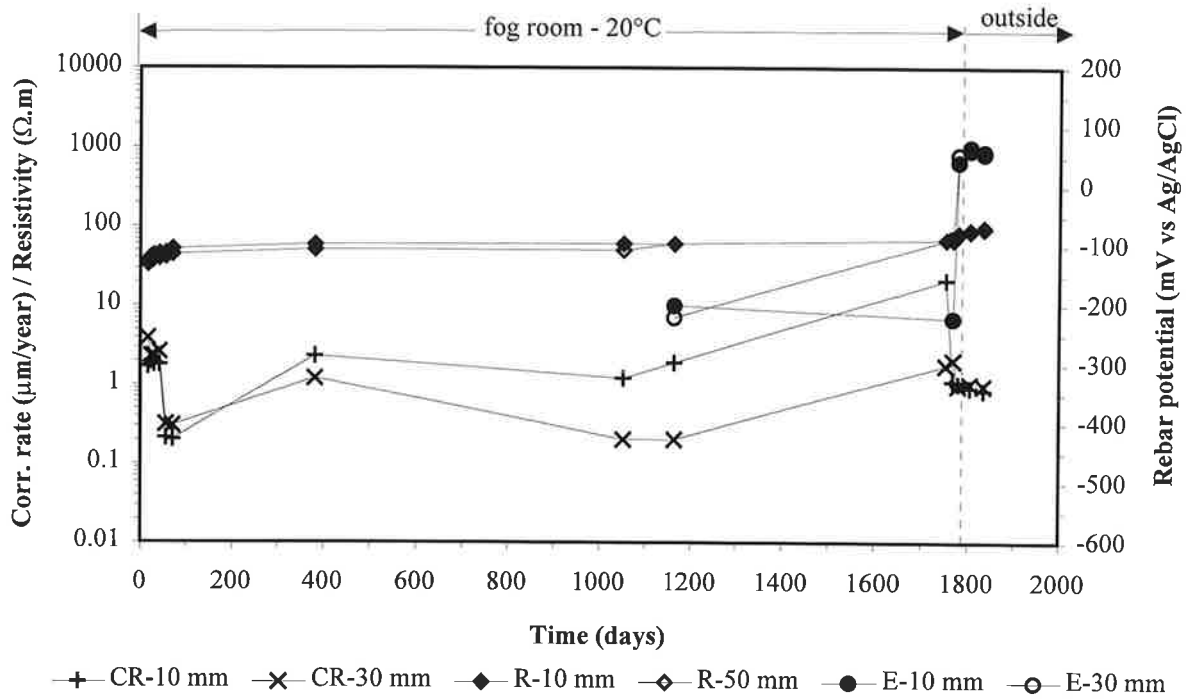
Figure A.29 - Corrosion rate of steel (CR), resistivity of concrete (R, measured with two-point method) and steel potential (E) against time in specimen *G3* (OPC cement, w/c 0.65, no Cl⁻), exposed in the fog room and outside.
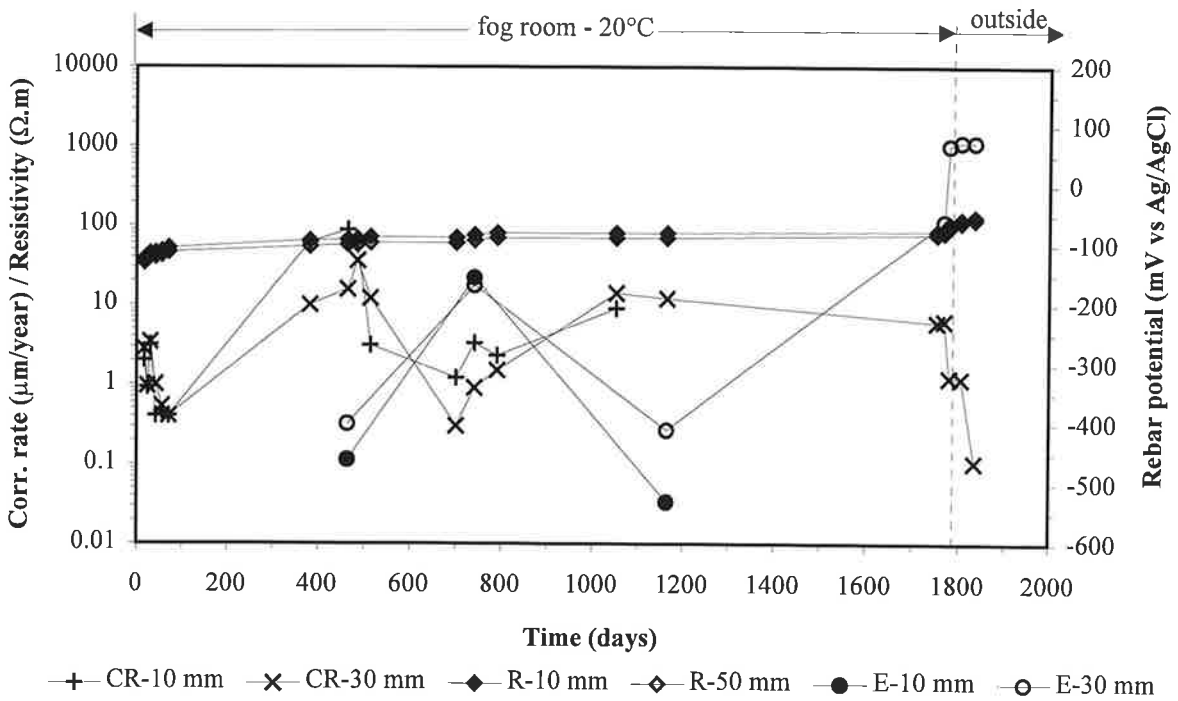
Figure A.30 - Corrosion rate of steel (CR), resistivity of concrete (R, measured with two-point method) and steel potential (E) against time in specimen *G4* (OPC cement, w/c 0.65, no Cl⁻), exposed in the fog room and outside.
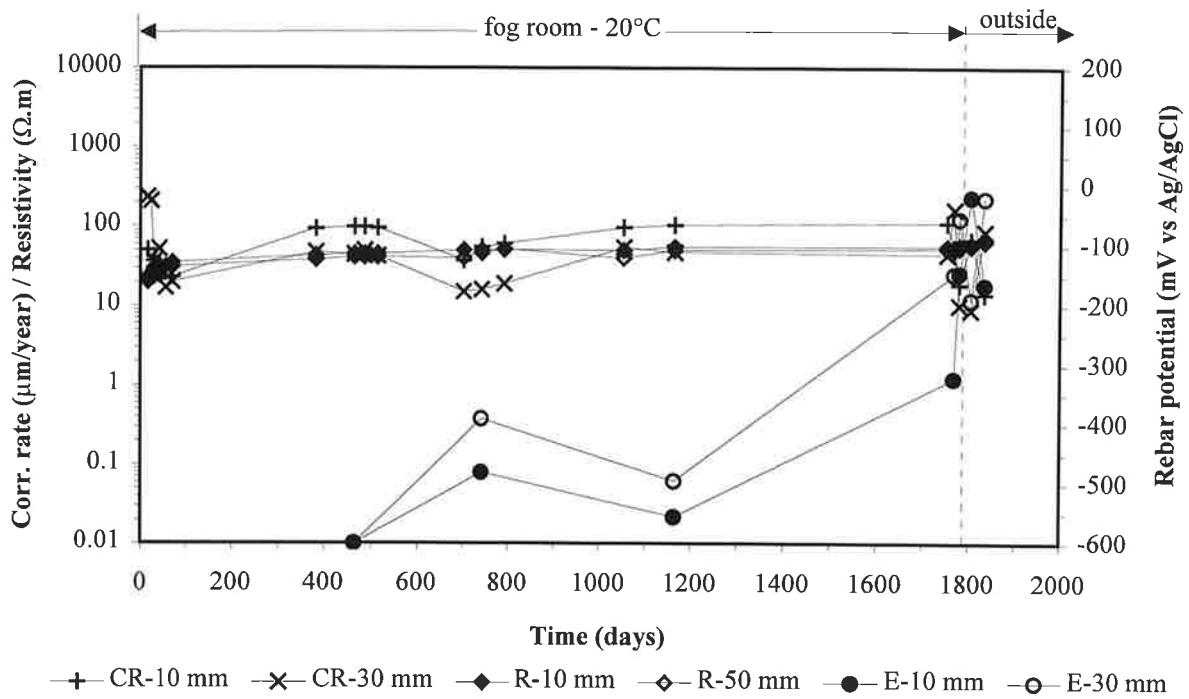
Figure A.31 - Corrosion rate of steel (CR), resistivity of concrete (R, measured with two-point method) and steel potential (E) against time in specimen *H3* (OPC cement, w/c 0.65, 2% Cl⁻), exposed in the fog room and outside.
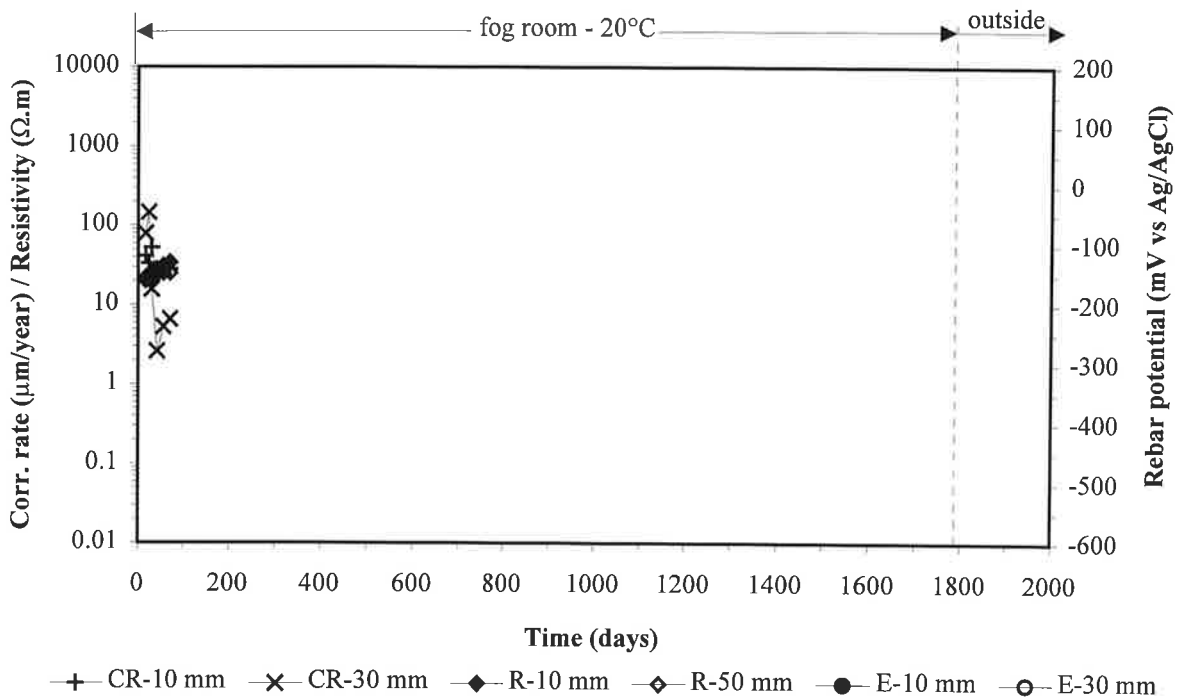
Figure A.32 - Corrosion rate of steel (CR), resistivity of concrete (R, measured with two-point method) and steel potential (E) against time in specimen *H4* (OPC cement, w/c 0.65, 2% Cl⁻), exposed in the fog room and outside.

APPENDIX B

Corrosion rate - resistivity and corrosion rate - potential correlations
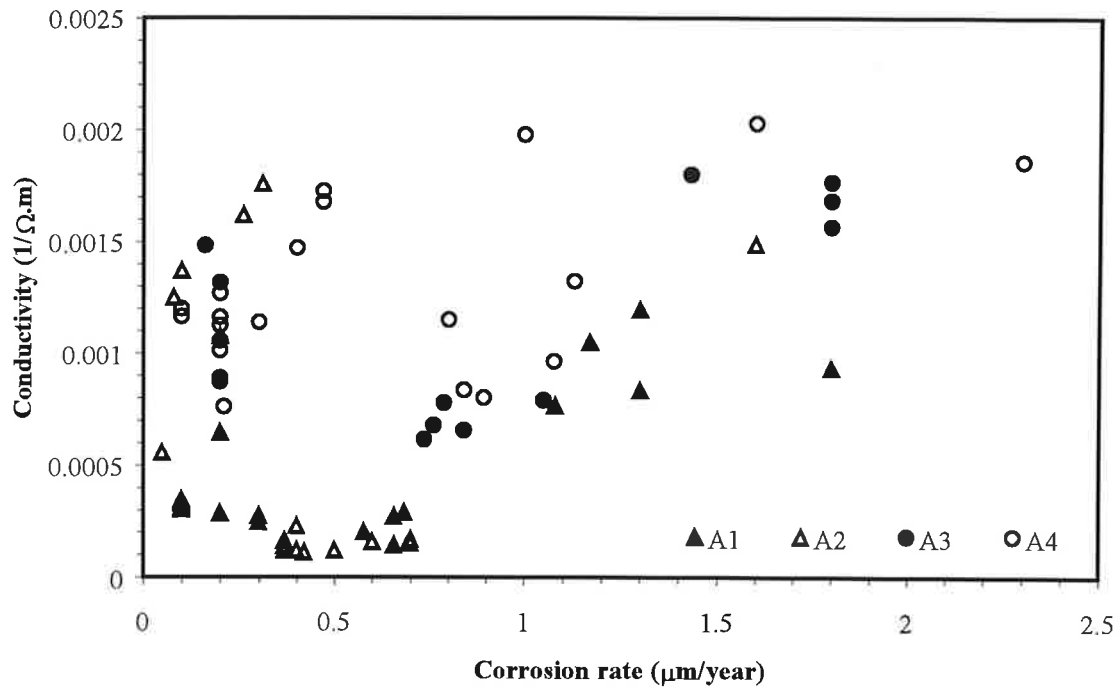
Figure B.1 - Conductivity of concrete (measured with two-point method at 10 mm depth) against corrosion rate of steel (rebars at 10 mm depth) in specimens with BFSC cement, w/c 0.45 and without chloride. Measurements at 80% R.H. (specimens A1 and A2) and in the fog room and outside (specimens A3 and A4) are reported.
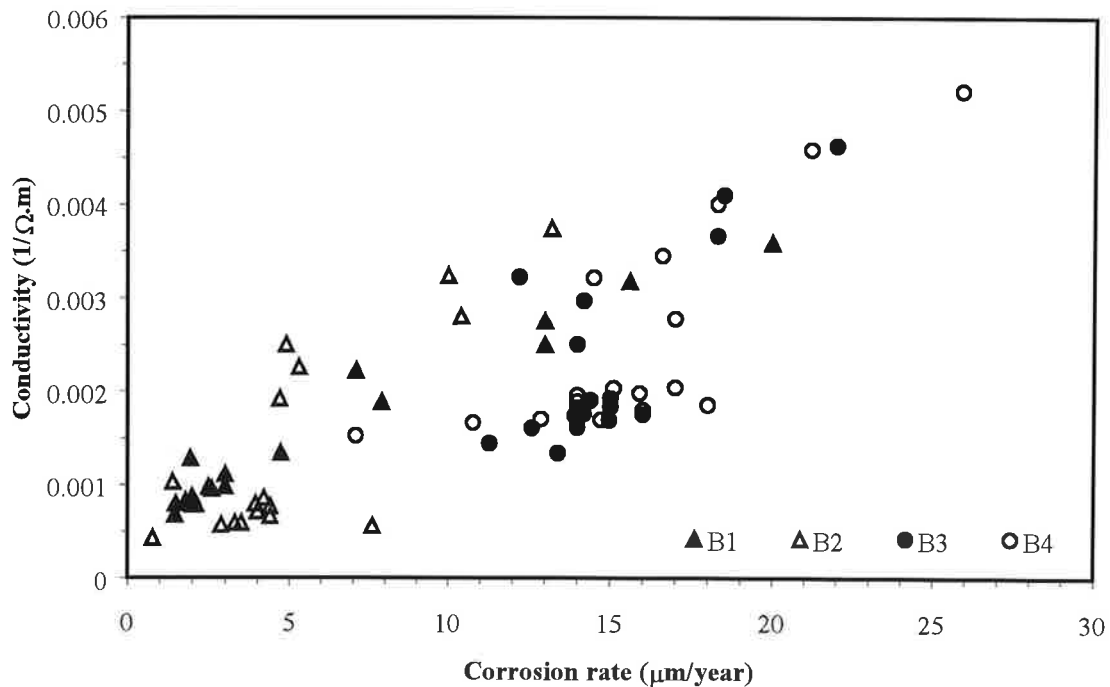
Figure B.2 - Conductivity of concrete (measured with two-point method at 10 mm depth) against corrosion rate of steel (rebars at 10 mm depth) in specimens with BFSC cement, w/c 0.45 and 2% chloride. Measurements at 80% R.H. (specimens B1 and B2) and in the fog room and outside (specimens B3 and B4) are reported.

Figure B.3 - Conductivity of concrete (measured with two-point method at 10 mm depth) against corrosion rate of steel (rebars at 10 mm depth) in specimens with BFSC cement, w/c 0.65 and without chloride. Measurements at 80% R.H. (specimens C1 and C2) and in the fog room and outside (specimens C3 and C4) are reported.

Figure B.4 - Conductivity of concrete (measured with two-point method at 10 mm depth) against corrosion rate of steel (rebars at 10 mm depth) in specimens with BFSC cement, w/c 0.65 and 2% chloride. Measurements at 80% R.H. (specimens D1 and D2) and in the fog room and outside (specimens D3 and D4) are reported.
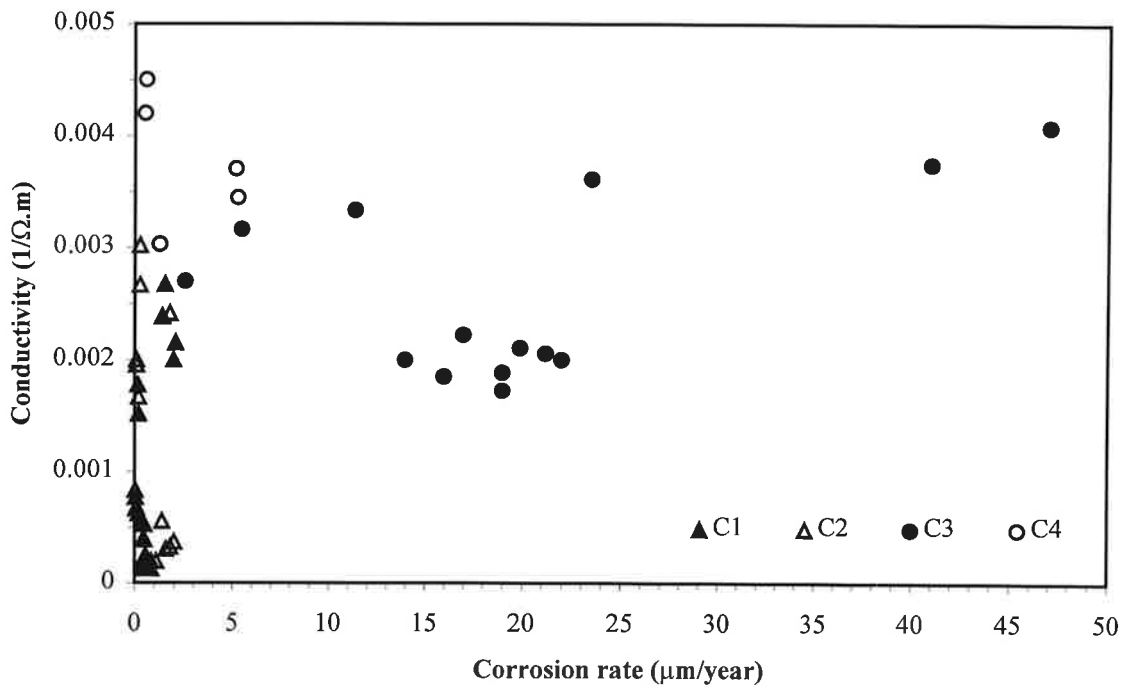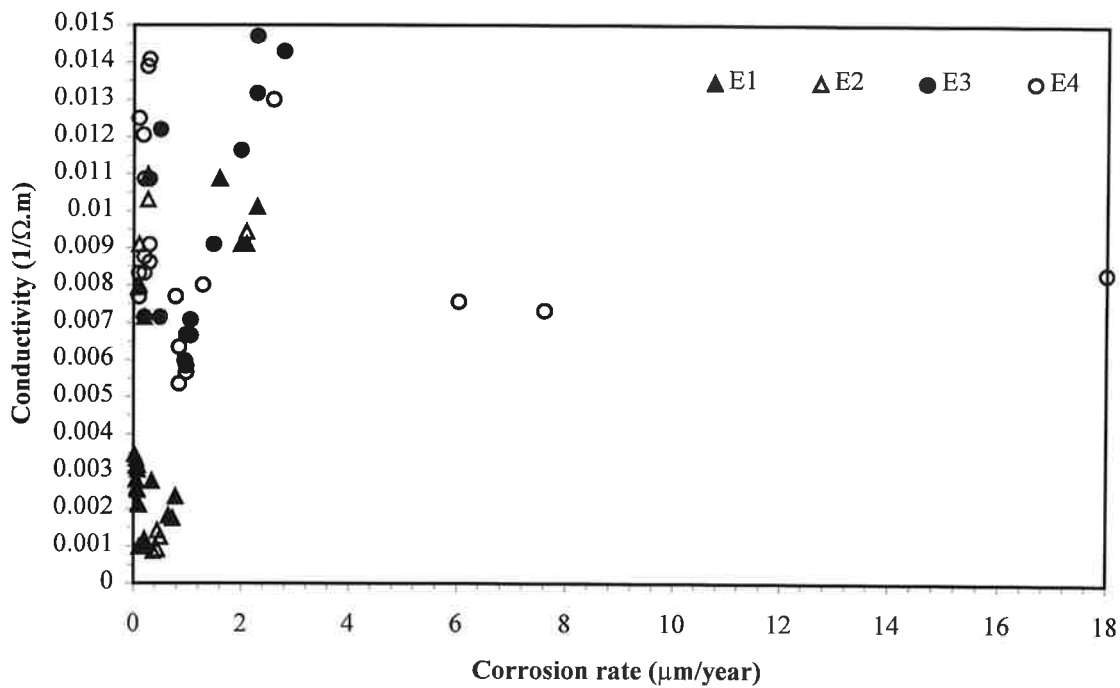
Figure B.5 - Conductivity of concrete (measured with two-point method at 10 mm depth) against corrosion rate of steel (rebars at 10 mm depth) in specimens with OPC cement, w/c 0.45 and without chloride. Measurements at 80% R.H. (specimens E1 and E2) and in the fog room and outside (specimens E3 and E4) are reported.
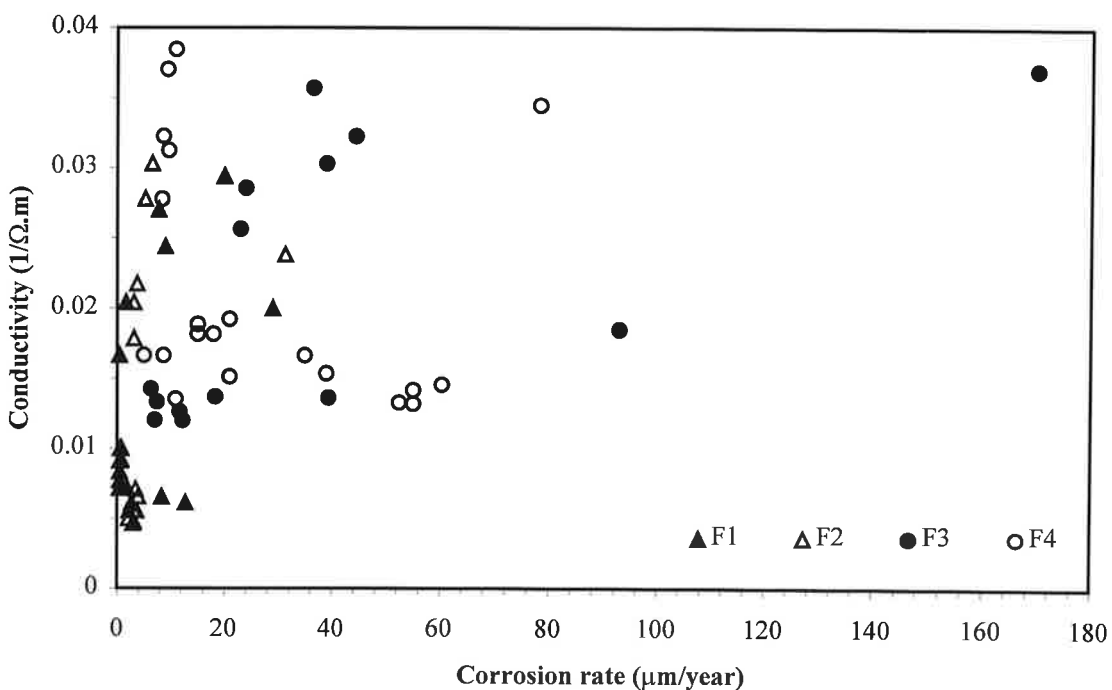
Figure B.6 - Conductivity of concrete (measured with two-point method at 10 mm depth) against corrosion rate of steel (rebars at 10 mm depth) in specimens with OPC cement, w/c 0.45 and 2% chloride. Measurements at 80% R.H. (specimens F1 and F2) and in the fog room and outside (specimens F3 and F4) are reported.
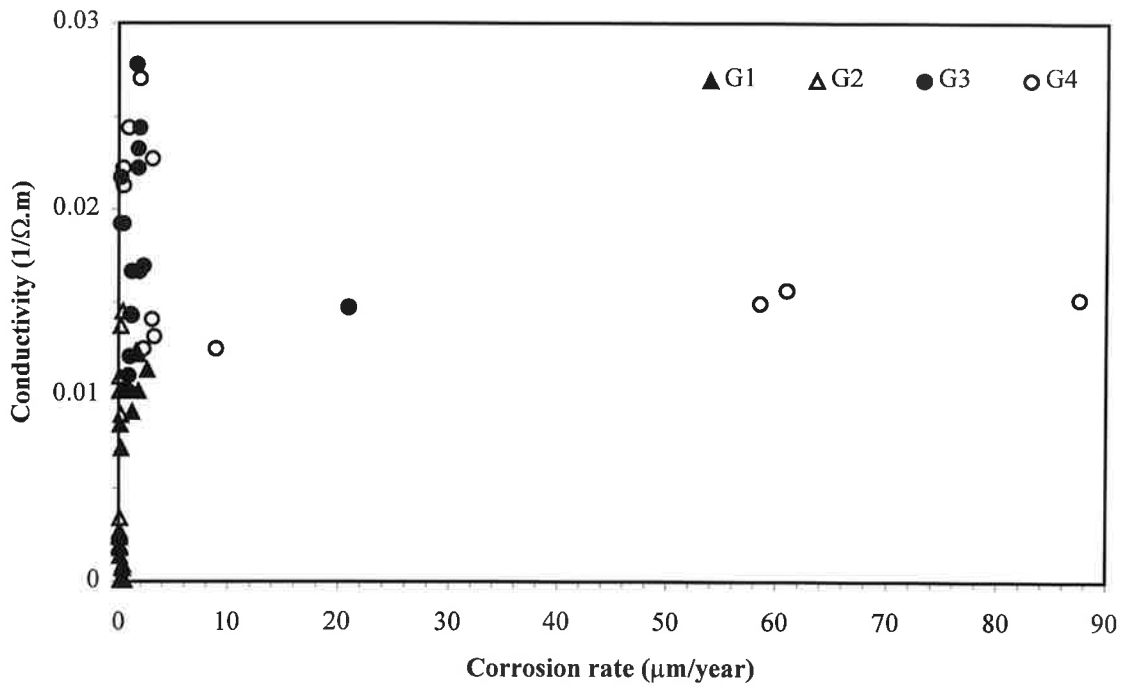
Figure B.7 - Conductivity of concrete (measured with two-point method at 10 mm depth) against corrosion rate of steel (rebars at 10 mm depth) in specimens with OPC cement, w/c 0.65 and without chloride. Measurements at 80% R.H. (specimens G1 and G2) and in the fog room and outside (specimens G3 and G4) are reported.
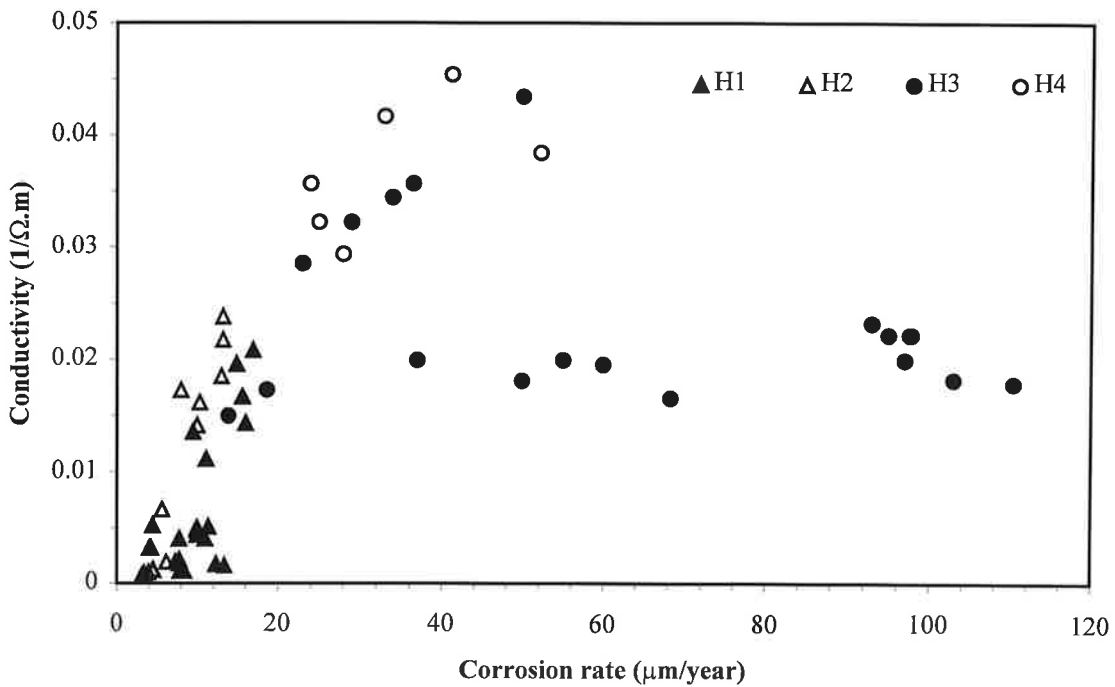
Figure B.8 - Conductivity of concrete (measured with two-point method at 10 mm depth) against corrosion rate of steel (rebars at 10 mm depth) in specimens with OPC cement, w/c 0.65 and 2% chloride. Measurements at 80% R.H. (specimens H1 and H2) and in the fog room and outside (specimens H3 and H4) are reported.
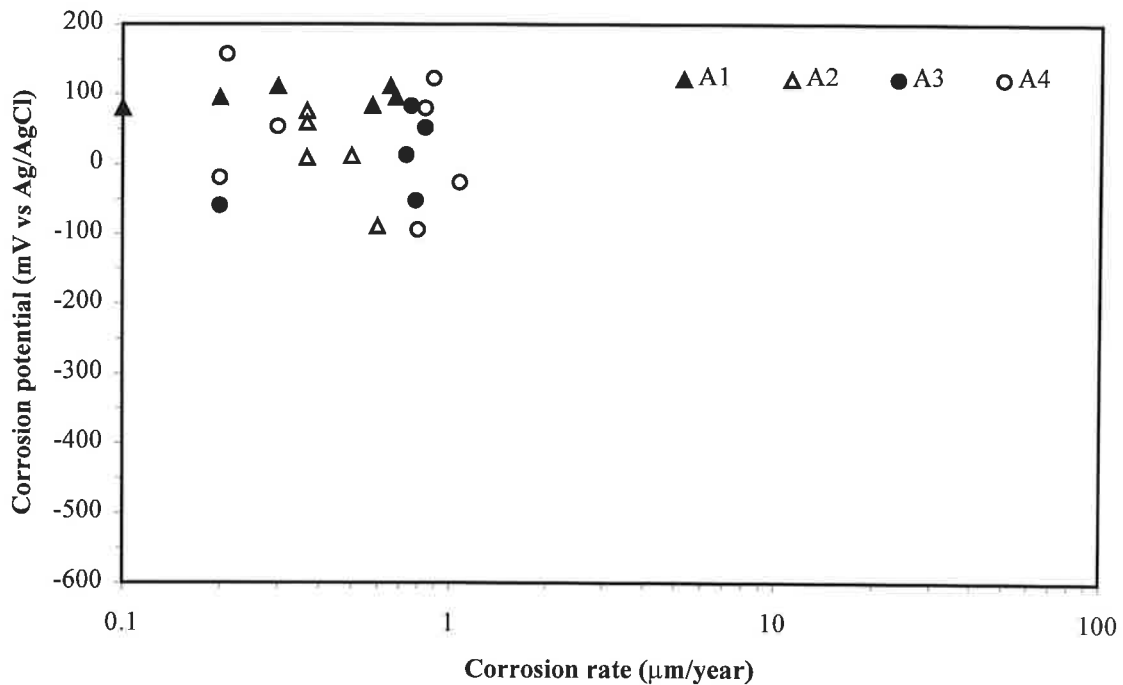
Figure B.9 - Corrosion potential against corrosion rate of steel (rebars at 10 mm depth) in specimens with BFSC cement, w/c 0.45 and without chloride. Measurements at 80% R.H. (specimens A1 and A2) and in the fog room and outside (specimens A3 and A4) are reported.
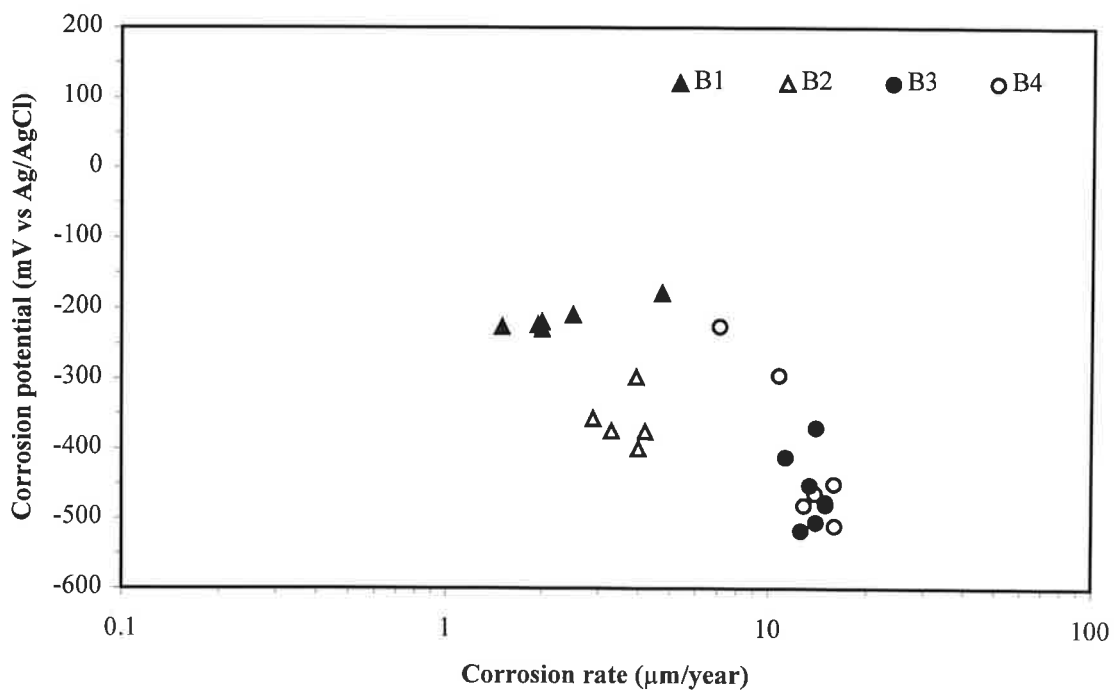
Figure B.10 - Corrosion potential against corrosion rate of steel (rebars at 10 mm depth) in specimens with BFSC cement, w/c 0.45 and 2% chloride. Measurements at 80% R.H. (specimens B1 and B2) and in the fog room and outside (specimens B3 and B4) are reported.
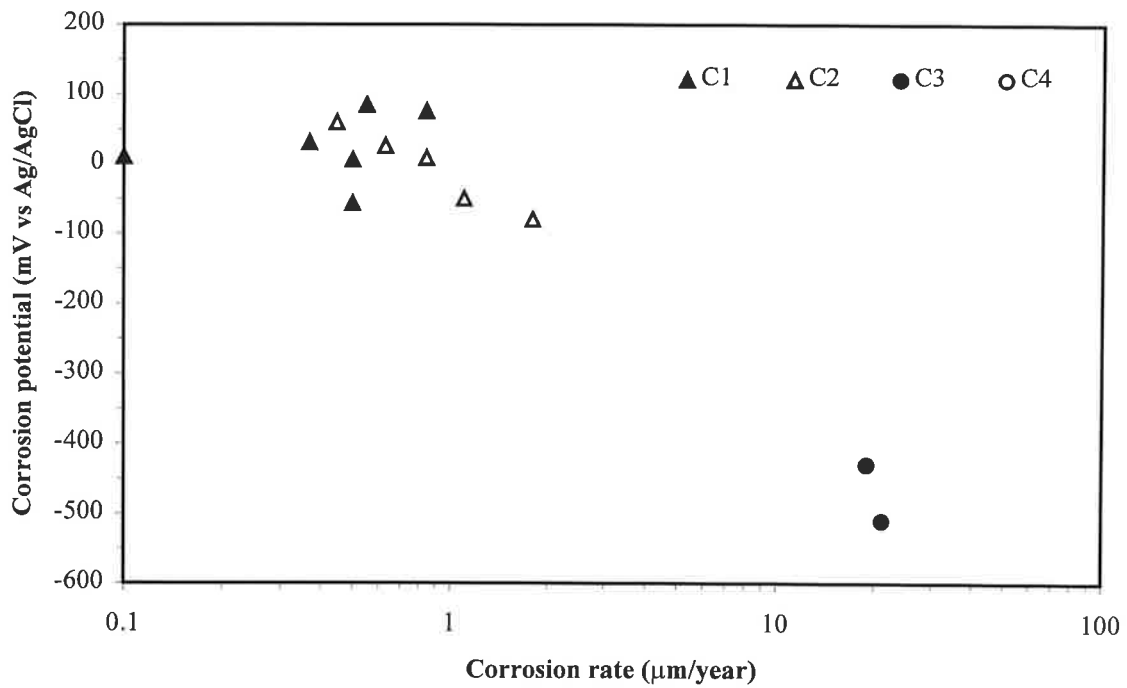
Figure B.11 - Corrosion potential against corrosion rate of steel (rebars at 10 mm depth) in specimens with BFSC cement, w/c 0.65 and without chloride. Measurements at 80% R.H. (specimens C1 and C2) and in the fog room and outside (specimens C3 and C4) are reported.
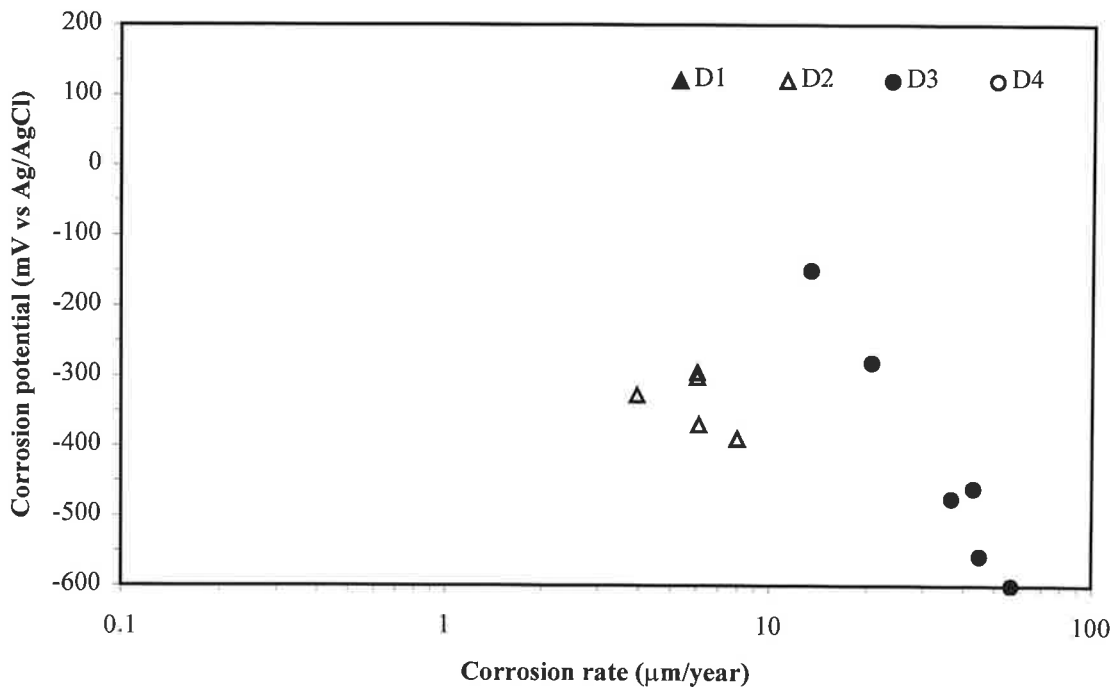
Figure B.12 - Corrosion potential against corrosion rate of steel (rebars at 10 mm depth) in specimens with BFSC cement, w/c 0.65 and 2% chloride. Measurements at 80% R.H. (specimens D1 and D2) and in the fog room and outside (specimens D3 and D4) are reported.
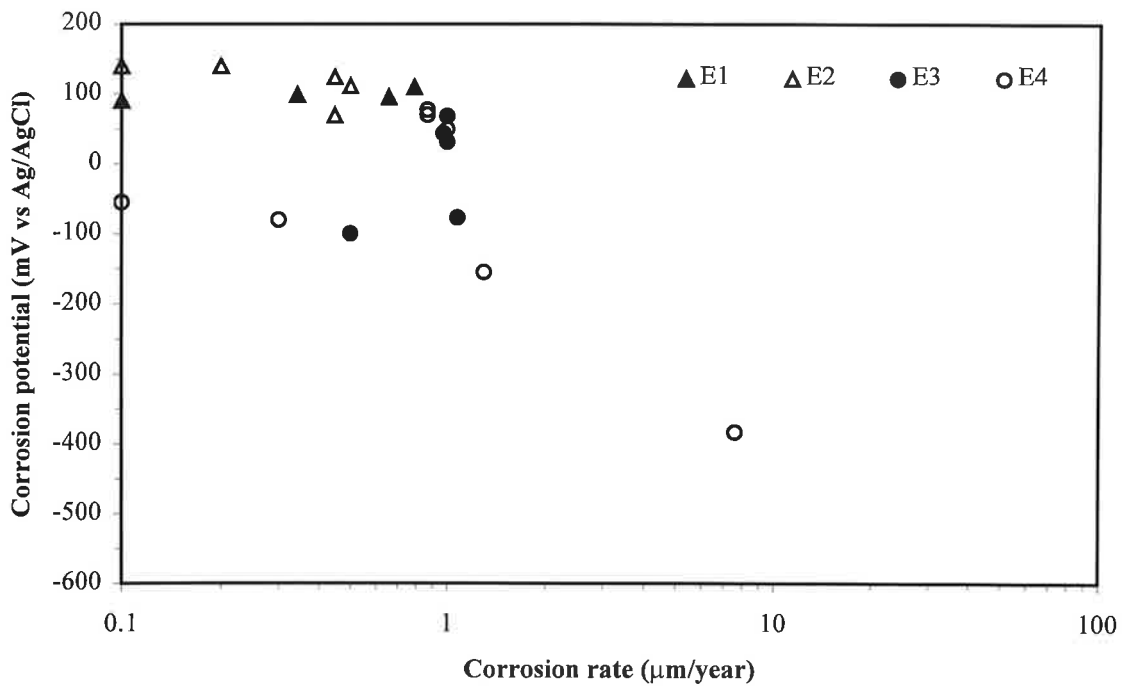
Figure B.13 - Corrosion potential against corrosion rate of steel (rebars at 10 mm depth) in specimens with OPC cement, w/c 0.45 and without chloride. Measurements at 80% R.H. (specimens E1 and E2) and in the fog room and outside (specimens E3 and E4) are reported.

Figure B.14 - Corrosion potential against corrosion rate of steel (rebars at 10 mm depth) in specimens with OPC cement, w/c 0.45 and 2% chloride. Measurements at 80% R.H. (specimens F1 and F2) and in the fog room and outside (specimens F3 and F4) are reported.
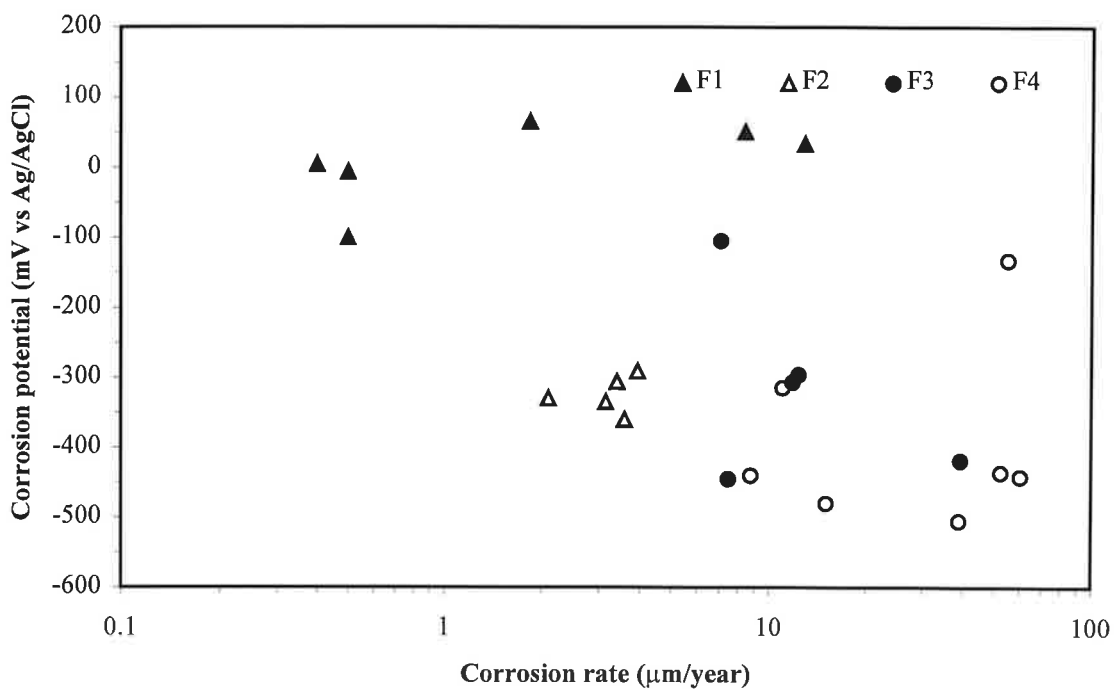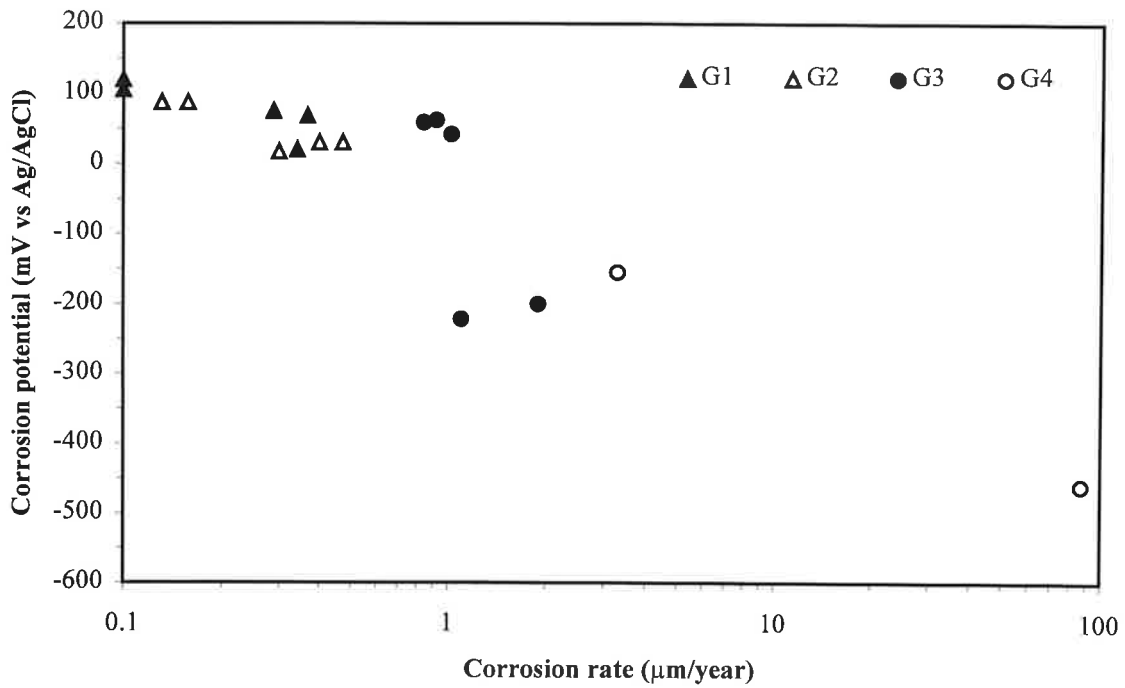
Figure B.15 - Corrosion potential against corrosion rate of steel (rebars at 10 mm depth) in specimens with OPC cement, w/c 0.65 and without chloride. Measurements at 80% R.H. (specimens G1 and G2) and in the fog room and outside (specimens G3 and G4) are reported.
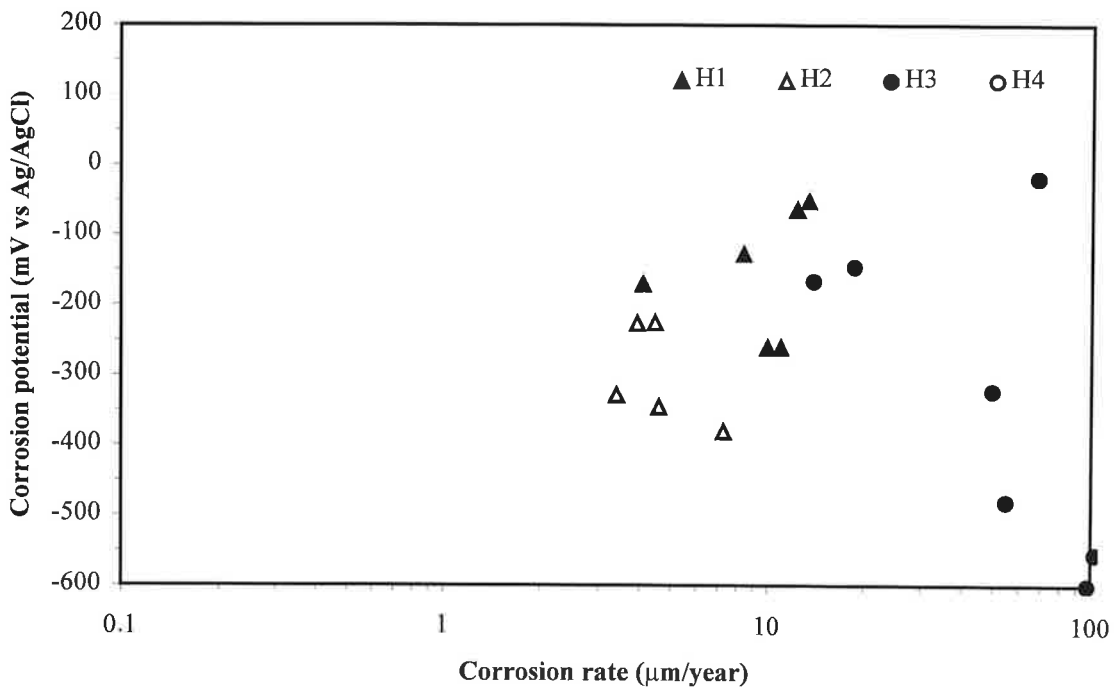
Figure B.16 - Corrosion potential against corrosion rate of steel (rebars at 10 mm depth) in specimens with OPC cement, w/c 0.65 and 2% chloride. Measurements at 80% R.H. (specimens H1 and H2) and in the fog room and outside (specimens H3 and H4) are reported.